



**DESIGN AND SYNTHESIS OF
17 α -(1-SUBSTITUTED-1,2,3-TRIAZOL-4-YL)-
19-NORTESTOSTERONE ACETATE DERIVATIVES USING
“CLICK CHEMISTRY” WITH PROGESTATIONAL
AND ANTICANCER ACTIVITIES**

A THESIS

Submitted in Partial Fulfillment of the Requirements
for the Master Degree of Pharmaceutical Science
(Pharmaceutical Medicinal Chemistry)

By

Zain El-Abdeen H. M. Ahmed

(B. Pharm. Sci. Assiut University, 2007)

Supervisors

Prof. Dr.

Adel F. Youssef

E. Professor of Pharm. Med. Chem.,
Faculty of Pharmacy,
Assiut University

Prof. Dr.

Nadia M. A. Mahfouz

Professor of Pharm. Med. Chem.,
Faculty of Pharmacy,
Assiut University

Prof. Dr.

Nawal A. El-koussi

Professor of Pharm. Med. Chem.,
Faculty of Pharmacy,
Assiut University

**Assiut University
(2014)**

٥٣٧/٥

بَيِّنَاتُ الْخَالِجِيَّةِ

قل إن صلاتي ونسكي ومحياي
ومماتي لله رب العالمين ﴿١٦٢﴾ لا
شريك له وبذلك أمرت وأنا أول
المسلمين ﴿١٦٣﴾



سورة الأنعام (١٦٢: ١٦٣)

Approval sheet

Title of the thesis:

Design and Synthesis of 17 α -(1-Substituted-1,2,3-Triazol-4-yl)-19-Nortestosterone Acetate Derivatives using "Click Chemistry" with Progestational and Anticancer Activities

Presented by: Zain El-Abdeen Hassep Mohamed Ahmed

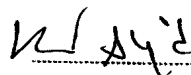
Committee in Charge

Signature

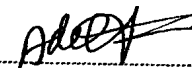
Prof. Dr. Hassan H. Farag
E. Prof. of Med. Chem.,
Faculty of Pharmacy, Assiut University



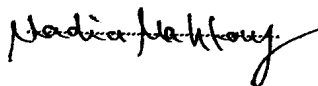
Prof. Dr. Khaled A. Mohamad
Prof. of Pharm. Chem.,
Faculty of Pharmacy, Ain Shams University



Prof. Dr. Adel F. Youssef
E. Prof. of Med. Chem.,
Faculty of Pharmacy, Assiut University



Prof. Dr. Nadia M. Mahfouz
E. Prof. of Med. Chem.,
Faculty of Pharmacy, Assiut University



Prof. Dr. Nawal A. El-Koussi
Prof. of Med. Chem.,
Faculty of Pharmacy, Assiut University

Nawal A. El-Koussi

Date: 8 /1/ 2014



To...

The memory of my Father,

My Mother who always stands beside me,

My Brothers for their continuous support,

My Wife for her patience and devotion,

My Son ☺

....Zain Hasep

Acknowledgment

To the Almighty God, ALLAH, Who has granted me all these graces to fulfill this work, supported me and blessed me by his mercy in all my life. To ALLAH I extended my heartfelt thanks.

*Intleed, my appreciation and profound gratitude are to E. **Prof. Dr. Adel F. Youssof**, Professor of Medicinal Chemistry, Faculty of Pharmacy, Assiut University, for suggesting the subject of this work, kind supervision, continuous encouragement, direct guidance and valuable support.*

*My cordial thanks is to **Prof. Dr. Nadia M. Mahfouz**, Professor of Medicinal Chemistry, Faculty of Pharmacy, Assiut University, for her kind supervision, valuable comments and the fruitful discussions.*

*I am also profoundly indebted to **Prof. Dr. Nawal A. El-koussi**, Professor of Medicinal Chemistry, Faculty of Pharmacy, Assiut University, for her admirable supervision, continuous support, generous consideration and indispensable advice.*

*I am greatly indebted to **Dr. Gehad Abdel Raheem**, Lecturer of Pharmacology, National Research Centre, Cairo, Egypt, for her participation by the biological investigation.*

My extreme thanks is to all staff members, colleagues and technicians of the medicinal chemistry department for their encouragement and help.

Zain Hassep Mohamed

2014

CONTENTS

	Page
Content.....	i
List of tables.....	iv
List of figures.....	v
List of abbreviation.....	vii
Abstract.....	ix
1. Introduction.....	1
1.1) Pharmacological aspects of progestational agents.....	1
1.1.1) Physiologic Effects of progesterone	2
1.1.2) Metabolism of progesterone.....	3
1.2) Synthetic progestins.....	5
1.2.1) Classification of progestins.....	5
1.2.1.1) Progestins structurally related to progesterone.....	5
1.2.1.1.1) Pregnane derivatives.....	5
1.2.1.1.2) 19-Norpregnane derivatives.....	7
1.2.1.2) Progestins structurally related to testosterone.....	9
1.2.1.2.1) Ethinylated progestins.....	9
1.2.1.2.2) Non-Ethinylated progestins.....	13
1.2.2) Other biologic activities of progestogens.....	13
1.3) Chemical aspects of click reaction.....	17

1.4) Applications of click chemistry.....	19
1.4.1) Bioconjugation field.....	19
1.4.2) Polymer field.....	22
1.4.3) Drug discovery field.....	25
2. Scope of investigation.....	34
3. Results and Discussion.....	38
3.1) Chemistry.....	38
3.1.1) Synthesis of <i>o</i> -, <i>m</i> -, and <i>p</i> -azido benzoic acids (2a-c).....	38
3.1.2) Synthesis of methyl azidobenzoates (3a-c).....	43
3.1.3) Synthesis of 17 α - (1-substituted-1,2,3-triazol-4-yl) -19-nor- testosterone acetates (5a-f).....	45
3.2) Biology.....	57
3.2.1) <i>In vivo</i> progestational activity.....	57
3.2.2) Anticancer activity.....	63
3.3) Molecular modeling, docking simulation studies and physicochemical calculations.....	67
3.3.1) Progesterone receptor structure.....	67

3.3.2) Progesterone receptor (PR) active site.....	69
3.3.3) Norethindrone binding with progesterone receptor.....	69
3.3.4) Docking simulation studies of target compounds (5a-f) with progesterone receptor.....	70
3.3.5) Physicochemical calculations.....	81
4. Experimental.....	85
4.1) Chemistry.....	85
4.1.1) General method for synthesis of azido benzoic acids (2a-c).....	87
4.1.2) General method for synthesis of methyl azidobenzoates (3a-c).....	89
4.1.3) General method for synthesis of 17 α - (1-substituted 1,2,3-triazol -4-yl)-19-nortestosterone acetate (5a-f).....	90
4.2) Biology.....	94
4.2.1) Progestational Screening.....	94
4.2.2) Anticancer Screening.....	96
4.3) Molecular Modeling.....	99
References.....	102
Arabic Summary.....	115

LIST OF TABLES

No.	Page
1	Biological activities of natural progesterone and synthetic progestins.....15
2	IR absorption bands (cm^{-1}) of compounds (5a-f).....49
3	^{13}C -NMR chemical shifts of compounds 5b and 5d.....56
4	<i>In vivo</i> progestational activity of 17- α (1-substituted-1,2,3-triazole -4-yl) 19-nortestosterone acetate (5a-f) at a daily dose level of 0.018 mg/ml.....58
5	<i>In vitro</i> anticancer activity for compounds (5a-f).....64
6	Interaction energies, ligand target interactions and <i>in vivo</i> biological activities of reference drug NETA and target compounds.....73
7	Calculated properties of the synthesized compounds (5a-f) in addition to Norethindrone acetate.....82
8	Physical data of <i>o</i> - , <i>m</i> - and <i>p</i> -azidobenzoic acids (2a-c).....88
9	Physical data of compounds (5a-f)91

LIST OF FIGURES

No.		Page
1	Steroid hormone levels across the human menstrual cycle and their functional impact on endometrial tissue.....	2
2	Biomolecules immobilization onto solid surfaces via click chemistry.....	22
3	General methods for preparation of azides.....	38
4	¹ H-NMR spectrum of compound 2c	43
5	IR spectrum of compound 3c	44
6	¹ H-NMR spectra of compound 5c	52
7	Numerical assignment of carbons of compound 5b and 5d	53
8	A) ¹³ C-NMR spectrum of compound 5b . B) DEPT spectrum of compound 5b	54
9	Effect of compounds (5a-f) and NETA on body and uterus weight.....	59
10	Effect of compounds (5a-f) and NETA on uterine thickness.....	59
11	A light micrograph of the uterus of a rat treated with compound 5b showing significant increase in endometrial thickness and distributed endometrial glands.....	61
12	Schematic representation of the progesterone receptor PR-A and PR-B proteins. The DNA-binding domain (DBD), the ligand-binding domain (LBD) and activation function domains (AFs) are indicated.....	68

No.		Page
13	Ribbon representation of progesterone receptor. Norethindrone depicted in black ball-and-stick representation with red oxygen atoms.....	68
14	Flexible ligand/active site docking simulation by LigX tool.....	71
15	Two-dimensional representation of the docking pose of norethindrone acetate in the PR binding site.....	72
16	Two-dimensional representation of the docking pose of compound 5a in the PR binding site.....	74
17	Two-dimensional representation of the docking pose of compound 5b in the PR binding site.....	75
18	A) Two-dimensional representation of the docking pose of compound 5f in the PR binding site. B) 3D representation of the same pose.....	76
19	Two-dimensional representation of the docking pose of compound 5d in the PR binding site.....	77
20	Two-dimensional representation of the docking pose of compound 5c in the PR binding site.....	78
21	Two-dimensional representation of the docking pose of compound 5e in the PR binding site.....	78

LIST OF ABBREVIATIONS

P	Progesterone
LH	Luteinizing hormone
E2	Estradiol
A	Androgens
GC	Glucocorticoids
FSH	Follicle stimulating hormone
IM	Intramuscular injection
MPA	Medroxyprogesterone acetate
MA	Megestrol acetate
CMA	Chlormadinone acetate
CPA	Cyproterone acetate
NOMAC	Nomegestrol acetate
NETA	Norethindrone acetate
AR	Androgen receptor
ER	Estrogen receptor
GR	Glucocorticoid receptor
MR	Mineralocorticoid receptor
OC	Oral contraception
CuAAC	Cu (I)-catalyzed azide/alkyne cycloaddition
PEG	Polyethylene glycol
hGH	Human growth hormone
CPY	Carboxypeptidase Y
PVA	Poly vinyl alcohol
HIV	Human immunodeficiency virus
MIC	Minimum inhibitory concentration

NRs	Nuclear receptors
LBD	Ligand binding domain
TPSA	Topological polar surface area
MOE	Molecular operating environment
DEPT	Distortionless enhancement by polarization transfer
COSY	Correlation spectroscopy
NOESY	Nuclear Overhauser effect spectroscopy
NCI	National Cancer Institute
DBD	DNA binding domains
NTD	Amino terminal domain
PDB	Protein data bank
ANOVA	Analysis of variance

ABSTRACT

Progestins are synthetic substances that mimics some or all of the actions of progesterone. The primary goal of the research on new progestins was to design orally active compounds depending on the progesterone metabolic pathways knowledge. These progestins have been developed for regulation of the menstrual cycle, prevention of endometrial hyperplasia, treatment of abnormal uterine bleeding, hormonal replacement therapy and contraception.

It is noteworthy that steroidal molecules with a hetero atom (N, O or S) at steroidal ring A and D showed a wide range of other biological activities such as antimicrobial, anti-inflammatory, antitumor, hypocholesterolemic and diuretic activities. As a result, a variety of heterocyclic units were introduced into the steroidal backbone.

On the basis of the above observation, a novel series of norethindrone acetate bearing substituted 1,2,3 triazole moiety at ring D was prepared using click chemistry, through reaction of the 17 α ethynyl of norethindrone acetate with different substituted phenyl azides selected according to the results of preliminary docking studies against progesterone receptor.

The click reaction conditions were adapted for temperature, time, solvent and copper catalyst to obtain good yield of the final target compounds (**5a-f**).

The following six azide intermediates were synthesized:

- 2-Azidobenzoic acid (**2a**).
- 3-Azidobenzoic acid (**2b**).
- 4-Azidobenzoic acid (**2c**).
- Methyl 2-azidobenzoate (**3a**).

- Methyl 3-azidobenzoate (**3b**).
- Methyl 4-azidobenzoate (**3c**).

Their structures were assigned by spectroscopic methods (IR, ¹H-NMR) and by comparing their melting points by the reported one.

These azides were used for the click reaction with norethindrone acetate (**4**) for the synthesis of the following target compounds:

- 2-(4-(17-Acetoxy-13-methyl-3-oxo-2,3,6,7,8,9,10,11,12,13,14,15,16,17-tetradecahydro-1H-cyclopenta[a]phenanthren-17-yl)-1H-1,2,3-triazol-1-yl)benzoic acid (**5a**).
- 3-(4-(17-Acetoxy-13-methyl-3-oxo-2,3,6,7,8,9,10,11,12,13,14,15,16,17-tetradecahydro-1H-cyclopenta[a]phenanthren-17-yl)-1H-1,2,3-triazol-1-yl)benzoic acid (**5b**).
- 4-(4-(17-Acetoxy-13-methyl-3-oxo-2,3,6,7,8,9,10,11,12,13,14,15,16,17-tetradecahydro-1H-cyclopenta[a]phenanthren-17-yl)-1H-1,2,3-triazol-1-yl)benzoic acid (**5c**).
- Methyl 2-(4-(17-acetoxy-13-methyl-3-oxo-2,3,6,7,8,9,10,11,12,13,14,15,16,17-tetradecahydro-1H-cyclopenta[a]phenanthren-17-yl)-1H-1,2,3-triazol-1-yl) benzoate (**5d**).
- Methyl 3-(4-(17-acetoxy-13-methyl-3-oxo-2,3,6,7,8,9,10,11,12,13,14,15,16,17-tetradecahydro-1H-cyclopenta[a]phenanthren-17-yl)-1H-1,2,3-triazol-1-yl) benzoate (**5e**).

- Methyl 4-(4-(17-acetoxy-13-methyl-3-oxo-2,3,6,7,8,9,10,11,12,13,14,15,16,17-tetradecahydro-1H-cyclopenta[a]phenanthren-17-yl)-1H-1,2,3-triazol-1-yl)benzoate (**5f**).

These compounds were purified by column chromatography and their structures were assigned by elemental analyses, IR, ¹H-NMR, ¹³C-NMR.

The evaluation of the progestational activity of the synthesized compounds (**5a-f**) was carried out *in vivo* on rat uterus using norethindrone acetate as reference drug. The histopathological study revealed that all the synthesized compounds have *in vivo* progestational activity with enhanced potency due to their induction of endometrial proliferation as compared to the control animals. Compounds **5a**, **5b**, **5d** and **5f** showed progestational activity more than that revealed by Norethindrone acetate while compounds **5c** and **5e** showed lower activity than Norethindrone acetate.

Moreover the synthesized compounds (**5a-f**) were evaluated for the anticancer activity according to NCI (national cancer institute) *in vitro* protocols, they were screened against a panel consisting of 60 human cancer cell lines, derived from nine cancer cell types (Leukemia, Non small cell lung cancer, Colon cancer, Central nervous system cancer, Melanoma, Ovarian cancer, Renal cancer, Prostate cancer and Breast cancer). The tested compounds showed variable activities against the different cell lines. All the active compounds in this test proved to be non-selective with broad spectrum anticancer activity. The esterified derivatives (**5d-f**) displayed higher activity than their respective free acids (**5a-c**). Among the esterified derivatives compound **5e** is the most active one showing broad spectrum anticancer activity. It revealed about 50% growth inhibition of CNS cancer SNB-75 cell line, 56% growth inhibition of renal cancer A498 cell line and 56.7% growth inhibition of prostate cancer PC-3 cell line.

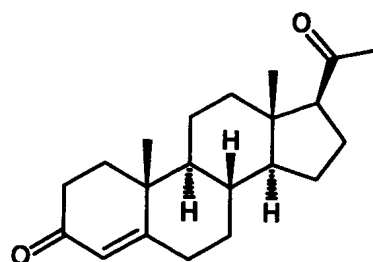
Molecular modeling (docking) study was performed using MOE software (V.10.2010) for *in silico* evaluation of the binding characters of the synthesized compounds (**5a-f**) in comparison to norethindrone acetate as reference ligand. The docking study revealed a significant effect of the added moiety on the binding of the tested compounds to the active site. Compound **5a**, **5b** and **5f** showed the highest scores due to their binding with the two essential amino acids Gln725 and Arg766 in addition to other hydrogen bond interaction with the active site Asn719. On the other hand compounds **5c**, **5d** and **5e** showed lower scores than the reference drug since they bind only with two essential amino acids in the active site. The effect of the structural modification on the physicochemical properties of the compounds was also studied and revealed that the modification slightly diminished the predicted water solubility of the target compounds but our design for introduction of the carboxyl group provides a wide capability of salt formation with several bases that can enhance water solubility.

1. INTRODUCTION

1. INTRODUCTION

1.1) Pharmacological aspects of progestational agents

Progesterone (P) (I) is a naturally occurring steroid hormone. In non-pregnant women, the main sites of progesterone biosynthesis are the ovaries and the adrenal cortices. Progesterone plays an important role in postovulatory regulation of the menstrual cycle. Under the influence of luteinizing hormone (LH), the corpus luteum secretes progesterone, which stimulates the endometrium to develop secretory glands and dominate the secretory phase. The corpus luteum produces progesterone for approximately 10 to 12 days of the cycle. If a fertilized ovum is not implanted, female sex hormones levels decline sharply, resulting in tissue breakdown and menstruation, **Figure 1**. If fertilization occurs, progesterone supports implantation of the ovum and maintains the pregnancy.^{1,2}



Progesterone (I)

Introduction

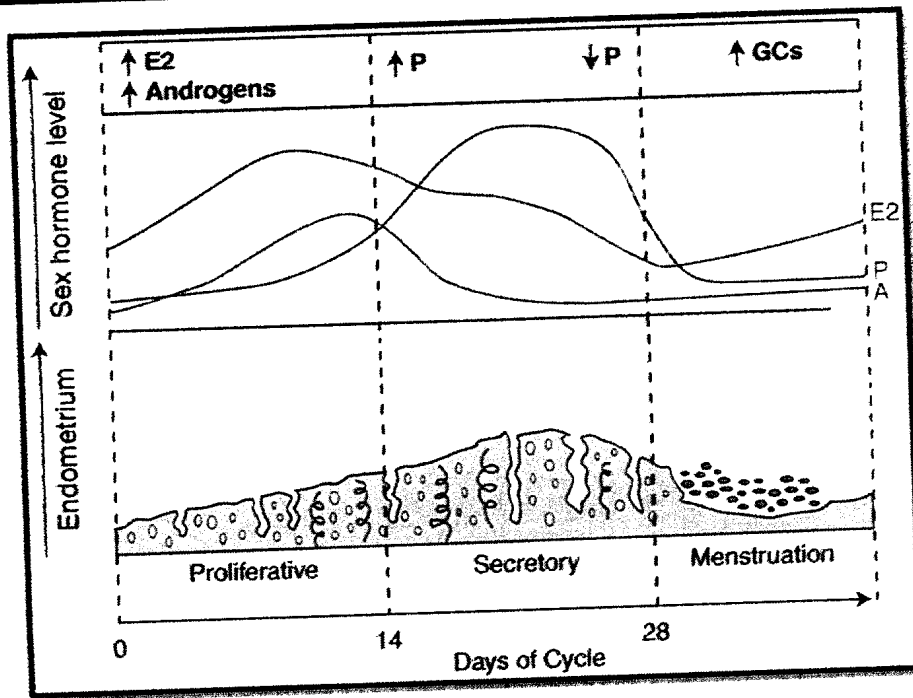


Figure (1): Steroid hormone levels across the human menstrual cycle and their functional impact on endometrial tissue. P= progesterone, E2= estradiol, A= androgens, GC= glucocorticoids.

1.1.1) Physiologic Effects of progesterone

The primary physiologic site of action of progesterone is the uterus. It acts on both the endometrium (inner mucous lining) and the myometrium (muscle mass) of the uterus. The effect of progesterone on the endometrium, already primed by estrogens, is to induce the secretory phase of the menstrual cycle. During this phase, the endometrial glands grow and secrete large amounts of carbohydrates that can be used by the fertilized ovum as an energy source. The primary function of progesterone with respect to the myometrium is to stop spontaneous rhythmic contractions of the uterus.³

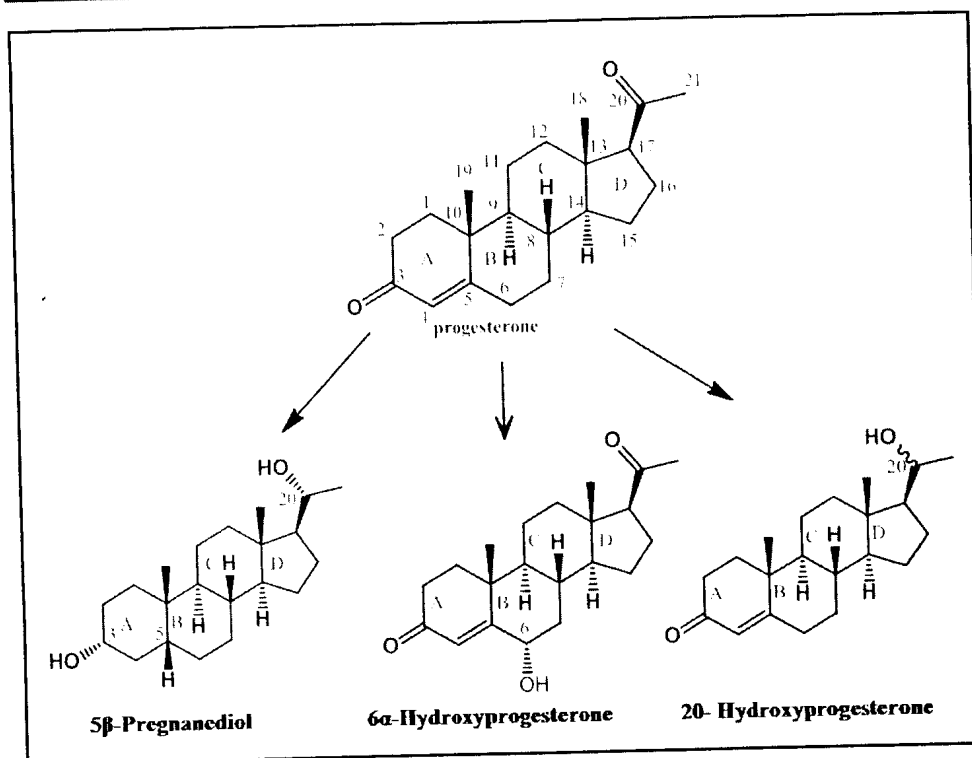
Progesterone often is referred to as the “hormone of pregnancy.” For the first trimester, the corpus luteum serves as the primary source of progesterone, at which point the developing placenta takes over as the major source of progesterone and estrogen. The high level of progesterone that is produced during pregnancy sends a signal to the hypothalamus via the negative feedback system to prevent release of the FSH and LH necessary for the development of new ova.³

In general, the non reproductive effects of progesterone such as the increase in sodium excretion and the temperature-raising effect are fairly insignificant.

1.1.2) Metabolism of progesterone

Progesterone is highly vulnerable to enzymatic reduction by reductases and hydroxysteroid dehydrogenases during hepatic first pass metabolism **scheme 1**, because its structure contains two ketone groups and a double bond, metabolic degradation of progesterone was shown to involve primarily reduction of the 20-keto group and the 4,5-double bond, followed by reduction of the 3-keto group.

As a result, the serious drawback of the natural hormone Progesterone was the poor bioavailability on oral administration due to this rapid metabolism in the liver: over 99% of the orally administered dose is metabolized in the liver before it reaches the general circulation. Intramuscular injection (IM) assures reliable absorption, but is related to low compliance. It is painful, can cause local irritation and cold abscesses, and therefore must be administered by trained medical personnel.⁴⁻⁶



Scheme (1): Metabolism of progesterone.³

Thus the primary goal of the research on new progestins was therefore to design orally active compounds depending on the progesterone metabolic pathways knowledge. This knowledge allowed the rational design of orally active analogues of progesterone: the 20-keto group could be protected by additional substituents in close proximity, e.g. at C-17 (acyl, alkyl, and halogen), C-16 (alkyl, cycloalkyl) and C-21 (OH, alkyl, halogen). Similarly reduction of double bond at ring A is slowed down by substituents at C-6 (methyl, halogen) and by extending the enone with an additional double bond.⁵

1.2) Synthetic progestins

A variety of oral, injectable and implantable synthetic analogs, called “progestins”, have been developed for regulation of the menstrual cycle, prevention of endometrial hyperplasia, treatment of abnormal uterine bleeding, hormone replacement therapy and contraception.^{1,7}

1.2.1) Classification of progestins

The classification of progestins has caused confusion. The designation of first-, second- or third-generation progestins is based on time since market introduction and not on structural and physiologic differences or efficacy. Another classification schemes were based on structural derivation and divides progestins into estranes, gonanes and pregnanes.¹ Others classifying them as following⁴:

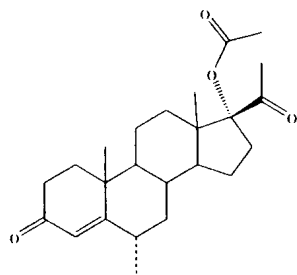
1.2.1.1) Progestins structurally related to progesterone

1.2.1.1.1) Pregnane derivatives:

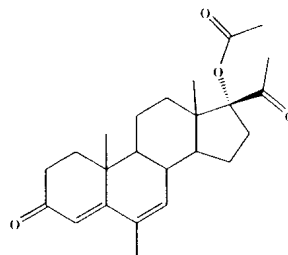
a. O-acetylated derivatives:

For the progestogenic activity the C17 position is of key importance. Progesterone loses its progestogenic activity with the introduction of a hydroxyl group at position C17. Accordingly, 17-hydroxyprogesterone is hormonally inactive but its acetate ester revealed weak progestogenic activity and also week oral bioavailability, but, esterification with caproate leads to a highly active progestin. On the other hand, methylation of 17-hydroxyprogesterone acetate ester at carbon 6 produce Medroxyprogesterone acetate (MPA) (II)^{8,9}. Chemical manipulation of the MPA molecule by addition of a double bond between carbons 6 and 7 gives rise to megestrol acetate (MA) (III). Substitution of the methyl group at carbon 6 of megestrol acetate with a chloro substituent gives rise to chlormadinone acetate (CMA) (IV).

Introduction

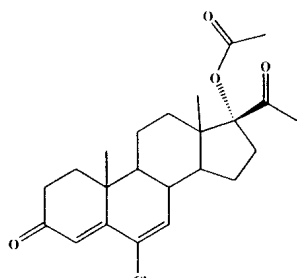


Medroxyprogesterone acetate (II)

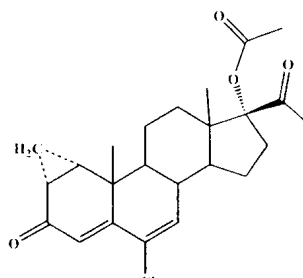


Megestrol acetate (III)

Attachment of carbons 1 and 2 of Chlormadinone acetate with a methylene moiety gives rise to Cyproterone acetate (CPA) (V). These three derivatives of Medroxyprogesterone acetate are more potent progestins¹⁰.



Chlormadinone acetate (IV)



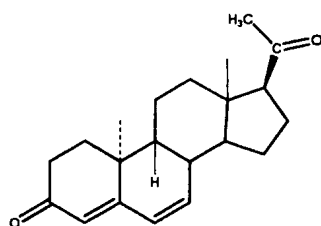
Cyproterone acetate (V)

b. Non-acetylated derivatives:

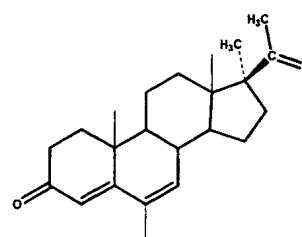
A unique progestin that has a methyl group at carbon 10 but lack O-acetyl moiety at C17 is dydrogesterone (VI) which is a retroprogesterone, a stereo-isomer of progesterone, with an additional double bond between carbon 6 and 7. The progesterone molecule is almost “flat”, the retroprogesterone molecule is bent by a change of the orientation of the methyl group at carbon 10 from the β to α position and the hydrogen at C9 from the α to the β position. This retrostructure binds almost exclusively to the progesterone receptor making dydrogesterone highly selective progestin, and showing no affinity for androgenic, estrogenic, glucocorticoid or mineralocorticoid receptors^{8,11}.

Introduction

Furthermore, medrogestone (VII) which has an α methyl group at the C17, another methyl moiety at C6 position in addition to a double bond between C6 and C7, revealed rapid and about 100% bioavailability.⁸



Dydrogesterone (VI)



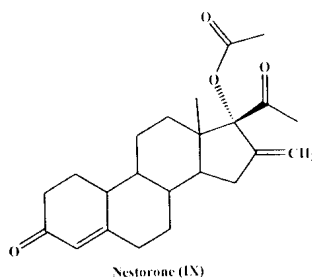
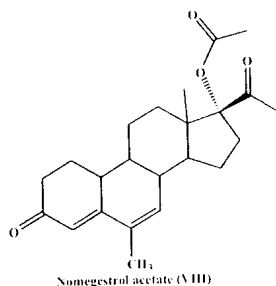
Medrogestone (VII)

1.2.1.1.2) 19-Norpregnane derivatives

These derivatives are characterized by lacking a methyl group at carbon 10 and subclassified to:

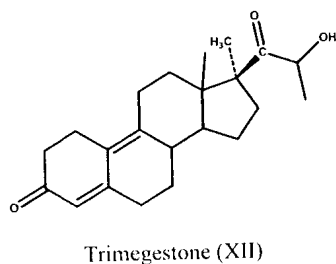
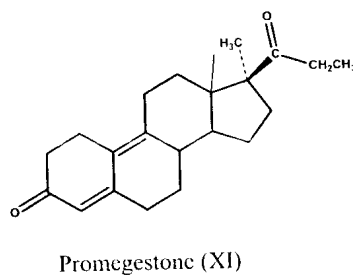
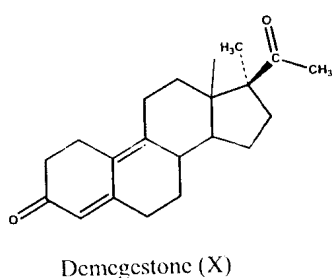
a. O-acetylated derivatives:

They are characterized by the presence of acetoxy moiety α - oriented at C17. They include nomegestrol acetate (NOMAC) (VIII) and nesterone (IX). Nomegestrol acetate characterized by the presence of a double bond between C6 and C7 which creates a so-called “conjugated double-bond system” over rings A and B. This conjugated system impaired a high stability and intrinsic potency in nomegestrol acetate action on progesterone receptor, a weak anti-androgenic effect and showed no binding to estrogen, glucocorticoid or mineralocorticoid receptors.¹² Nesterone is only active when administered parenterally because of its rapid metabolism and inactivation.¹³ The 16-methylene substituent enhanced progestational activity far more than either 16 α or 16 β -methyl substituents.¹⁴



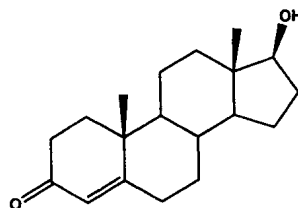
b. Non-acetylated:

This group includes Demegestone (X), promegestone (XI), and its active metabolite trimegestone (XII). They are characterized by the presence of an α methyl group at carbon 17 instead of the acetoxy group and a further double bond between C9 and C10.^{8, 10} Trimegestone, the most potent of the 19-norprogesterones, contains an unusual C21 hydroxyl group. It has very high affinity for the progesterone receptor but only weak affinity for the mineralocorticoid receptor, and on the other hand displays no glucocorticoid, androgenic, or antiandrogenic action. Trimegestone undergoes metabolic hydroxylation to produce metabolites with substantial progestogenic action.³



1.2.1.2) Progestins structurally related to testosterone

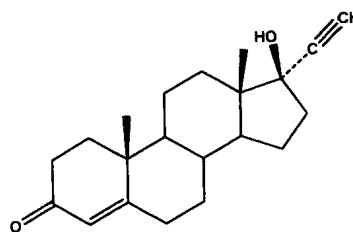
Using the testosterone (XIII) molecule as the starting point, we can show how manipulation of its chemical structure alters its biologic activity dramatically.⁹



Testosterone (XIII)

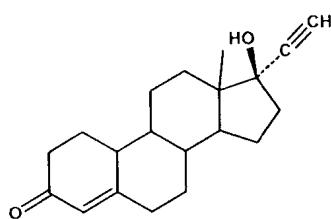
1.2.1.2.1) Ethynylated progestins:

Addition of an ethynyl group to the molecule causes loss of androgenic activity and enhances both the progestational activity and oral bioavailability e.g. 17 α – ethynyl testosterone, which was given the common name ethisterone (XIV).¹⁰

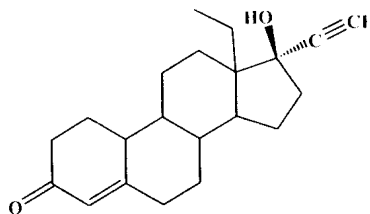


Ethisterone (XIV)

Furthermore removal of the methyl group at carbon 10 of ethisterone increases the progestational activity and enhances the oral bioavailability of the molecule and virtually eliminates its androgenicity. The resulting product is norethindrone, which is also called norethisterone (XV). It has 5 to 10 fold more progestin activity. Replacement of the methyl group at carbon 13 of norethindrone by an ethyl moiety yields a more active derivative, norgestrel (XVI), which consists of a racemic mixture of D-(-)-norgestrel (levonorgestrel) and L-(+)-norgestrel (dextronorgestrel).^{3, 9, 15}



Norethisterone (XV)



Norgestrel (XVI)
a : Dextronorgestrel
b : Levonorgestrel

Ethynylated progestins are subclassified to:

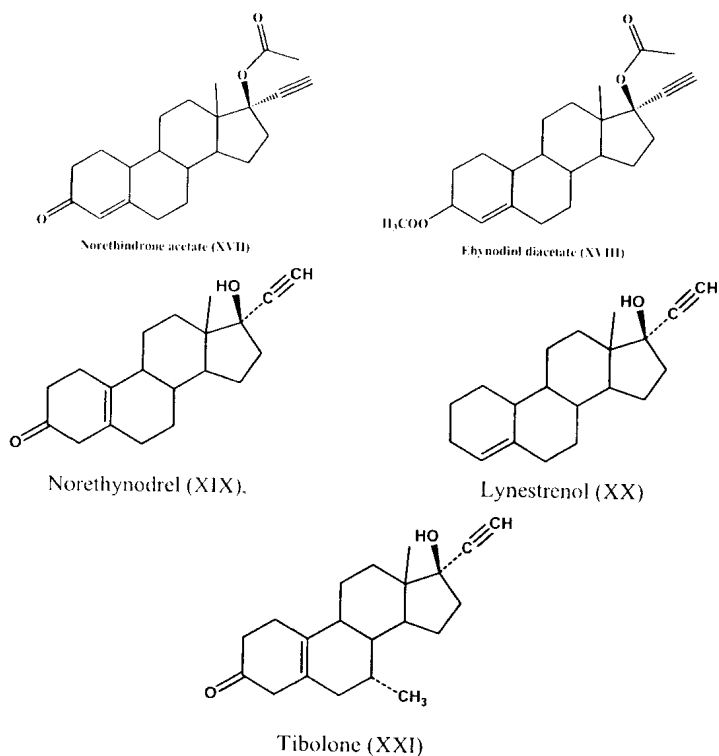
a. Estranes:

They have 18 carbon atoms as the parent steroid, estrane. The norethindrone family of progestins includes norethindrone acetate (NETA) (XVII), ethynodiol diacetate (XVIII), norethynodrel (XIX), and lynestrenol (XX). It was reported that acetylation of the 17β -OH of norethindrone increases the duration of action of the drug. Shift of the double bond between carbons 4 and 5 of norethindrone to carbons 5 and 10 gave norethynodrel molecule which has approximately one-tenth the progestational activity of norethindrone.¹⁰ Lynestrenol differs from norethindrone in structure by the absence of an oxygenated functional group at carbon 3. Introduction of α methyl group at carbon 7 of norethynodrel produces tibolone (XXI) which revealed increased hormonal activity.

It is generally considered that the progestins structurally related to norethindrone are prodrugs and their progestational activity is due to norethindrone. After oral administration, norethindrone acetate and ethynodiol diacetate (an extremely potent oral progestin) are rapidly converted to the parent compound by esterases during hepatic first pass metabolism. Although little is known about the biotransformation of lynestrenol (XX) and norethynodrel (XIX), it appears that lynestrenol first undergoes hydroxylation at carbon 3 and then oxidation of the hydroxyl group, forming norethindrone.¹⁶ The possibility that some norethynodrel is metabolized by pathways not involving norethindrone as an intermediate has not

Introduction

been excluded, but there is no evidence in its favor. Thus, it generally appears that the pharmacokinetics of progestins structurally related to norethindrone is determined by the pharmacokinetics of norethindrone.^{9, 10, 15}

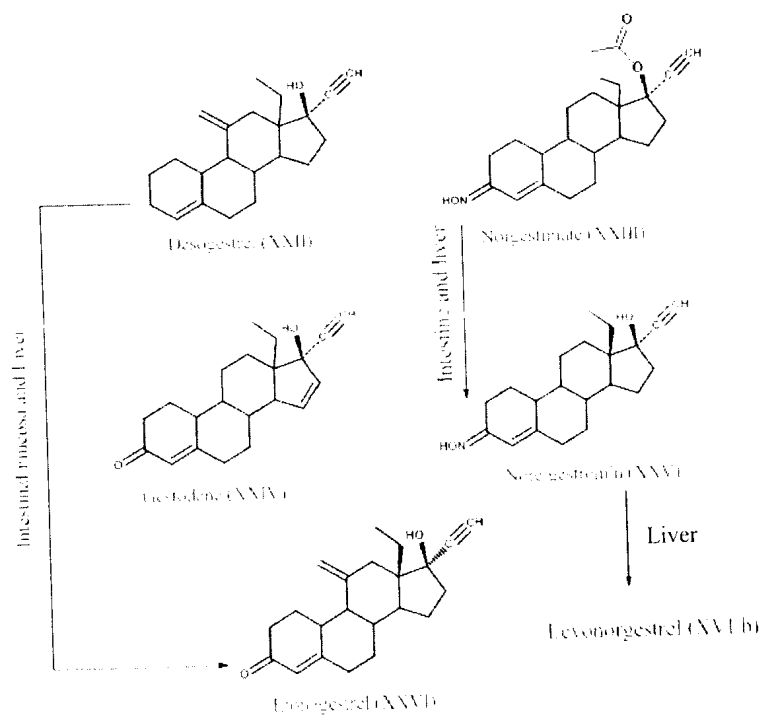


b. 13-Ethylgonanes:

These compounds are often referred to "new" progestins because they were marketed more recently compared with levonorgestrel (XVI), norethindrone (XV), and progestins structurally related to norethindrone. They include desogestrel (XXII), norgestimate (XXIII), gestodene (XXIV) and etonogestrel (XXVI). In comparison to the chemical structure of levonorgestrel (XVI b), desogestrel is a prodrug lacking oxygenated functional group at carbon 3 and has a methylene group at carbon 11. It is rapidly metabolized in the intestinal mucosa and in liver via first pass to its active metabolite, etonogestrel (XXVI). Whereas the progestin norgestimate (XXIII) has an oxime group at carbon 3 and acetoxy

Introduction

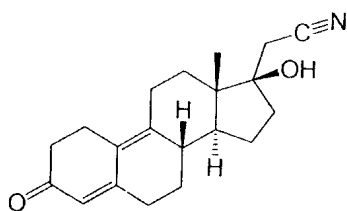
group at carbon 17. Norgestimate rapidly undergoes a two-step metabolic transformation to form two active products, norgestromin (XXV) (levonorgestrel 3-oxime) and levonorgestrel (XVI b). Deacetylation of norgestimate occurs in the intestine and liver, whereas conversion of the 3-oxime to the corresponding ketone occurs primarily in the liver. Both desogestrel (XXII) and norgestimate (XXIII) exhibit high selectivity for the progesterone receptor and have low androgenic activity. In contrast, gestodene (XXIV) which is not a prodrug differs from levonorgestrel only in that it has a double bond between carbons 15 and 16 exhibiting nearly 100% oral bioavailability and excellent progesterone receptor binding affinity. The synthetic progestin norgestromin (XXV) which is 17-deacetylnorgestimate (active metabolite of norgestimate) and etonogestrel (XXVI) which is the active metabolite of the prodrug, desogestrel are newer derivatives of this group^{3, 9, 10, 17, 18}.



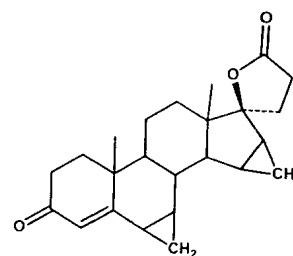
Introduction

1.2.1.2.2) Non-ethinylated derivatives:

The non-ethinylated subgroup of progestins includes dienogest (XXVII) and drospirenone (XXVIII). Comparing with the chemical structure of norethindrone, dienogest (XXVII) contains the isosteric cyano group instead of an ethynyl moiety at carbon 17, and a double bond between carbons 10 and 11. Dienogest is 10 times more potent than the standard levonorgestrel.¹⁹ Drospirenone (XXVIII) has the basic chemical structure of the parent compound, androstane (19 carbons) and is an analog of spironolactone. It is the only progestin with antimineralocorticoid activity. Its affinity for the mineralocorticoid receptor is five fold greater than that of aldosterone. Drospirenone has progestogenic action, but only 10% that of levonorgestrel. It contains one methylene group attached to carbons 6 and 7, another attached to carbons 15 and 16 and a γ -carbolactone group at carbon 17.^{3, 9, 10}



Dienogest (XXVII)



Drospirenone (XXVIII)

1.2.2) Other Biological Activities of Progestogens

It is very difficult to deduce various biological actions and activities of steroids with progestational activity from the chemical structure alone. One of the essential requirements of any compound with such an activity is of course: being able to bind to the progesterone-receptor but interaction with other steroid hormone receptors as androgen receptor (AR), estrogen receptor (ER), glucocorticoid receptor (GR) and mineralocorticoid receptor (MR) may occur. These interactions add to the physiological effects of progestogens; variably, anti-estrogenic, androgenic, anti-androgenic, and/or anti-mineralocorticoid activities **Table 1**. The most controversial and confusing of these activities is the androgenicity of certain

Introduction

progestins. Adding to the confusion is the fact that there appears to be several different forms of the progesterone receptors, usually called PR-A and PR-B, the difference being a sequence of amino-acids in the B-form that is not found in PR-A. Also biologically both forms have different specifications, interpreted by authors as: the PR-B is the “normal” receptor, the intermediate in the agonistic activity in several organs whereas the PR-A is capable of antagonising the effects stimulated by an activated PR-B. Relatively little is known yet on the composition of PR in different tissues during specific periods of development. Binding of the steroids to both forms is expected not to show differences as the steroid binding domain of both isoforms are identical.^{4, 8, 10, 20}

Progesterone derivative progestogens are similar to progesterone in that they are potent PR agonists, display weak affinity for the GR and have no detectable affinity for the ER. They differ though with respect to MR and AR binding. While progestogens of the 19-nortestosterone group show potent PR binding, only weak binding to the GR and MR receptors, virtually no detectable affinity for the ER, and have androgenic and anti-androgenic properties, The two most notable androgenic progestins are levonorgestrel and norethindrone.^{10, 20}

The desired biologic effect of progestins used in oral contraception (OC) is progestational activity, causing the endometrium to change from the proliferative to the secretory state. Undesired pharmacologic properties, such as androgenic activity, are not necessary for contraception and increase the potential for adverse effects (e. g., acne, hirsutism, weight gain, alterations in carbohydrate and lipoprotein metabolism, and hypertension). Consequently, there has been interest in synthesizing progestins that better mimic the natural hormone and attempts have been made to alter the current progestins to reduce the relative androgenicity.^{1, 21}

Introduction

Table (1): Biological activities of natural progesterone and synthetic progestins.⁸

Progestin	Progesto- genic	Anti- estrogenic	Estro- genic	Andro- genic	Anti- andro- genic	Gluco- corticoid	Anti- mineralo- corticoid
Progesterone	+	+	-	-	±	+	+
Dydrogesterone	+	+	-	-	±	-	±
Medrogestone	+	+	-	-	±	-	-
Chlormadinone acetate	+	+	-	-	+	+	-
Cyproterone acetate	+	+	-	-	++	+	-
Megestrol acetate	+	+	-	±	+	+	-
Medroxyprogesterone acetate	+	+	-	±	-	+	-
Nomegestrol acetate	+	+	-	-	±	-	-
Promegestone	+	+	-	-	-	-	-
Trimegestone	+	+	-	-	±	-	±
Drospirenone	+	+	-	-	+	-	+
Norethisterone	+	+	+	+	-	-	-
Lynestrenol	+	+	+	+	-	-	-
Norethinodrel	±	±	+	±	-	-	-
Levonorgestrel	+	+	-	+	-	-	-
Norgestimate	+	+	-	+	-	-	-
Etonogestrel	+	+	-	+	-	-	-
Gestoden	+	+	-	+	-	+	+
Dienogest	+	±	±	-	+	-	-

(+) effective; (±) weakly effective; (-) not effective.

Introduction

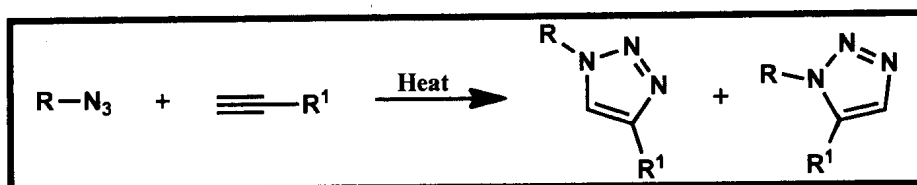
A selective progestin has progestational effects at relatively low concentrations or doses and androgenic effects at only relatively high concentrations or doses. The degree to which progestational activity is maximized and androgenic activity is minimized is a measure of a progestin's selectivity. The ratio of its affinity for progesterone receptors to its affinity for androgen receptors is the selectivity index. To minimize the androgenic side effects associated with the older progestins, the doses used in OCs have been reduced over the years. These dose reductions have decreased the potential for undesired androgenic effects but also have negatively affected cycle control thus the need for synthesizing new progestins with higher selectivity is an urgent need.²¹

1.3) Chemical aspects of click reaction

1.3.1) Preface :^{22, 23}

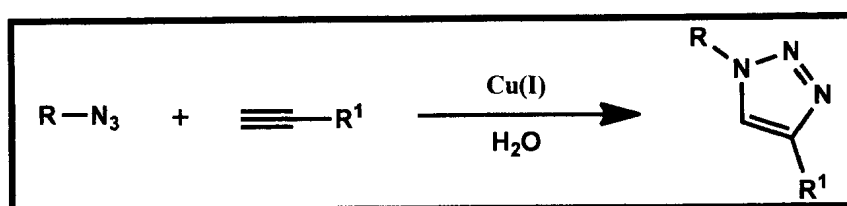
In 2001, Kolb, Finn and Sharpless defined the very useful and “green” concept of a “click” reaction, with the aim of binding two molecular building blocks together in a facile, selective, high-yield reaction under mild water-tolerant conditions with little or no by-products.

An examination of the azide-alkyne cycloaddition shows that it fulfills many of the prerequisites. Unfortunately, the thermal Huisgen 1,3-dipolar cycloaddition of alkynes to azides requires elevated temperatures and often produces mixtures of 1,4 and 1,5-disubstituted products when using asymmetric alkynes **Scheme 2**. In this respect, the classic 1,3-dipolar cycloaddition fails as a true click reaction.



Scheme (2): Huisgen 1,3-dipolar cycloaddition of alkynes to azides

A copper-catalyzed variant that follows a different mechanism can be conducted under aqueous conditions, even at room temperature. Additionally, whereas the classic Huisgen 1,3-dipolar cycloaddition often gives mixtures of regioisomers, the copper-catalyzed reaction allows the synthesis of the 1,4-disubstituted regioisomers specifically, **Scheme 3**.

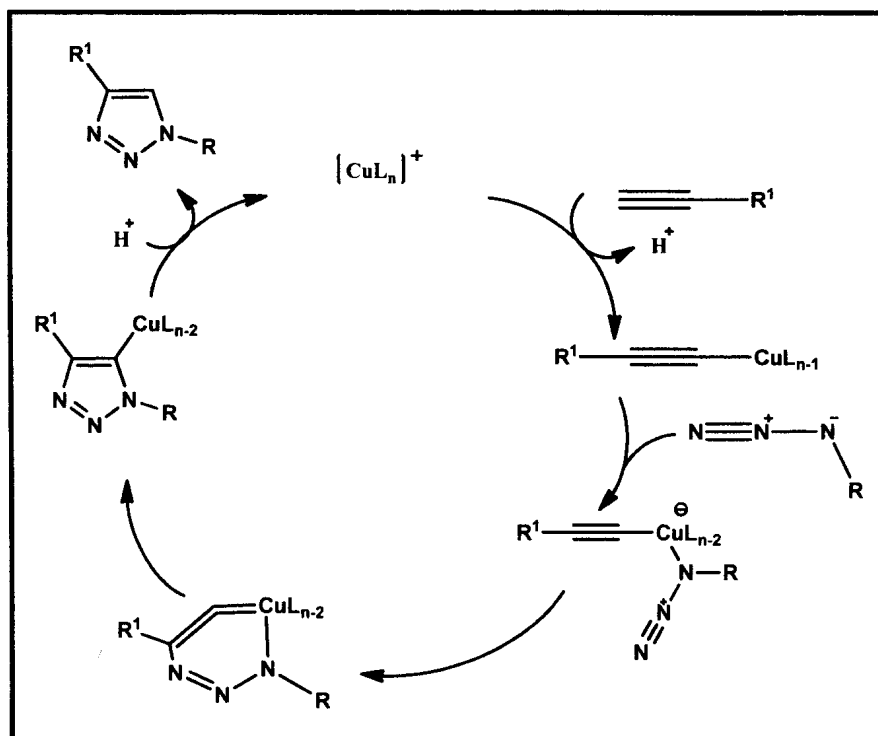


Scheme (3): Cu (I) -catalyzed azide/alkyne cycloaddition (CuAAC).

1.3.2) Mechanism of click reaction

The Cu (I)-catalyzed azide/alkyne cycloaddition (CuAAC) reaction proceeds via the following steps: **Scheme 4**

- 1- Copper acetylide formation via coordination of Cu (I) to the alkyne which is slightly endothermic in MeCN, but exothermic in water, which is in agreement with observed rate acceleration in water instead.
- 2- The azide displaces another ligand and binds to the copper.
- 3- Formation of six-membered copper (III) metallacycle.
- 4- Ring contraction to a triazolyl-copper derivative is followed by protonolysis that delivers the triazole product and closes the catalytic cycle.



Scheme (4): Cu (I)-catalyzed azide/alkyne cycloaddition (CuAAC) mechanism

1.4) Applications of click chemistry

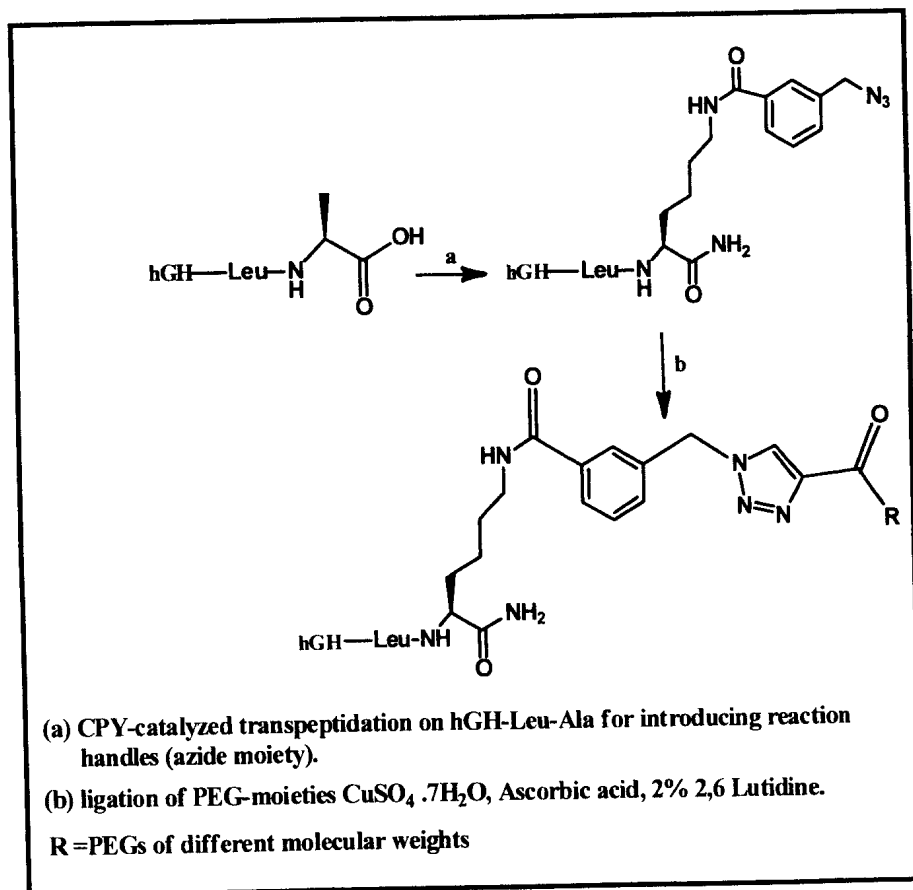
Click chemistry is a modular synthetic approach towards the assembly of new molecular entities. The wide scope of CuAAC is firmly demonstrated by its use in different areas of life such as drug discovery, bioconjugation, polymer and materials science and related areas including supramolecular chemistry.²⁴

1.4.1) Bioconjugation field

Bioconjugation refers to the covalent derivatization of biomolecules for several applications in research laboratories, industrial facilities, and medical clinics. Bioconjugation method should be highly site-specific and cause minimal perturbation to the active form of the biomolecule because poor control over the site of modification often results in loss of the biological function of the target biomolecule²⁵. Among the bioconjugation linkages, the click reaction is unique in that the azide moiety is absent in almost all naturally existing compounds, lacks reactivity with natural biomolecules, and consequently, only undergoes ligation with a limited set of partners. This click reaction utilizes functional groups that are mostly compatible with enzymes under physiologic conditions and can be readily incorporated into diverse organic building blocks.²⁶

Introduction

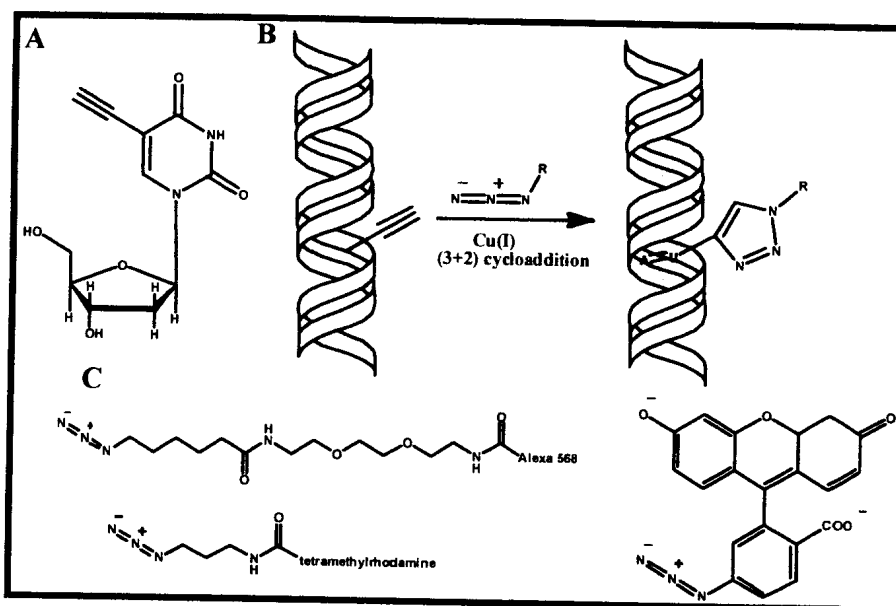
Two-step strategy was used for the preparation of C-terminally PEGylated hGH-derivatives. In the first step, a CPY-catalyzed transpeptidation was performed on hGH-Leu-Ala, introducing reaction handles, which were used in the second step for the ligation of PEG-moieties. Copper (I) catalyzed [2+3]-cycloaddition reactions were used for the attachment of PEG-moieties in order to increase its plasma half-life **Scheme 5**. The biological data show a dependency of the potency of the hGH-derivatives on both size as well as shape of the PEG-group.²⁷



Scheme (5): Preparation of C-terminally PEGylated hGH-derivatives.

Introduction

A new method to detect DNA synthesis in proliferating cells, based on the incorporation of 5-ethynyl-2-deoxyuridine (EdU) and its subsequent detection by a fluorescent azide through a Cu(I)-catalyzed [3+2] cycloaddition reaction (click chemistry) **Scheme 6**. Detection of the EdU label is highly sensitive and can be accomplished in minutes. The small size of the fluorescent azides used for detection results in a high degree of specimen penetration, allowing the staining of whole-mount preparations of large tissue and organ explants.²⁸



Scheme (6): (A) Structure of 5-ethynyl-2-deoxyuridine. (B) Schematic of the click reaction for detecting EdU incorporated into cellular DNA. (C) Structures of the fluorescent azides.

The applicability of azide-alkyne [3+2] cycloaddition reactions (click chemistry) for the immobilization of carbohydrates and proteins onto a solid surface was demonstrated, **Figure 2**. A poly (ethylene glycol) (PEG) linker carrying alkyne and cyclodiene terminal groups was synthesized and immobilized onto a functionalized glass slide via an aqueous Diels-Alder reaction. In the

Introduction

process, an alkyne-terminated PEGylated surface was provided for the conjugation of azide-containing biomolecules via click chemistry.²⁹

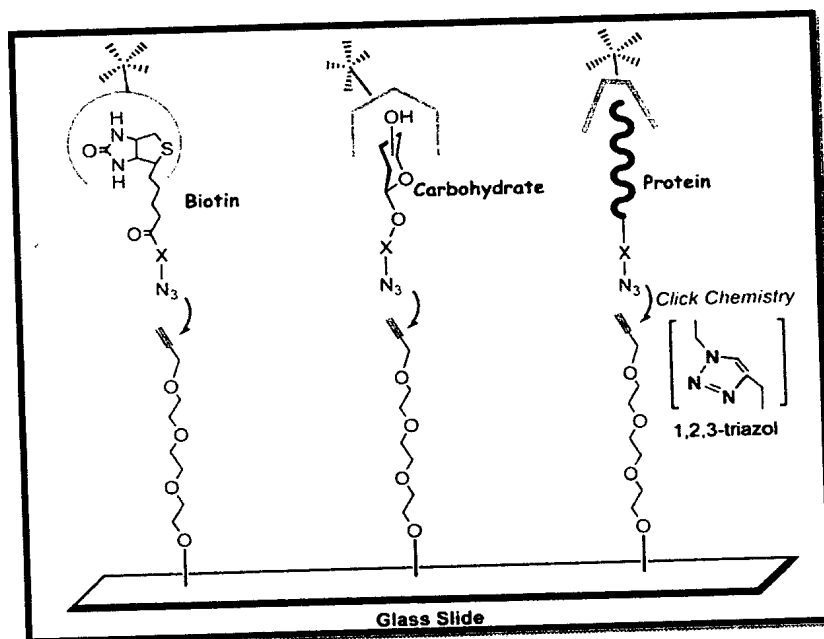


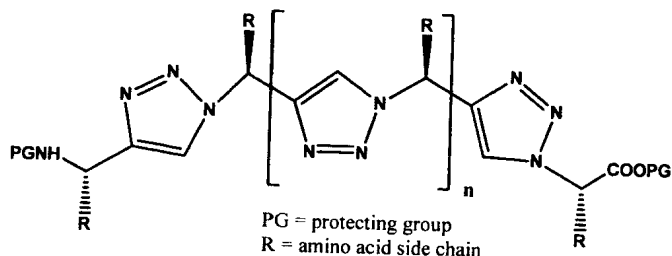
Figure (2): Biomolecules immobilization onto solid surfaces via click chemistry.

1.4.2) Polymer field

During the last decades, great efforts have been devoted to design polymers for reducing the toxicity, increasing the absorption, and improving the release profile of drugs. Advantage has been also taken from the inherent multivalency of polymers and dendrimers for the incorporation of diverse functional molecules of interest in targeting and diagnosis. The introduction of the click concept by Sharpless and coworkers in 2001 focusing the attention on modularity and orthogonality has greatly benefited polymer synthesis, an area where reaction efficiency and product purity are significantly challenged.³⁰

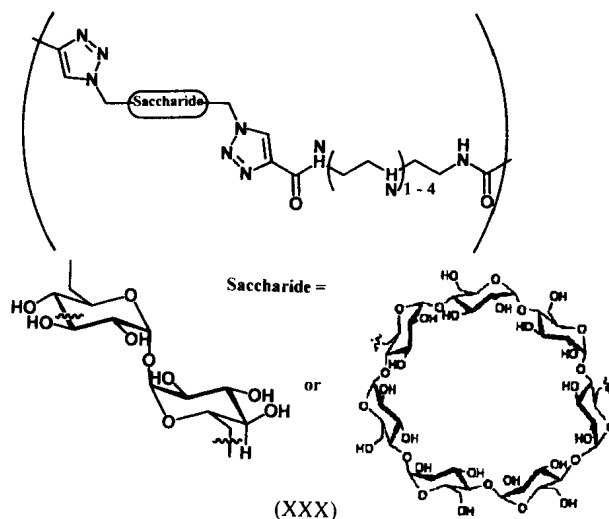
Introduction

The first biologically relevant polymers (XXIX) prepared by CuAAC presented by the group of Arora, in this work advantage was taken from the planar and polarized structure of triazols to prepare oligomers with similar properties to peptides but improved *in vivo* stability.³¹



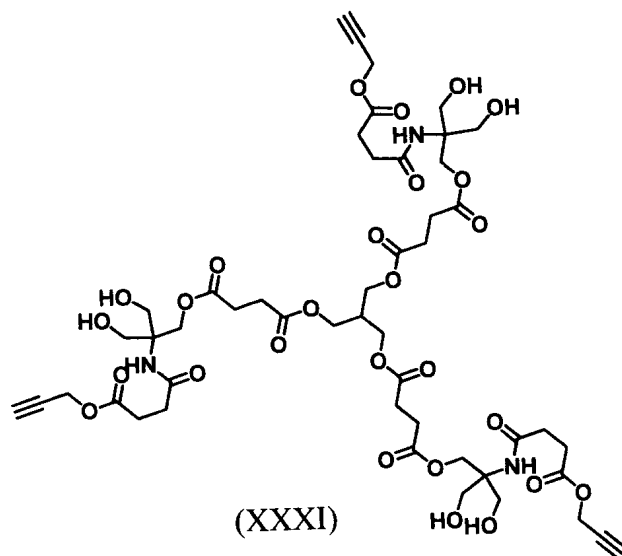
(XXIX)

Synthesis of high molecular weight polymers (XXX) (up to 331 kDa) that contain trehalose or cyclodextrin diazide monomers copolymerized with linear oligoamine monomers was described. The presence of carbohydrates was envisioned to grant biocompatibility, water solubility, and stability against aggregation. The oligoamine monomers facilitated DNA complexation and interaction with cell surfaces. Indeed, the carbohydrate-oligoamine copolymers prepared by this way exhibited low cytotoxicity and facilitated a high cellular uptake and gene expression in HeLa and H9c2 (2-1) cells.^{30, 32}

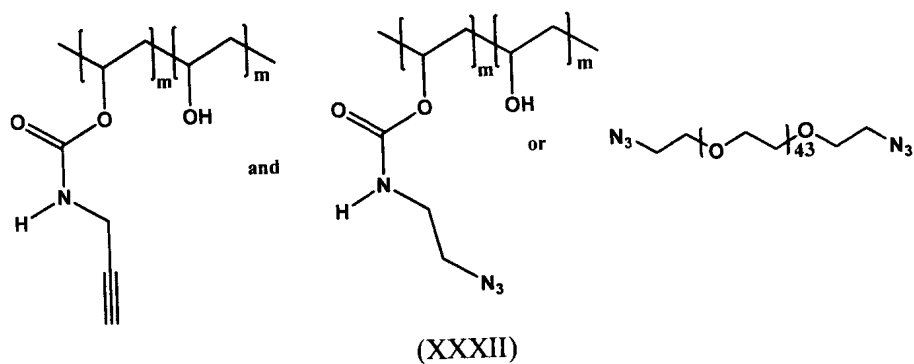


Introduction

The preparation of bifunctional dendrimers bearing up to 24 hydroxyl groups at the periphery and 21 internal alkyne/azide groups distributed throughout the dendrimer backbone was described. These dendrimers (XXXI) were amenable for further functionalization by means of CuAAC.³³



Poly vinyl alcohol (PVA) was modified either with azides or alkynes, producing two different polymers (XXXII) that yielded transparent hydrogels upon mixing in the presence of CuSO₄/ascorbate.^{30, 34}

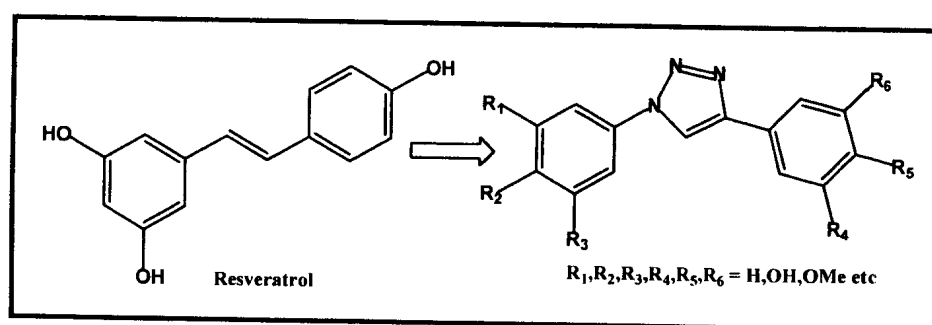


1.4.3) Drug discovery field

The emerging field of click chemistry offers a unique approach to the synthesis of 1,2,3-triazole-containing molecules. 1,2,3-Triazole moieties are attractive connecting units because they are stable to metabolic degradation and capable of hydrogen bonding, which can be favorable in the binding of biomolecular targets and can improve the solubility. The basic heterocyclic rings present in the various medicinal agents are mainly 1,2,3-triazole or 1,2,4-triazole. A large volume of research has been carried out on triazole and their derivatives, which has proven the pharmacological importance of this heterocyclic nucleus.

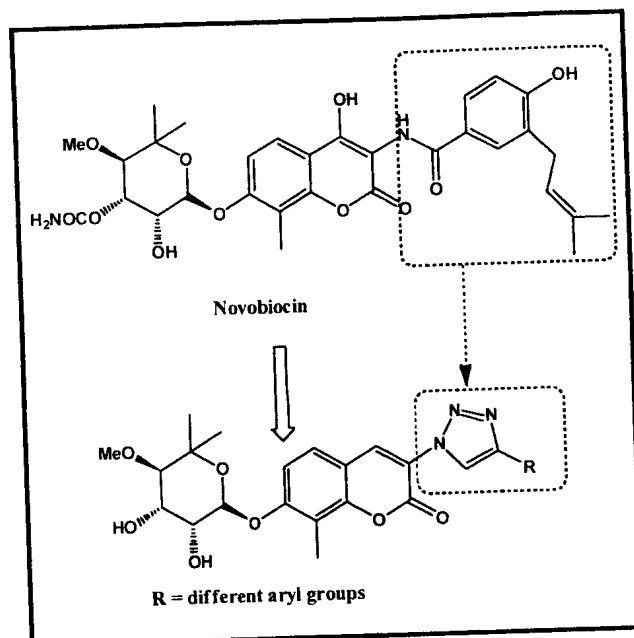
1.4.3.1) Antiproliferative activity

Many triazole derivatives of resveratrol (stilbenoid, natural phenol) were synthesized by means of a parallel combinatorial approach that used a typical click reaction. Some of these compounds exhibited antiproliferative activity,³⁵ **Scheme 7**



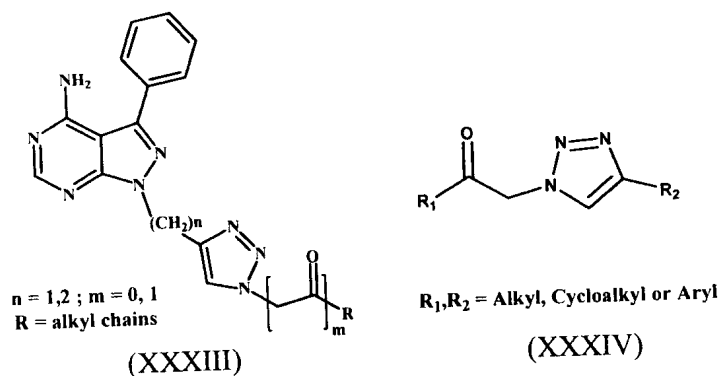
Scheme (7): Triazole derivatization of resveratrol.

A series of triazole-containing novobiocin analogues has been designed, synthesized and their inhibitory activity determined. These compounds contain a triazole ring in lieu of the amide moiety present in the natural product. The antiproliferative effects of these compounds were evaluated against two breast cancer cell lines (SKBr-3 and MCF-7), and manifested activity similar to their amide-containing counterpart **Scheme 8**.³⁶



Scheme (8): Triazole derivatization of novobiocin.

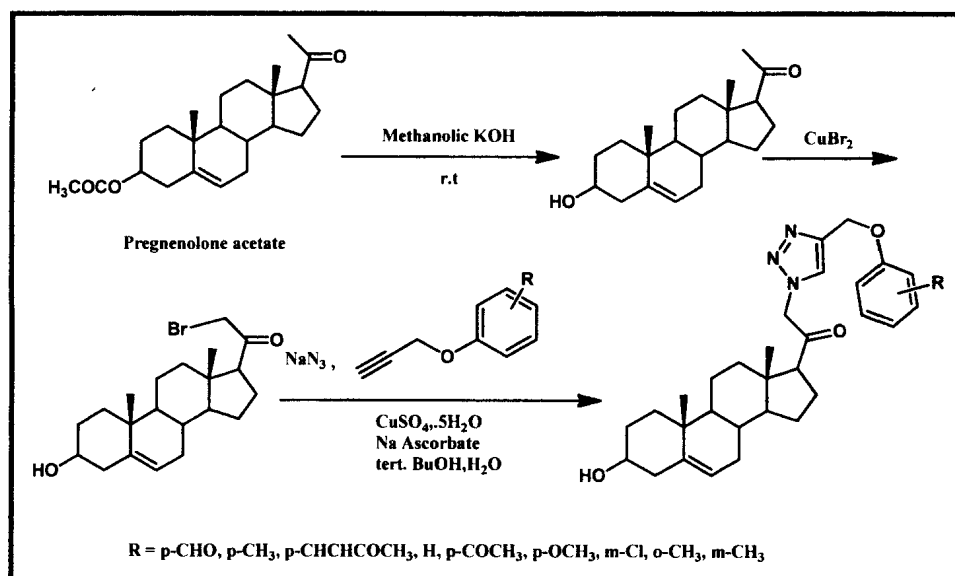
Two classes of 1,4-disubstituted 1,2,3-triazoles (XXXIII) and (XXXIV) were synthesized using a click chemistry approach. Some derivatives exhibited modest Src kinase inhibitory activity.^{24, 37}



A facile synthesis of 21-triazolyl derivatives of pregnenolone, **Scheme 9** and their potential antitumor activity is reported.³⁸ The scheme involves the transformation of the starting pregnenolone acetate into pregnenolone, which is

Introduction

converted to 21-bromo pregnenolone and finally the one-pot, two-step in situ conversion of the bromo derivative to the 21-triazolyl pregnenolone using the 'click chemistry' approach. These derivatives were screened for their anticancer activity against seven human cancer cell lines. Some of these derivatives exhibited significant anticancer activity.



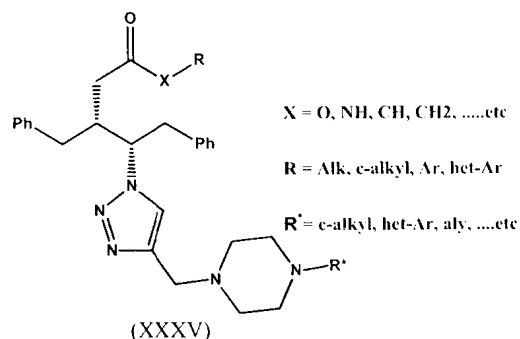
Scheme (9): Synthesis of 21-triazolyl derivatives of pregnenolone

1.4.3.2) Antiviral activity

A novel series of potent human immunodeficiency virus type 1 protease (HIV-1-Pr) inhibitors (XXXV) has been developed. The copper (I)-catalyzed azide-alkyne cycloaddition (CuAAC) was used to unite a focused library of azide-containing fragments with a diverse array of functionalized alkyne-containing building blocks. In combination with direct screening of the crude reaction products, this method led to the rapid identification of a lead structure and readily enabled optimization of both azide and alkyne fragments and obtaining these compounds exhibited high binding efficiency to human immunodeficiency virus type-1 protease (HIV-1-Pr). Replacement of the triazole with a range of alternative

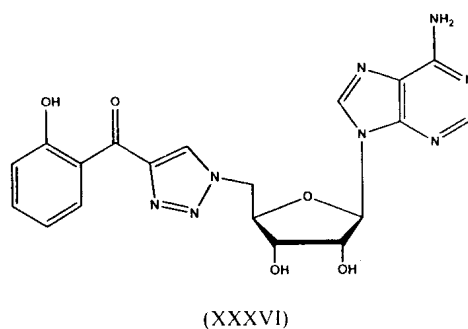
Introduction

linkers led to greatly reduced protease inhibition; however, further functionalization of the triazoles at the 5-position gave a series of compounds with increased activity.³⁹



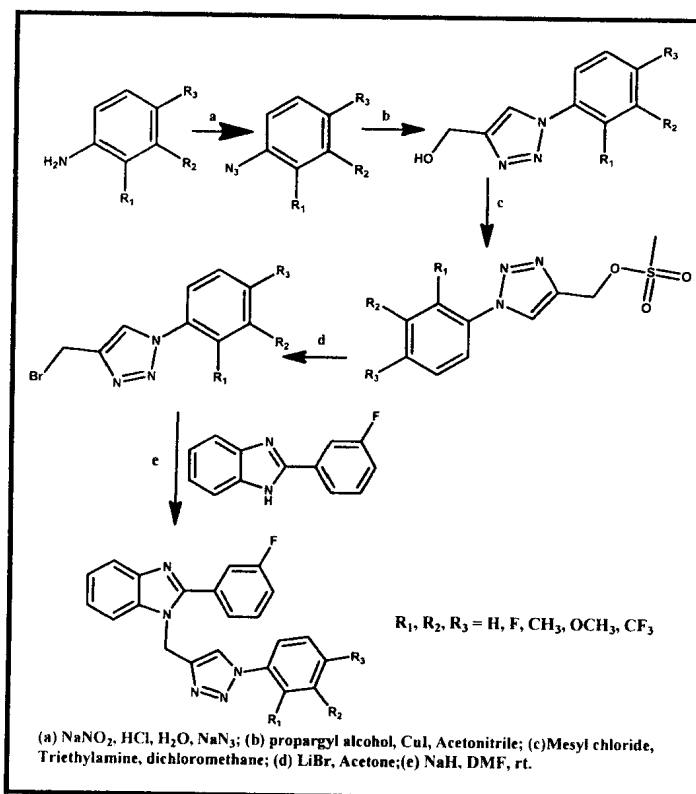
1.4.3.3) Antitubercular activity

Somu et al. reported the synthesis of a rationally designed nucleoside (XXXVI) using click reaction. This compound was found to be inhibitor of *Mycobacterium tuberculosis* that disrupts siderophore biosynthesis. The activity is due to inhibition of the adenylate-forming enzyme MbtA, which is involved in biosynthesis of the mycobactins.^{24, 40}



On the basis of promising results of the preliminary study, novel *Mycobacterium tuberculosis* H37Rv strain inhibitors with fluorine and 1,2,3-triazole containing benzimidazoles for the treatment of tuberculosis were disclosed by Gill et al.⁴¹ First a series of 4-(bromomethyl)-1-substituted-phenyl-1H-[1,2,3]-

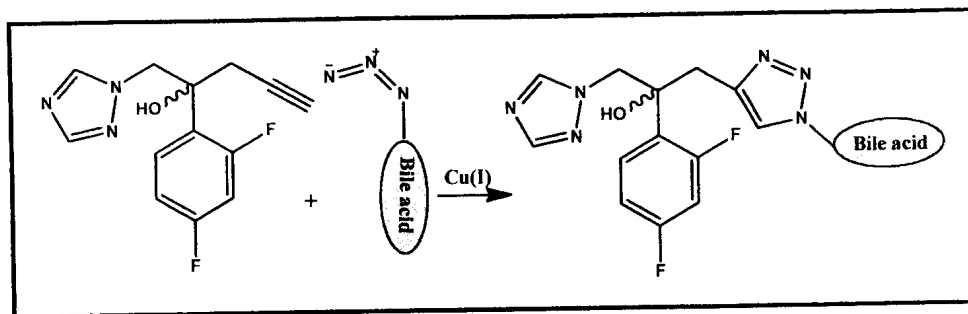
triazole was prepared and then condensed with 2-(3-fluorophenyl)-1H-benzimidazole, **Scheme 10**



Scheme (10): Synthesis of 2-(3-fluorophenyl)-1-[1-(substituted phenyl)-1H-[1,2,3]-triazol-4-yl methyl]-1H-benzimidazole derivatives.

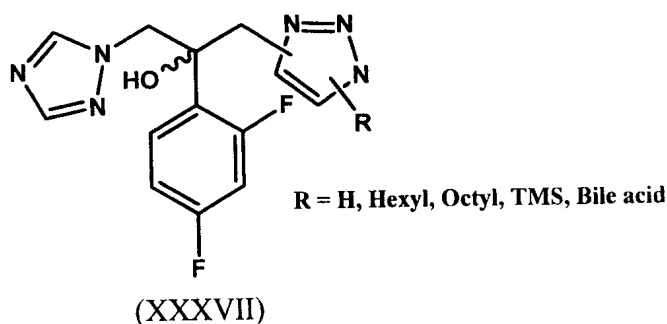
1.4.3.4) Antifungal activity

Novel fluconazole/bile acid conjugates were designed and their regioselective synthesis was achieved in very high yield via Cu(I) catalyzed intermolecular 1,3-dipolar cycloaddition, **Scheme 11**. These new molecules showed very good antifungal activity against *Candida* species with MIC values ranging from 3.12 to 6.25 mg mL^{-1} . In this conjugate, the bile acid part acts as a drug carrier and the fluconazole part acts as an inhibitor of 14α -demethylase enzymes in the fungal cell.⁴²



Scheme (11): Synthesis of fluconazole/bile acid conjugate.

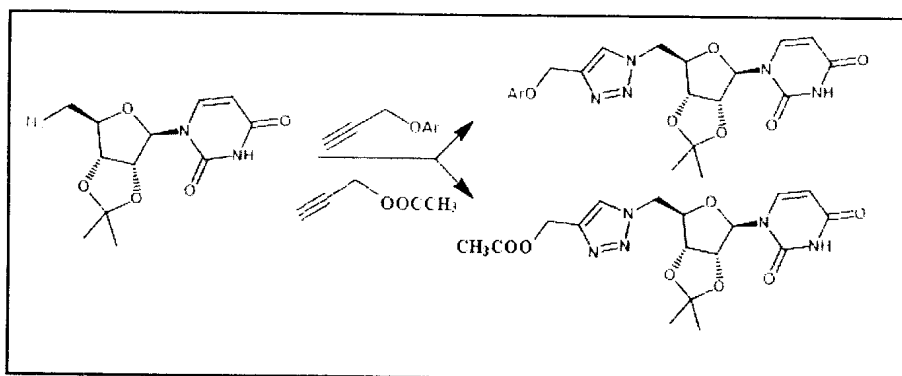
Fluconazole based novel mimics containing 1,2,3-triazole (XXXVII) were designed and synthesized as antifungal agents. Their antifungal activity was evaluated *in vitro* by measuring the minimal inhibitory concentrations (MICs). Some derivatives were found to be more potent against *Candida* fungal pathogens than control drugs fluconazole and amphotericin B. Furthermore, these molecules were evaluated *in vivo* against *Candida albicans* in Swiss mice and also their antiproliferative activity was tested against human hepatocellular carcinoma Hep3B and human epithelial carcinoma A431. It was found that these compounds resulted in 97.4% reduction in fungal load in mice and did not show any profound proliferative effect at lower dose (0.001 mg/ml).⁴³



Chaudhary et al.⁴⁴ synthesized several novel 1,4-disubstituted-1,2,3-triazolyluridine derivatives by means of a click chemistry approach, **Scheme 12**.

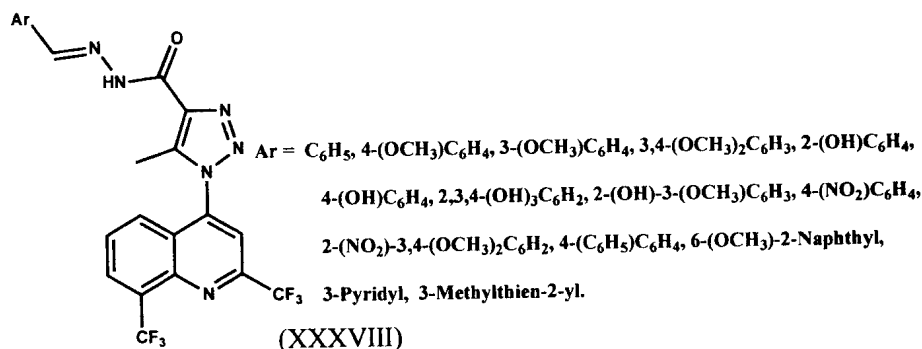
Introduction

Most of which showed significant antifungal activity. One of the compounds showed potent antifungal activity against *C. neoformans* with a MIC of 8mg/mL (0.018mg/mL for Fluconazole). Some other compounds in the series showed antifungal activity with MIC values of 24–32mg/mL (0.048–0.067mg/mL for Nikkomycin) against *C. albicans*. These compounds were proposed as leads chitin synthase inhibitors for further modifications. They also have potential for applications in health care and in agriculture.



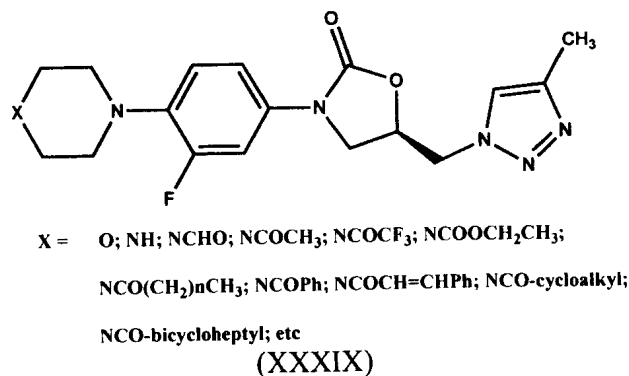
Scheme (12): Novel 1,4-disubstituted-1,2,3-triazolyluridine derivatives tested as antifungal agents.

Sumangala and co-workers⁴⁵ synthesized a series of 1,2,3-triazole-containing quinoline (XXXVIII). They studied their antimicrobial and antifungal activity by using cyclopiroxolamine as standard antifungal agent. Investigation of the structure activity relationships revealed that the nature of the substituent on the 4-position of the triazole ring influences the antimicrobial activity. Most of the newly synthesized compounds showed significant antimicrobial activity at a concentration of 6.25 $\mu\text{g mL}^{-1}$.



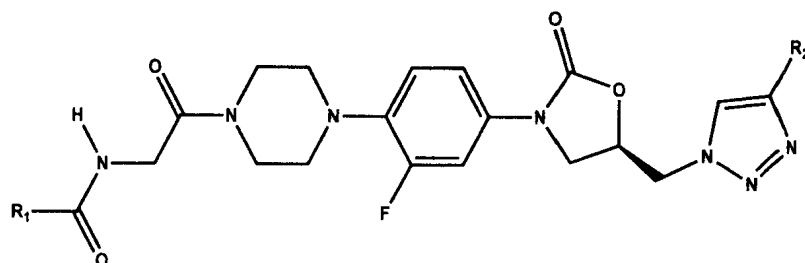
1.4.3.5) Antibacterial activity

A series of 5-(4-methyl-1,2,3-triazol-1-yl)methyl oxazolidinones (XXXIX) were synthesized by Phillips and co-workers.⁴⁶ The synthesized compounds then tested for their antibacterial activity against a panel of Gram-positive and Gram-negative clinical isolates in comparison with linezolid and vancomycin. Most of the compounds demonstrated strong to moderate *in vitro* antibacterial activity against susceptible and resistant Gram-positive pathogenic bacteria. The observed antibacterial activity varied with substitutions at the phenyl C4 position with bulky alkylcarbonyl and alkoxy carbonyl substitutions on the piperazine N4. Whereas the presence of the 4-methyl-1,2,3-triazole moiety in the acyl-piperazine containing analogs resulted in increased protein binding, and decreased antibacterial activity particularly against *Streptococcus pneumoniae* strains.



Introduction

Phillips and co-workers⁴⁷ also synthesized a series of 1H-1,2,3-triazolyl piperazino oxazolidinone analogs (XXXX) with optionally varied glycinyl substitutions. Their antibacterial activity was assessed against a panel of susceptible and resistant Gram-positive and selected Gram-negative bacteria including clinical isolates.



R_1 = Alkyl, halogenated alkyl, cycloalkyl, phenyl, heteroaryl;

R_2 = H, CH₃

(XXXX)

2. SCOPE OF INVESTIGATION

2. SCOPE OF INVESTIGATION

Steroidal compounds are widely existent in natural world and display a variety of biological activities. Beside the naturally occurring substances, the majority of steroidal drugs are semi-synthetic compounds. Increasing the selectivity and minimizing the side effects are still the priority of the medicinal chemists.⁴⁸

In the past decade, an extensive focus of research was directed towards the rational modifications of steroidal molecules. Steroidal molecules with a hetero atom (N, O or S) in ring A and D showed a wide range of biological activities such as anti-microbial, anti-inflammatory, anti-tumor, hypocholesterolemic and diuretic activities. As a result, variety of heterocyclic units such as pyrazoles, pyrazolines, isoxazoles, isoxazolines, thiazoles, and thiadiazoles were introduced into the steroidal backbone.^{38, 49-53}

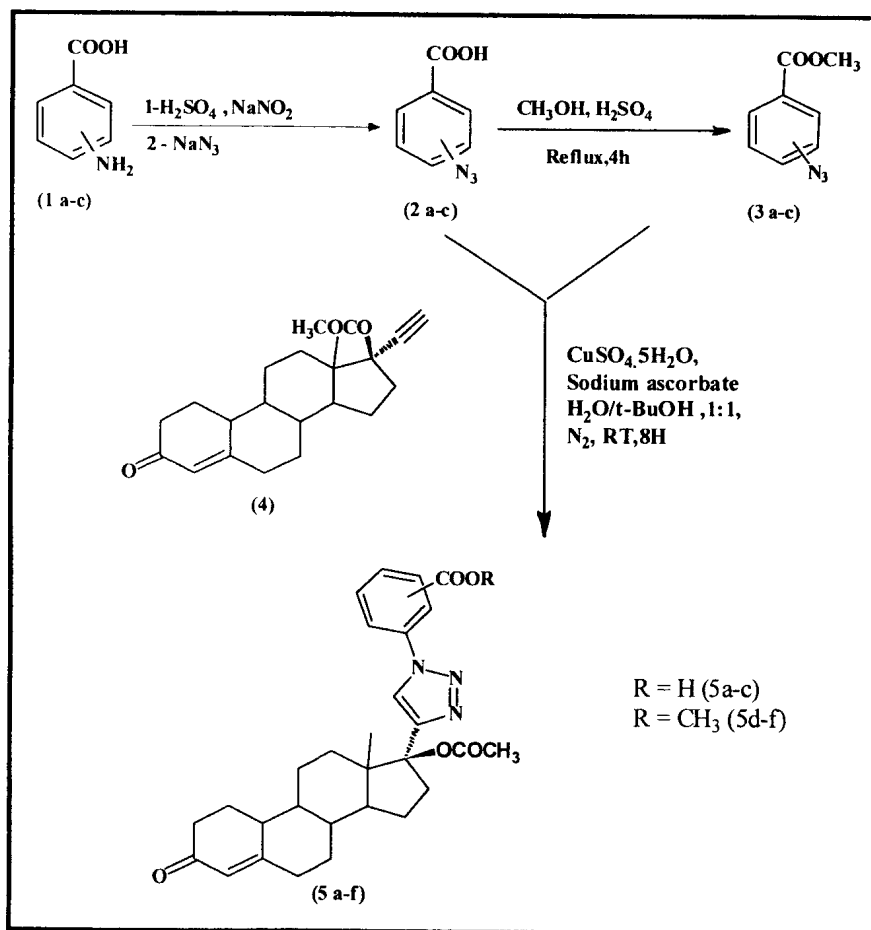
The basicity and hydrophilicity of an azole in theory might alter the biological function of a steroid. Moreover, the azole ring might interact with some enzymes, e.g. cytochrome P450. In addition, steroidal azoles have also been found to be potent inhibitors of 17 α -Hydroxylase/C17,20 Lyase, the enzyme which catalyzes the conversion of progesterone and pregnenolone into the androgens. Since androgens are implicated in the etiology of number of androgen dependant diseases, e.g. prostate cancer, inhibitors of such enzymes are useful for the treatment of these diseases. Steroidal azoles have also been found to have strong inhibitory effect on 5 α -reductases which makes them promising agents against various types of tumors.^{38, 54}

It was reported that nuclear receptors such as progesterone receptor pockets can rearrange to accommodate different agonists.⁵⁵ Accordingly

Scope of Investigation

the PR potency & selectivity of synthetic steroid agonist can be enhanced by even larger chemical moieties at 17 α -position of steroid backbones.⁵⁶

Based on these finding, we were endeavored to design and synthesize novel hybrid molecules through insertion of substituted 1,2,3- triazole moiety at a strategic position of steroidal nucleus, 17 α -position, and biologically evaluate their activity in the aim that they will be new candidates as progestational and anticancer agents. Click reaction will be used for the synthesis of the target compounds (5a-f), Scheme 13.



Scheme (13): Design of the novel steroidal azoles using click reaction.

Scope of Investigation

The objectives of the designed compounds **5(a-f)** are:

1- Enhancing the binding characters of the steroidal molecule such as hydrogen bonding, ionic and lipophilic interactions through linking of substituted 1,2,3-triazole moiety at 17 α of steroidal nucleus. 1,2,3-triazole possess a strong dipole moment, an aromatic character and a good hydrogen-bond-accepting ability. Furthermore, they are very stable to both metabolic and chemical degradations, being rather inert to severe hydrolytic, oxidizing and reducing conditions, even at high temperatures.⁵⁷

2- In addition, the added moiety plays a significant role to alter the physicochemical properties of the steroid such as lipophilicity, solubility, topological polar surface area (TPSA) and molecular volume, which can be studied with chemical computing software, that in turn affect the biological characters of molecules.

3- Furthermore, insertion of carboxylic moiety at different positions of phenyl nucleus is considered as water solubility enhancer of the highly lipophilic steroidal molecule through salt formation with a suitable counter base.

Our design strategy for selection of new scaffolds was based on molecular docking study in which a large number of azides with different substituents at different positions was suggested and the resulted triazoles were *in-silico* examined against the progesterone receptor (PR) using MOE software. Triazoles that showed a good binding with the essential amino acids of the active site of the receptor were selected for laboratory synthesis.

In vivo progestational activity study will be carried to evaluate the progestational activity and potency of the novel compounds. In addition,

Scope of Investigation

in vitro anticancer activity study will be carried out to evaluate the predicted anticancer activity.

Further, molecular docking study of the novel compounds will be carried to PR to verify the biological evaluation results and show the binding mode with the receptor.

Finally *in silico* computing of the physicochemical properties of the novel compounds will be carried out to evaluate the alteration of these Properties due to the structural modification.

3. RESULTS AND DISCUSSION

3.1. CHEMISTRY

3) RESULTS AND DISCUSSION

3.1) CHEMISTRY

3.1.1) Synthesis of *o*-, *m*-, and *p*-azido benzoic acids (2a-c):

Generally, organic azides may be prepared through five different methods⁵⁸, **Figure 3**:

- Insertion of the azido group (N₃) (substitution or addition).
- Insertion of a diazo group (N₂) (diazo transfer).
- Insertion of a nitrogen atom (diazotization).
- Cleavage of triazines and analogous compounds.
- Rearrangement of azides.

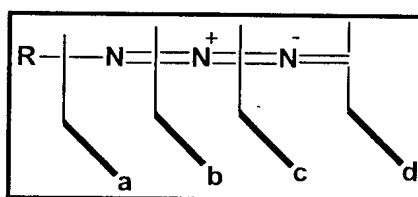


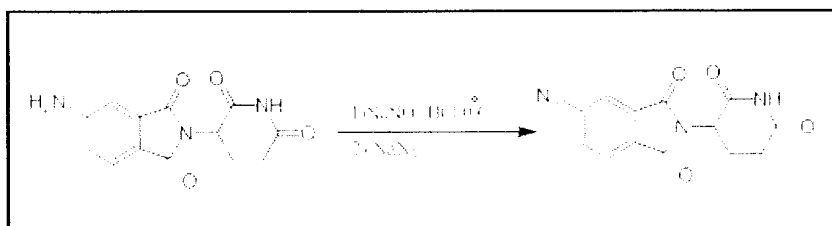
Figure (3): General methods for preparation of azides

1- Aryl Azides from Diazonium Compounds

Aryl diazonium salts react directly without catalysts with azide ions to form the corresponding aryl azides. Alkali azides or trimethylsilyl azide act as source of the azido group. Unlike the Sandmeyer reaction, this reaction does not take place with cleavage of the C-heteroatom bond but occurs through attack of the azide on the diazonium ion with formation of the intermediate pentazenes and

pentazoles then these intermediates lose nitrogen and the corresponding azides are obtained at low reaction temperatures^{58,59}.

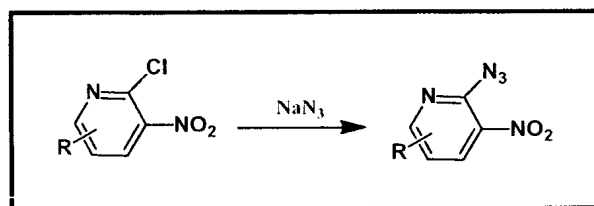
e.g. azido-thalidomide⁶⁰, **Scheme 14**.



Scheme (14): Synthesis of azido-thalidomide

2-Nucleophilic Aromatic Substitution

Activated aromatic systems such as fluoro- and chloronitro arenes⁶¹ and few heteroaromatic systems⁶² can undergo nucleophilic substitution by azide ions. They are generally sufficiently nucleophilic to produce aryl azides in good yields. e.g. azidonitropyridines from chloronitropyridines⁶³, **Scheme 15**.

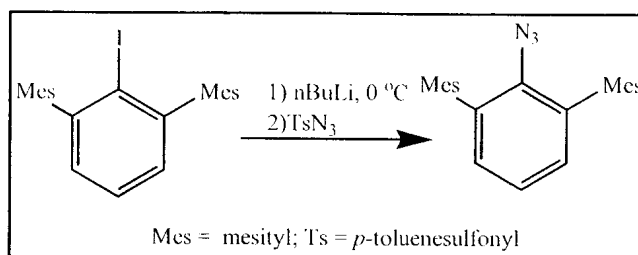


Scheme (15): Synthesis of azidonitropyridines

3. Aryl Azides from Organometallic Reagents

Numerous methods for the preparation of aryl azides with organometallic reagents have been developed. For example, tosyl azide reacts with Grignard or lithium reagents to form novel aryl azides⁵⁸. Accordingly dimesityl phenyl azide was prepared via reaction of 2,6-dimesitylphenyliodide with nBuLi at 0 °C in hexane

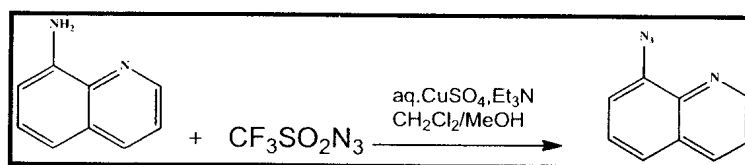
and the resulting lithium salt was treated with *p*-toluenesulfonyl azide to provide 2,6-dimesitylphenyl azide⁶⁴ **Scheme 16**.



Scheme (16): Preparation of dimesityl phenyl azide

4- Aryl Azides by Diazo Transfer

Aryl and heteroaryl azides may be prepared by the reaction of aromatic/heteroaromatic amines with triflyl azide. The mild reaction conditions and very high yields, make these transformations the method of choice for the preparation of numerous aromatic azides. e.g. 8-azidoquinoline from 8-aminoquinoline.⁶⁵ **Scheme 17**.



Scheme (17): Preparation of 8-azidoquinoline

5- Aryl Azides from Nitrosoarenes

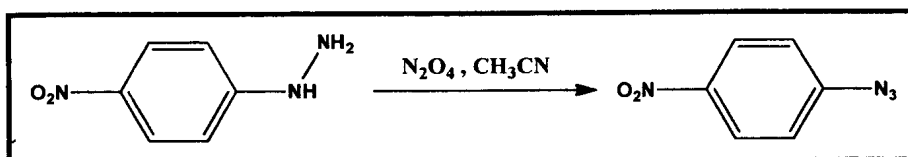
The reaction of nitrosoarenes with hydrogen azide leads to formation of aryl azides in good yields. However, the diazonium ions must first be formed and then treated with azide ions as the second step; thus, 2 equivalents of hydrogen azide are required.⁵⁸

6-Diazotization of Hydrazines

The reaction of hydrazines with nitrosyl ions or their precursors is a well-established procedure that is equally suitable for the preparation

Results & Discussion, Chemistry

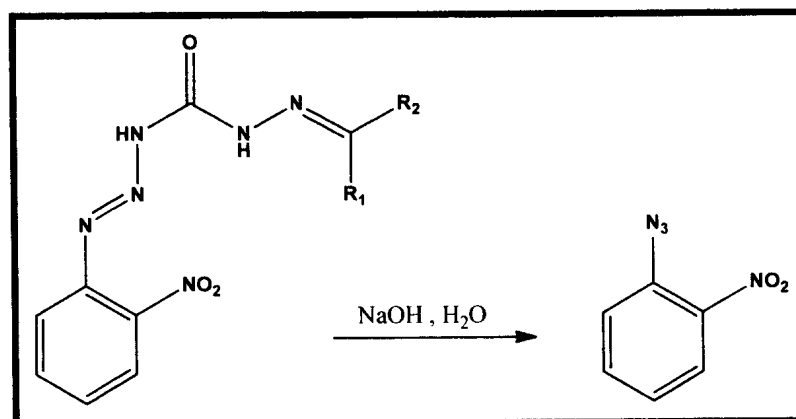
of different classes of compounds such as aromatic and aliphatic azides, acyl azides, and sulphonyl azides. Dinitrogen tetroxide, mixtures of nitrogen oxide/oxygen, nitrosylsalts and sodium nitrite are particularly suitable. **Scheme 18.**^{58, 66}



Scheme (18): Conversion of p-nitrophenyl hydrazine into corresponding azide.

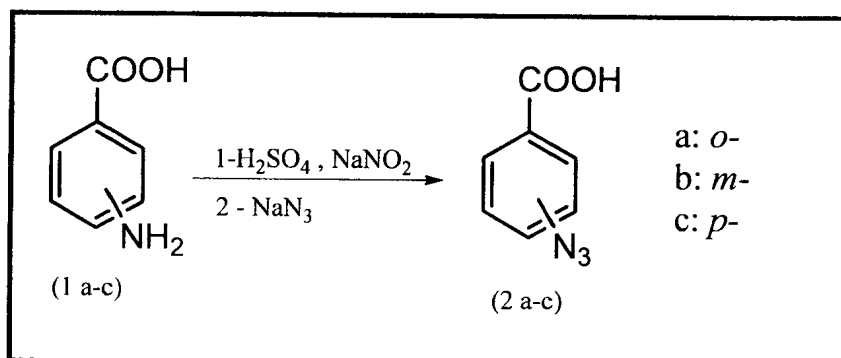
7- Modification of Triazenes and Related Compounds

An older method for the preparation of azides is based on the rearrangement of triazenes into azides. In particular, the base-induced cleavage of triazene derivatives can be used for the preparation of azides **Scheme 19.**⁵⁸



Scheme (19): Synthesis of the aryl azide from the semicarbazone derivatives

In the present investigation benzoic acid azides (**2a-c**) were prepared by diazotization of the corresponding commercially available aminobenzoic acids (**1a-c**) with sodium nitrite in presence of sulphuric acid at 0-5°C, followed by azidation of the resulting diazonium salts with sodium azide as reported⁶⁷ **Scheme 20**.



Assignment of the structures of compounds (**2a-c**) was confirmed by comparing its physical and spectroscopic data (IR and ¹H-NMR) with the literature one.⁶⁸

The IR spectra of the prepared azido benzoic acids (**2a-c**) revealed broad absorption bands respectively at 3670-3060, 3625-3380 and 3755-3090 cm⁻¹ attributed to their OH groups. Strong absorption bands at 1684, 1647, 1668 cm⁻¹ are assigned to stretching vibrations of carbonyl groups. The appearance of absorption bands at 2100, 2345, 2095 cm⁻¹ was assigned to the asymmetric stretching vibrations of N=N⁺=N⁻ (N₃) groups.

Comparing the ¹H-NMR spectra of compounds (**2a-c**) revealed the absence of a broad hump at δ 6.19- 5.13 ppm in the spectra of (**1a-c**) which indicated the transformation of NH₂ to azido group. Broad singlet signals at δ 11.21, 9.16, 8.63 ppm exchangeable with D₂O were assigned

Results & Discussion, Chemistry

for COOH protons. Furthermore the aromatic protons appeared either as multiplet signals at 7.42-7.09 ppm (H3,5), 7.81- 7.42 ppm (H4) and 8.29-8.03 ppm (H6) for compound **2a**, or as one multiplet signal at 8.09-7.13 ppm integrated for 4 protons (H2,4-6) for compound **2b** or as a pair of doublets at δ 7.33 - 7.03 ppm (H3,5) and δ 8.29 - 7.93 ppm (H2,6) for compound **2c**, **Figure 4**

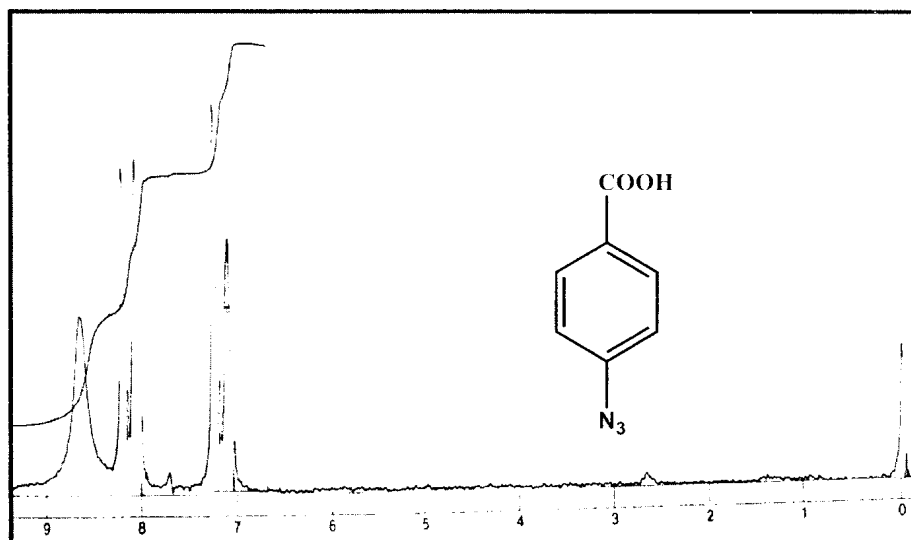
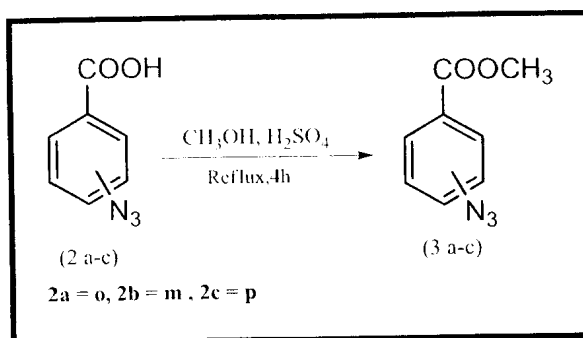


Figure (4): ¹H-NMR spectrum of compound (**2c**)

3.1.2) Synthesis of methyl azidobenzoates (**3a-c**):

Preparation of methyl azidobenzoates (**3a-c**) was achieved via esterification of the corresponding acids (**2a-c**) by refluxing with absolute methanol in presence of concentrated sulphuric acid, **Scheme 21**. The yields of the products were 63%- 80%. Methyl *o*-azidobenzoate showed the lowest yield (63%) whereas the *p*-isomer gave the highest yield (80%). This may be attributed to the steric effect of azido moiety on the neighboring carboxyl.



Scheme (21): Synthesis of compounds (3a-c)

Assignment of the structure of compounds (3a-c) was confirmed by comparing their physical and spectroscopic data (IR and $^1\text{H-NMR}$) with the reported ones.^{69, 70}

Comparison of the IR spectra of the prepared methyl azidobenzoate (3a-c) with their precursor acids (2a-c), revealed the disappearance of the broad absorption band at $3755\text{-}3060\text{ cm}^{-1}$ attributed to carboxylic OH group. Moreover, the absorption band of carbonyl group of the azidobenzoate esters were shifted to $1715\text{ - }1710\text{ cm}^{-1}$ compared with their corresponding acids ($1684\text{-}1647\text{ cm}^{-1}$), **Figure 5**.

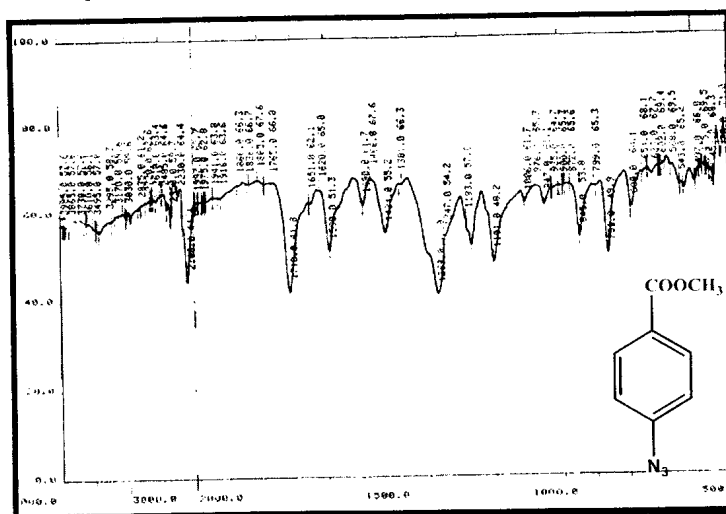


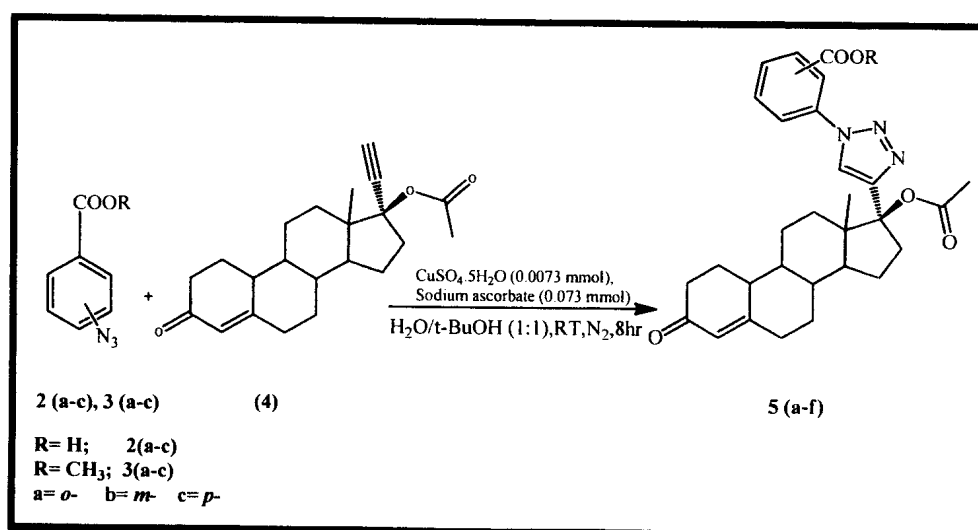
Figure (5): IR spectrum of compound (3c)

Results & Discussion, Chemistry

¹H-NMR spectra of compounds (**3a-c**) revealed the disappearance of the broad singlet signal of COOH protons in (**2a-c**) and appearance of singlet signal at δ 3.89, 3.86 and 3.86 ppm integrated for 3 protons, assigned for methyl protons. The aromatic protons appeared either as multiplets at δ 8.00- 6.93 and 7.73- 6.83 ppm for compound **3a** and **3b** respectively or as pair of doublets at δ 7.33- 7.00 and 8.06- 7.76 ppm for compound **3c**.

3.1.3) Synthesis of 17 α -(1-substituted-1,2,3-triazol-4-yl)-19-nortestosterone acetates (**5a-f**)

The target compounds (**5a-f**) were prepared using click reaction through cycloaddition of norethindrone acetate (**4**) with the respective azide (**2a-c** and **3a-c**), **Scheme 22**. Copper catalyzed azide/alkyne cycloaddition reaction has become very popular as a “click reaction” since it facilitates stereoselective formation of 1, 4-disubstituted triazoles and produces high yield under mild water tolerant conditions with little or no by products.



Scheme (22). Synthesis of compounds (**5a-f**)

Results & Discussion, Chemistry

In our investigation several attempts were tried for optimization of the conditions required to keep the catalytic capacity of Cu (I) in the reaction for preparation of 1, 4 disubstituted isomer. Copper (I) chloride was first used as a direct source of Cu (I), however air oxidation to Cu (II) and the partial solubility of Copper (I) in water restricted its use. In-situ formation of Cu (I) from copper sulphate pentahydrate together with a reducing agent, sodium ascorbate, was also tried to inhibit the air oxidation to Cu (II) or Cu⁰ compounds. Ten equivalents sodium ascorbate in a mixture of water and t-BuOH according to Fokin and Sharpless procedures was used. Furthermore, the reaction performed under nitrogen condition to prevent air oxidation to Cu (II).

A variety of solvents was tried, for example water/ DMSO mixture was used, but difficult separation of the product from this solvent restricted its use. Also a water/ ethanol mixture was tried as an attempt for yield improvement of some derivatives, however no significant increase in the yield was observed. The use of water only as a solvent was reported²³ for the CuAAC reaction, but in the present investigation it was unsuitable because both the azides and norethindrone acetate were highly water insoluble. The most commonly used mixture of solvents is water/ t-BuOH (1:1) which solubilized the substrate and retained favorable aqueous media.

The Cu (I)-catalyzed azide-alkyne cycloadditions are normally performed at room temperature but in some cases additional heating has an accelerating effect. Similarly, microwave irradiation and sonication can dramatically reduce the reaction times without affecting the yields or the formation of undesired side reactions⁷¹. In our work heating was used to accelerate the synthesis of compound **5c** but a great decomposition of the reaction constituent was observed as demonstrated by TLC

Results & Discussion, Chemistry

monitoring. Sonication was also tried in the preparation of compound **5a**; this led to transformation of the azide **2a** to the respective amine as demonstrated by TLC monitoring. So stirring at room temperature with increasing of the reaction time was adopted for preparation of our targets (**5a-f**).

With regard to the reaction yields, it was reported that the reaction is not significantly affected by the steric and electronic properties of the groups attached to the azide and alkyne centers. Electron-deficient, electron-rich, aliphatic, aromatic, and heteroaromatic azides usually react well with variously substituted terminal alkynes⁷². The reaction proceeds in many protic and aprotic solvents, including water, and is unaffected by most organic and inorganic functional groups⁷². On the other hand other publications concluded that the fastest reactions were observed for azides with electron-withdrawing and less sterically congested azides⁷³.

Accordingly, in the present investigation aromatic azides with electron withdrawing group at *o*, *m* and *p* position were selected. An obvious variation in the product yields was observed. Triazoles **5a** and **5d** derived from ortho azidobenzoic acids and its methyl ester showed the lowest yield (45-50%) comparing to their meta and para congeners. This may be attributed to steric congestion due to ortho substitution.

Four equivalents of azides with one of the steroid were used to ensure complete consumption of the highly expensive hormone during the reaction time and to avoid its loss as much as possible. Column chromatography was used to get rid of the excess azide.

The structures of the compounds (**5a-f**) were confirmed by IR, ¹H-NMR, and ¹³C-NMR for certain derivatives.

Results & Discussion, Chemistry

The IR spectra of the prepared compounds (**5a-c**) **Table 2** revealed broad absorption bands at $2530-3695\text{ cm}^{-1}$ attributed to OH group, where these bands not observed in their corresponding methyl esters (**5d-f**). The appearance of absorption bands at $2915-2928\text{ cm}^{-1}$ was assigned to the $\text{sp}^3\text{C-H}$ stretching vibrations in the prepared compounds (**5a-f**).

Comparison between the published infrared spectra of norethindrone⁷⁴ and norethindrone acetate⁷⁵ indicated that the absorption band of the acetyl carbonyl group appeared at higher wave number than that at C3 ketonic carbonyl. It is also reported that the absorption band of carboxylic carbonyl group almost appears at a wave number lower than that of ketones and esters.

The absorption bands of the acetyl carbonyl group of (**5a-c**) appeared as separate bands at $1714-1718\text{ cm}^{-1}$ whereas their corresponding esters (**5d-f**) showed strong overlapped bands of both acetyl and ester carbonyl groups at $1715-1722\text{ cm}^{-1}$.

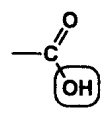
The absorption band of the C3 ketonic carbonyl group of the acid derivatives (**5a,b**) appeared as a broad band at 1651 cm^{-1} overlapped with carboxylic carbonyl group. Whereas the C3 ketonic carbonyl group of compound **5c** appeared at 1645 cm^{-1} separated from carboxylic carbonyl group which appeared at 1615 cm^{-1} . On the other hand the ketonic carbonyl moiety of the ester derivatives (**5d-f**) appeared as separate bands at $1655-1657\text{ cm}^{-1}$.

Aromatic C-H out of plane bending is a characteristic feature in the IR spectrum of disubstituted benzenes. Compounds **5a** and **5d** with ortho disubstituted benzene ring showed a strong band at 758 and 760 cm^{-1} respectively. While compounds **5b** and **5e** with meta disubstituted benzene ring showed three bands at $(693,752,874\text{ cm}^{-1})$ and $(674,750,893$

Results & Discussion, Chemistry

cm⁻¹) respectively. Finally compounds **5c** and **5f** with para disubstituted benzene ring showed a strong band at 856 and 855 cm⁻¹ respectively.

Table (2): IR absorption bands (cm⁻¹) of compounds (**5a-f**)

No.	IR (KBr, ν cm ⁻¹)					
	C-H		CH ₃ C=O	Ph-C=O Carboxyl/ester	3-C=O	Ar C-H out of plane bending
Acid derivatives						
5a	2915	2590-3695	1718	1651		758
5b	2925	2530-3435	1718	1651		693,752,874
5c	2928	2565-3455	1714	1615	1645	856
Ester derivatives						
5d	2915	--	1722		1656	760
5e	2915	--	1719		1657	674,750,893
5f	2920	--	1715		1655	855

Results & Discussion, Chemistry

For the $^1\text{H-NMR}$ spectra of compounds (**5a-f**) we focused on the interpretation of the newly added moiety, in addition to the significant protons of the steroid nucleus and not on the all steroidal protons because of the need of additional techniques for their interpretation such as $^1\text{H-}^{13}\text{C-COSY}$ or NOESY.

The protons of norethindrone acetate are in the upfield range ($\delta=0.54 - 3.75$ ppm) and the most deshielded C4-H appeared at δ 5.75 ppm while all the protons of the newly added 1-phenyl-1,2,3-triazole moiety appeared in the aromatic range.

In $^1\text{H-NMR}$ spectra of compounds **5a** and its esterified derivative **5d**, the steroidal C4-H appeared as singlet at δ 5.81 and 5.77 ppm respectively integrated for one proton.

The aromatic protons of compound **5a** appeared as doublet at δ 8.03-8.01 ppm integrated for one proton assigned for Ar H6, multiplet at δ 7.68-7.64 ppm integrated for one proton assigned for Ar H4 and multiplet at δ 7.58-7.52 ppm integrated for three protons assigned for Ar H3, 5 and H5 of triazole.

On the other hand the aromatic protons of compound **5d** appeared as multiplet at δ 7.98-7.94 ppm integrated for one proton assigned for Ar H6 and multiplet at δ 7.64-7.49 ppm integrated for four protons assigned for Ar H3,4,5 and H5 of triazole. The O-CH₃ protons of compound **5d** appeared at δ 3.67-3.60 ppm as separate singlet signal integrated for three protons.

$^1\text{H-NMR}$ spectra of compound **5b** and its esterified derivative **5e** showed the steroidal C4-H as singlets at δ 5.82 and 5.67 ppm respectively integrated for one proton.

Results & Discussion, Chemistry

The aromatic protons of compound **5b** appeared as singlet at δ 8.34 ppm integrated for one proton assigned for Ar H2, multiplet at δ 8.14-8.12 ppm integrated for two protons assigned for Ar H4,6 and triplet at δ 7.64-7.60 ppm integrated for one proton assigned for Ar H5. The triazole H5 appeared as separate singlet proton at δ 7.84 ppm.

The aromatic protons of compound **5e** appeared as singlet integrated for one proton at δ 8.84 ppm assigned for Ar H2, multiplet integrated for one proton at δ 8.24-8.22 ppm assigned for Ar H6, doublet integrated for one proton at δ 8.06-8.02 ppm assigned for Ar H4 and multiplet integrated for one proton at δ 7.76-7.71 ppm assigned for Ar H5. The triazole H5 of compound **5e** appeared as multiplet at δ 8.44 ppm and integrated for one proton. The O-CH₃ protons of compound **5e** appeared as separate singlet signal integrated for three protons at δ 3.90 ppm.

¹H-NMR spectra of compound **5c** and its esterified derivative **5f** indicate the presence of steroidal C4-H as singlet integrated for one proton at δ 5.81 and 5.63 ppm respectively. The aromatic protons of both compounds appeared as pair of doublet which is a characteristic feature of the para substituted benzene ring.

For compound **5c**, Ar H2,6 appeared as doublet integrated for two protons at δ 8.23-8.21 ppm and Ar H3,5 appeared as doublet integrated for two protons at δ 7.89-7.86 ppm. The triazole H5 proton of compound **5c** appeared as singlet integrated for one proton at δ 7.82 ppm **Figure 6**.

Ar H_{2,6} for compound **5f** appeared as doublet integrated for two protons at δ 8.11-8.09 ppm and Ar H3,5 appeared as doublet integrated for two protons at δ 8.08-8.05 ppm. The triazole H₅ proton of compound **5f** appeared as singlet signal integrated for one proton at δ 8.78 ppm.

Results & Discussion, Chemistry

The O-CH₃ protons of compound **5f** appeared as separate singlet integrated for three protons at δ 3.83 ppm.

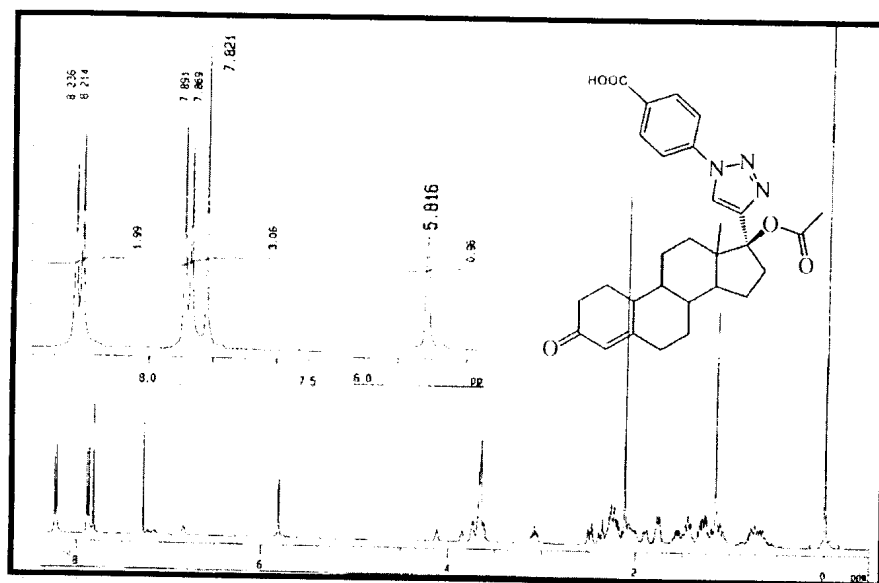


Figure (6): ¹H-NMR spectra of compound **5c**.

It is reported that the C5-H of 1,2,3 triazole can be included in hydrogen bond and this leads to deshielding of the proton in ¹H-NMR depending on the strength of the hydrogen bond⁷⁶. We tried several approaches to correlate the effect of the nature and position of the aromatic substitution on the chemical shift of the triazole H5 proton. Partial charge calculations at the heavy atoms, linear distances and dihedral angles determinations between the target centers was carried out, however no definite results were obtained, this may be due to other factors affecting the possible intra molecular hydrogen bonding between C5-H and COOR group on the benzene ring. Anisotropic effect of the carbonyl group and its conformation may affect the degree of shielding of the proton.

The ^{13}C -NMR data of compound **5b** and **5d** Figure 7 are shown in Table 3. Assignment of each signal to its corresponding carbon atom was followed by comparison with the chemical shift of reported structurally related compounds and was confirmed by DEPT experiments at 135° .^{77, 78}

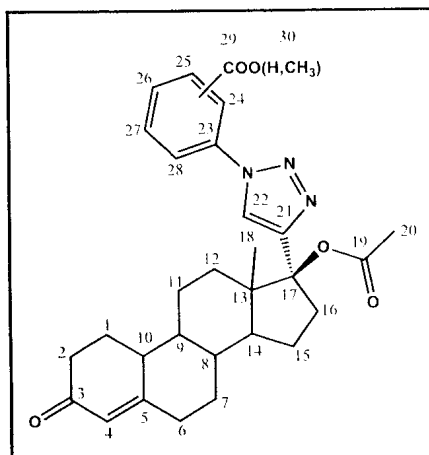


Figure (7): Numerical assignment of carbons of compound **5b** and **5d**

The ^{13}C -NMR spectrum of compound **5b** revealed 10 CH carbons, 4 resonated up field (δ 40.72-48.65ppm) and 6 resonated downfield (δ 119.39-130.11 ppm). The spectrum showed also two signals upfield shifted at δ 14.82 and 21.73 ppm corresponding to C18 and C20 respectively. All these signals are confirmed by their pointing up in the DEPT spectrum. The spectrum revealed also 7 signals assigned to 8 CH_2 carbon atoms of the steroidal nucleus. It was observed that C1 and C12 are totally overlapped and appeared as one signal at δ 36.33 ppm. These carbon atoms are further confirmed by pointing down in the DEPT spectrum. Additionally, the spectrum show 6 signals corresponding to 6 completely substituted carbon atoms which are easily identified by their low intensity and not observed in DEPT spectrum. C13 of the steroidal nucleus resonates at upfield region (δ 47.61 ppm) while C17 is relatively downfield shifted (δ 88.11ppm). The remaining completely substituted carbon atoms resonate in the downfield region.

Results & Discussion, Chemistry

Finally the mostly downfield shifted signal at δ 200.37 ppm assigned to C3. C19 and C29 are totally overlapped and appeared as one signal at δ 170.51 ppm **Figure 8**.

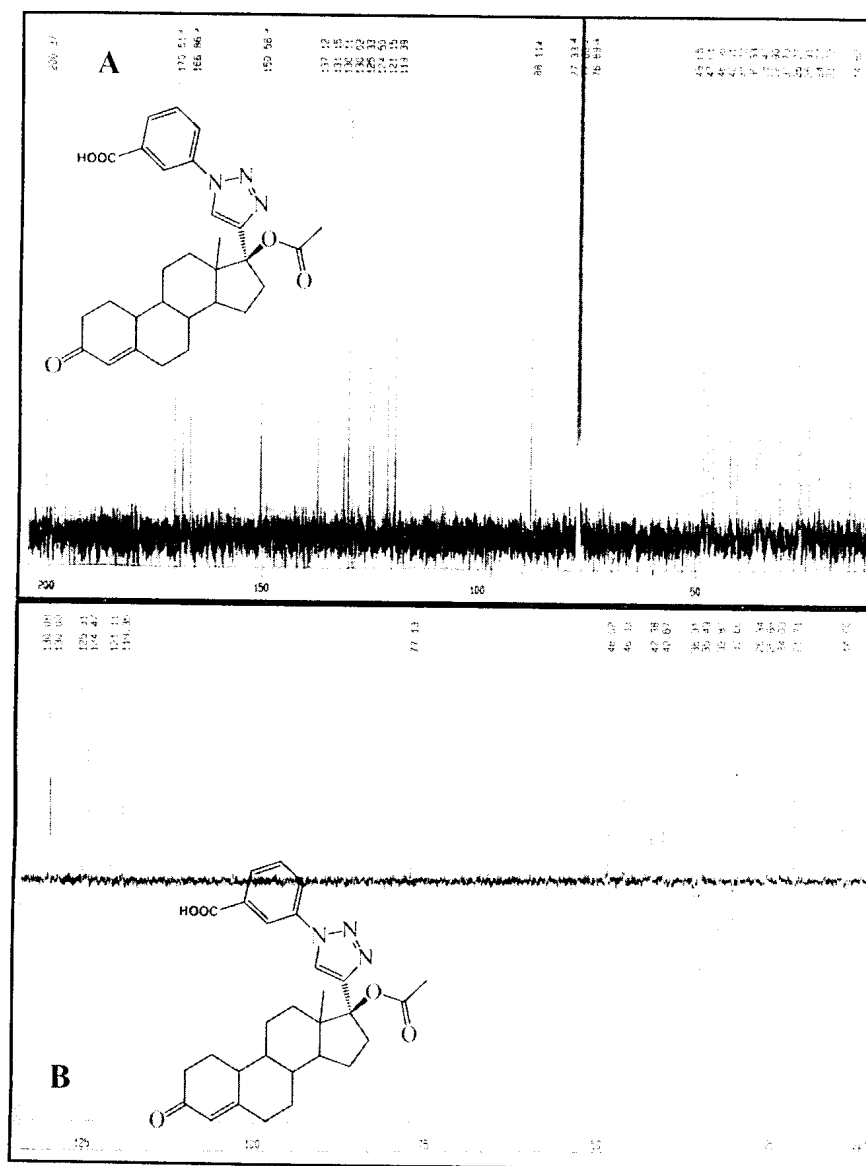


Figure (8): A) ^{13}C -NMR spectrum of compound 5b.
B) DEPT spectrum of compound 5b.

Results & Discussion, Chemistry

The ^{13}C -NMR spectrum of compound **5d** revealed 10 CH carbons, 4 resonated up field (δ 40.75-48.91 ppm) and 6 resonate at the downfield region (δ 118.32-129.83 ppm). It was observed that C25 and C22 of the triazole ring are totally overlapped and appeared as one signal at 129.83 ppm. The spectrum showed also three signals upfield shifted at δ 14.52, 21.55 and δ 52.53 ppm corresponding to C18, C20 and C30 respectively. The spectrum revealed also 8 signals assigned to the 8 CH_2 carbons, all are resonating at the up field region (δ 24.07-36.44 ppm). Additionally, the spectrum show 6 signals corresponding to 6 quaternary and carbonyl carbon atoms, C13 of the steroidal nucleus resonated at upfield region (δ 48.91 ppm), C17 is relatively downfield shifted (δ 88.07ppm). The remaining completely substituted carbon atoms resonated in the downfield region (131.27 – 166.46 ppm). Finally the most downfield shifted signal at δ 218.26 ppm was assigned to C3. C19 and C29 resonated at 195.03 and 166.45 ppm respectively.

Results & Discussion, Chemistry

Table (3): ^{13}C -NMR chemical shifts of compounds **5b** and **5d**.

Carbon atom	5b(δ ppm)	5d(δ ppm)
(C1,C2,C12) ^a	36.33 ^b , 35.37	36.44, 35.47, 32.77
C ₃	200.37	218.26
(C4,C27) ^a	125.33, 124.50	124.57, 123.47
C5	166.86	166.46
C6	30.70	29.45
(C7,C11,C15) ^a	26.37, 25.91, 24.07	26.57, 24.07, 26.02
C8	40.72	40.75
C9	48.65	48.91
C10	42.71	42.45
C13	47.61	48.91
C14	46.36	46.13
C16	32.90	30.83
C17	88.11	88.07
C18	14.82	14.52
C20	21.73	21.55
C19, C29	170.51 ^b	195.03, 166.45
C25	137.12	129.83 ^b
C24	119.39	132.63
C23	150.58	150.95
C28	121.15	118.32
C26, C22	(130.11, 130.02) ^a	126.02, 129.83 ^b
C21	131.15	131.27
C30	-	52.53

a) It is difficult to assign each signal to its corresponding C-atom exactly, since the difference in their chemical shift is ≤ 2 ppm and needed other techniques for their assignment e.g. ^1H - ^{13}C -COSY or NOESY

b) Totally overlapped signals.

3.2. BIOLOGY

3.2) BIOLOGY

3.2.1) *In vivo* progestational activity:

The preliminary *in vivo* progestational activity of the synthesized 17 α -(1-substituted-1, 2, 3-triazol- 4-yl)-19-nortestosterone acetate (**5a-f**) was evaluated using adult female Wistar rats showing at least two consecutive 4-day estrous cycles. Norethindrone acetate (NETA) and its synthesized derivatives were dissolved in DMSO at a concentration of 0.018 mg/ ml. Rats received 1 ml s.c. injections of tested compounds daily, for 8 days. For all experiments the treatment was started when the animals were in estrus phase. Initial body weight before treatment and final body weight at the time of sacrifice were recorded. Twenty-four hours after the final dose, rats were killed, and their uteri were carefully excised, trimmed of extraneous tissue, blotted filter paper to remove excess fluid, weighed on electronic balance to calculate the uterus weight as the following:

$$\text{Relative organ weight (kg)} = [\text{organ weight (g)}/\text{body weight (g)}] \times 1000$$

Then it was fixed, and stained. Paraffin sections of fixed uteri were evaluated for endometrial gland. The thickness of endometrium, myometrium and the uterine epithelial cell heights were measured using an objective lens of magnification 10, and eye lens 10 the total magnification was 100.

Results of *in vivo* progestational activity of the tested compounds as well as Norethindrone acetate (reference drug) in relation to the solvent as control are shown in **Table 4**, **Figure 9** and **Figure 10**.

Results & Discussion, Biology

Results showed that the compounds exhibited variable activities and variable effects on both uterus weight and histology compared with control and reference drug Norethindrone acetate.

Table (4): *In vivo* progestational activity of 17 α -(1-substituted-1,2,3-triazol-4-yl)-19-nor-testosterone acetate (**5a-f**) at a daily dose level of 0.018 mg/ml.

Compound	% increase in body weight	Relative Uterus weight	Endometrial thickness (μ m)	Myometrial thickness (μ m)	Epithelial cell height (μ m)
control	17.7 \pm 1.6	1.5 \pm 0.03	154.47 \pm 1.19	122.40 \pm 2.37	57.80 \pm 0.92
NETA	28.6 \pm 1.1	1.7 \pm 0.05	302.35 \pm 2.2*	228.60 \pm 2.86*	68.22 \pm 0.71*
5a	17.2 \pm 0.64**	1.9 \pm 0.18	452 \pm 12.67***	170.80 \pm 8.87***	45.50 \pm 1.063***
5b	18.6 \pm 1.63**	2.0 \pm .13	375.5 \pm 13.99***	176 \pm 10.27***	43.60 \pm 0.89***
5c	17.6 \pm 1.43**	3.9 \pm 0.35***	277.5 \pm 10.42*	113.60 \pm 3.78**	39.60 \pm 1.27***
5d	16.5 \pm 1.1**	1.3 \pm 0.1	343.7 \pm 1.86***	197.70 \pm 7.92***	64.60 \pm 1.31*
5e	17.7 \pm 1.6**	1.9 \pm 0.13	214.04 \pm 2.21***	319.80 \pm 7.91***	59.10 \pm 0.75***
5f	34.5 \pm 3.1*	1.9 \pm 0.09	417.6 \pm 7.17***	221.80 \pm 2.56*	29.60 \pm 0.49***

Values represent the mean \pm SEM of six animals per group.

* Significantly different from control group at P < 0.05.

** Significantly different from NETA group at P < 0.05.

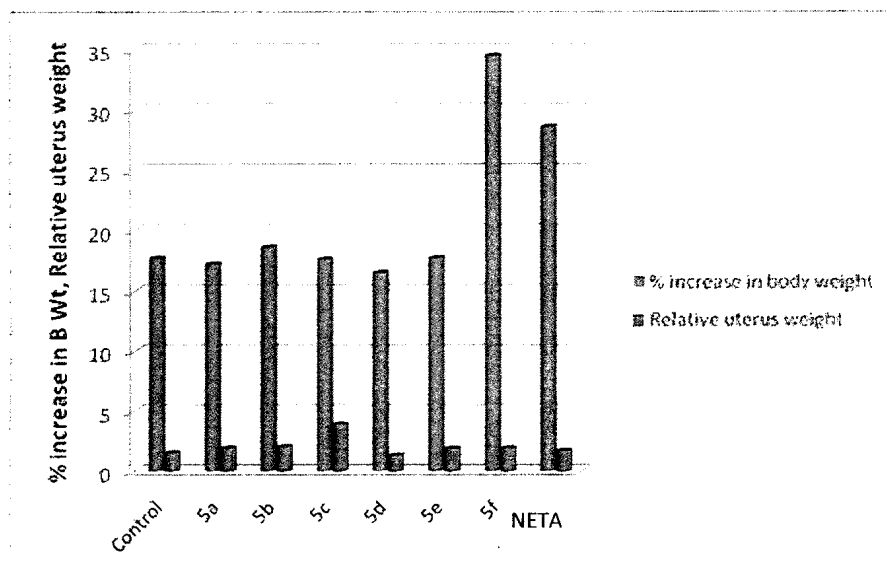


Figure (9): Effect of compounds (5a-f) and NETA on body and uterus weight.

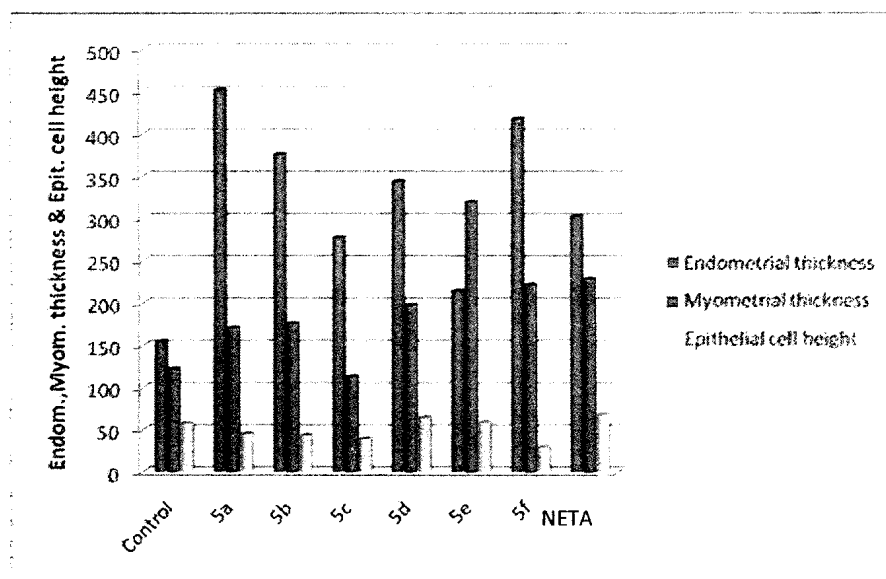


Figure (10): Effect of compounds (5a-f) and NETA on uterine thickness.

3.2.1.1) Effect on body and uterus weight:

In all animals, there was an increase in the final body weight compared to the initial body weight. Rats treated with tested compounds showed no significant increase in the body weight as compared to the control rats except compound **5f** which showed an increase in the body weight compared to both control and Norethindrone acetate treated rats, but the increase was significant compared to control rats.

All the tested compounds except **5d** showed an increase in uterus weight compared to both the control and Norethindrone acetate. This increase was significant with compound **5c**, but the uterus was abnormally edematous and filled with fluids and this was mainly the cause of increased weight not the endometrial proliferation.

3.2.1.2) Effect on uterine histology:

An examination of the uterine histology of the rats treated with the tested compounds showed a significant increase in both endometrial and myometrial thickness compared to the control animals except compound **5c** which showed myometrial atrophy. This increase in the lining thickness of the uterus may be the cause of the increase in uterus wet weight with most compounds. The increase in the endometrial thickness was accompanied by appearance of endometrial glands **Figure 11**.

Compounds (**5a,b,d,f**) showed significant increase in endometrial thickness as compared to Norethindrone acetate, while compounds **5c** and **5e** showed decrease in the endometrial thickness. With regard to the myometrium, only compound **5e** showed significant increase in the thickness while all the other compounds showed decrease in the thickness of the myometrium.

Results & Discussion, Biology

Finally, all compounds showed a decrease in the epithelial cell height as compared to the control and Norethindrone acetate except **5d** and **5e** which showed an increase in the epithelial cell height comparing to control.



Figure (11): A light micrograph of the uterus of a rat treated with compound **5b** showing significant increase in endometrial thickness and distributed endometrial glands.

Consequently, the results indicated that:

- 1- All the synthesized compounds have *in vivo* progestational activity due to their induction of endometrial proliferation as compared to the control animals.
- 2- Compounds **5a**, **5b**, **5d** and **5f** showed progestational activity more than that revealed by Norethindrone acetate while compounds **5c** and **5e** showed lower activity than Norethindrone acetate.
- 3- According to the effect on the endometrial thickness, the progestational activity can be arranged in the following order:
5a > 5f > 5b > 5d > 5c > 5e.

Results & Discussion, Biology

- 4- The esterified derivatives **5d** and **5e** showed lower activity than their corresponding acids **5a** and **5b** while the opposite was observed with the ester **5f** and its acid precursor **5c**.
- 5- The *ortho* derivatives **5a** and **5d** displayed higher activity than the *meta* isomers **5b** and **5e**.

3.2.2) Anticancer activity

Six newly synthesized compounds (**5a-f**) were screened for their anticancer activity according to NCI *in vitro* protocols, against a panel consisting of 60 human tumor cell lines. These cell lines are derived from nine cancer types as follows : Leukemia (L) lines CCRF-CEM, HL-60(TB), K-562, MOLT-4, RPMI-8226, SR; Non small cell lung cancer (NSCLC) lines A549/ATCC, EKVX, HOP-62, HOP-92, NCI-H226, NCI-H23, NCI-H322M, NCI-H460, NCI-H522; Colon cancer (CL) lines COLO 205, HCC-2998, HCT-116, HCT-15, HT29, SW-620; Central nervous system cancer (CNSC) lines SF-268, SF-295, SF-539, SNB-19, SNB-75, U251; Melanoma (M) lines LOX IMVI, M14, SK-MEL-2, SK-MEL-28, SK-MEL-5, UACC-257, UACC-62; Ovarian cancer (OC) lines IGR-OV1(Restricted Use), OVCAR-3, OVCAR-5, OVCAR-8, SK-OV-3; Renal cancer (RC) lines 786-0, A498, ACHN, CAKI-1, RXF 393 (Restricted Use), SN12C, TK-10(Restricted Use), UO-31; Prostate cancer (PC) line PC-3 and Breast cancer (BC) lines MCF7, NCI/ADR-RES, MDA-MB-231/ATCC, HS 578T, MDA-MB-435, BT-549, T-47D . The activity results of compounds (**5a-f**) against different cancer cell lines except melanoma lines are listed in **Table 5**.

3.2.2.1) 60-Cell panel results and discussion

3.2.2.1.1) Leukemia (L) cell lines

Compound **5e** showed antitumor activity against RPMI-8226 and SR cell lines with 29.59 % and 27.58% growth inhibition respectively, while compound **5d** showed 23% growth inhibition of RPMI-8226

Results & Discussion, Biology

Table (5): *In vitro* anticancer activity for compounds (5a-f)

Cell line		Growth Percentage (%)					
		5a	5b	5c	5d	5e	5f
Leukemia	RPMI-8226	94.11	91.60	83.16	77.11	70.41	90.00
	SR	102.31	102.35	103.61	92.69	72.24	87.71
Non-Small Cell Lung cancer	A549/ATCC	95.55	95.73	84.99	92.02	68.57	87.89
	NCI-H522	90.41	117.20	66.54	72.64	75.69	87.48
Colon cancer (HT29)		102.06	110.02	93.50	97.72	79.16	100.28
CNS Cancer	SNB-75	76.79	72.11	68.32	66.46	53.60	73.88
	SF-295	104.44	103.90	92.85	89.47	74.94	93.66
	SNB-19	91.28	98.03	96.41	90.77	74.93	82.72
ovarian cancer (OVCAR-4)		98.07	95.43	77.20	92.60	69.60	78.59
Renal cancer	A498	94.79	77.5	156.59	72.61	43.93	82.76
	UO-31	82.69	80.60	83.16	62.22	62.09	73.58
	CAKI-1	93.74	96.31	96.25	86.45	67.79	92.57
	RXF393	100.35	122.63	107.34	96.84	69.13	114.66
Prostate cancer (PC-3)		94.83	83.89	79.39	65.99	43.30	73.54
Breast cancer	MCF7	109.54	88.82	99.69	97.48	76.87	96.84
	MDA-MB-468	95.48	108.97	90.65	82.67	73.27	88.15

3.2.2.1.2) Non Small Cell Lung Cancer (NSCLC) cell lines

Compound **5c** showed 33.46 % of growth inhibition of NCI-H522 cell line while compound **5d** and **5e** revealed 27.36% and 24.31% of growth inhibition respectively on the same cell line. Additionally compound **5e** showed 31.43% percent of growth inhibition of A549/ATCC cell line.

3.2.2.1.3) Colon cancer (CL) cell lines

None of the tested compounds showed clear inhibition of growth with any of the six colon cancer cell lines, except Compound **5e** which showed 21.84% of growth inhibition of HT29 cell line.

3.2.2.1.4) Central Nervous System Cancer (CNSC) cell lines

The most prominent activity was on SNB-75 cell line. All compounds revealed a prominent growth inhibition and the most active compound was **5e** with about 46.40% inhibition of growth followed by **5d**, **5c**, **5b**, **5f** and **5a** with 33.54%, 31.68%, 27.89%, 26.12% and 23.21% inhibition of growth respectively. Compound **5e** showed also 25.06% inhibition of growth of both SF-295 and SNB-19 cell lines.

3.2.2.1.5) Ovarian Cancer (OC) cell lines

Compound **5e** showed 30.40% inhibition of growth of OVCAR-4 cell line, while compounds **5c** and **5f** showed 22.8% and 21.41% inhibition of growth respectively on the same cell line.

3.2.2.1.6) Renal Cancer (RC) cell lines

The most prominent activity was on A498 cell line and the most active compound was **5e** with about 56.07% inhibition of growth followed by **5d** and **5b**, with 27.4% and 22.5 % inhibition of growth respectively. On the other hand compounds **5d**, **5e** and **5f** showed additional activity against UO-31 cell line causing 37.8%, 38% and 26.5% inhibition of

growth respectively. Compound **5e** also showed 32.2% inhibition of growth of CAKI-1 cell line and 30.87 % inhibition of growth of RXF 393 cell line.

3.2.2.1.7) Prostate Cancer (PC) cell line

The most prominent activity was on PC-3 cell line and the most active compound was **5e** with about 56.7 % inhibition of growth followed by **5d** and **5f** with 34 % and 26.5 % inhibition of growth respectively.

3.2.2.1.8) Breast Cancer (BC) cell lines:

Only compound **5e** showed growth inhibition of MDA-MB-468 and MCF7 cell lines by 26.7% and 23.13% inhibition of growth respectively.

To summarize the results of the anticancer screening against the challenged cell lines, the esterified derivatives (**5d-f**) displayed higher activity than their respective free acids (**5a-c**). Among the esterified derivatives compound **5e** is the most active one showing broad spectrum anticancer activity. It revealed about 50% growth inhibition of CNS cancer SNB-75 cell line, 56% growth inhibition of renal cancer A498 cell line and 56.7% growth inhibition of prostate cancer PC-3 cell line. No effect for the position of the substituent (*o*, *m* and *p*) was observed.

**3.3. MOLECULAR
MODELING, DOCKING
SIMULATION STUDIES
AND PHYSICOCHEMICAL
CALCULATIONS**

3.3) MOLECULAR MODELING, DOCKING SIMULATION STUDIES AND PHYSICOCHEMICAL CALCULATIONS

3.3.1) Progesterone receptor structure

Progesterone receptor (PR) is one of the nuclear receptors (NRs) which are ligand-dependent transcription factors that regulate the expression of a variety of important target genes involved in a wide spectrum of developmental and physiological processes⁷⁹. PR and Steroid hormone receptors are multi-domain proteins composed of conserved well-structured regions, such as ligand (LBD) and DNA binding domains (DBD), plus other naturally unstructured regions including the amino-terminal domain (NTD) and the hinge region between the LBD and DBD. The hinge is more than just a flexible region between the DBD and LBD and is capable of binding coregulatory proteins. PR is expressed as two isoforms, PR-A and PR-B, which arise from the same gene by utilization of two promoters. The two receptors are identical in the C-terminal ligand binding domain (LBD) and DNA binding domain (DBD) and most of the amino-terminal domain (NTD) except for an 164 amino acid extension of the NTD unique to PR-B, **Figure 12**.⁸⁰

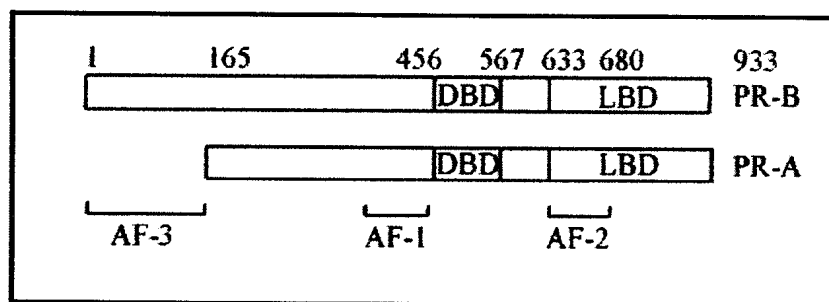


Figure (12): Schematic representation of the progesterone receptor PR-A and PR-B proteins. The DNA-binding domain (DBD), the ligand-binding domain (LBD) and activation function domains (AFs) are indicated.

The three-dimensional structure of progesterone receptor complexed with Norethindrone is described (PDB Id: 1SQN) **Figure 13.**⁵⁶

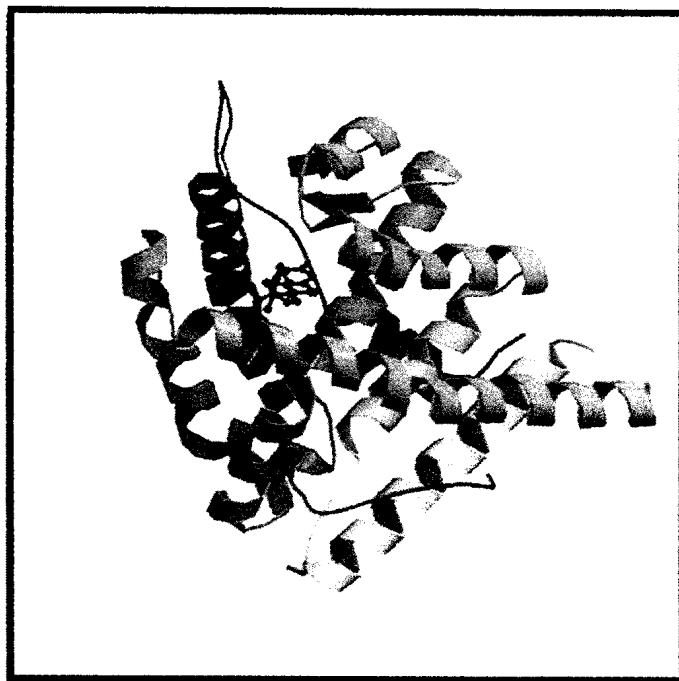


Figure (13): Ribbon representation of progesterone receptor. Norethindrone depicted in black ball-and-stick representation with red oxygen atoms.

3.3.2) Progesterone receptor (PR) active site

Our understanding of how various progestin ligands interact at the molecular level has been greatly enhanced by the elucidation of crystal structures of these ligands bound to ligand-binding domain of the PR. To date, ligand-bound PR structures have been solved for the natural ligand, progesterone (P)⁸¹, other C₁₇ substituted steroids such as Metribolone, Mometasone furoate, Norethindrone⁵⁶ and the non-steroidal ligand Tanaproget⁸². These structures reveal ligand-binding pockets that vary in shape and size depending on the nature of the bound ligand and provide interesting insights into receptor flexibility, which allow these ligands to be accommodated. For example, when compared to P, which has a bound molecular volume of 349 Å³, tanaproget has a much smaller molecular volume of 290 Å³, yet both these ligands are potent PR agonists⁸³. Examination of the bindings between the different ligands and the receptor revealed that the active site amino acids are Leu-715, Cys-891, Thr-894, Tyr-890, Leu-797, Leu -887, Met-756, Met-801, Met-759, Phe-778, Arg-766, Gln-725, Leu-721, Leu-718, Trp-755, Asn-719, Met-909 and Phe-905.

3.3.3) Norethindrone binding with progesterone receptor

As observed in other PR/steroid complexes, a hydrogen bond was observed between oxygen atom of C₃ carbonyl of the steroid A-ring of norethindrone and the side chain of Gln725. This hydrogen bond between a conserved glutamine and the A-ring oxygen has been observed in all crystal structures of 3-keto steroid receptors. The side chain of a conserved arginine, PR Arg766, formed the linchpin of a hydrogen bond network centered on the A-ring C₃ carbonyl oxygen. This network also

included a hydrogen bond between Arg766 and Phe778, which made vander Waals contact with the steroid A-ring. Most of the remaining PR-ligand interactions were hydrophobic, but some polar interactions involving the D-ring may be responsible for molecular recognition and increased affinity.⁵⁶

3.3.4) Docking simulation studies of target compounds (5a-f) with progesterone receptor

Molecular docking simulation of the tested compounds (**5a-f**) was performed to rationalize the obtained *in vivo* biological results. Furthermore, molecular docking studies help in understanding the binding mode and various interactions between the ligand and progesterone receptor.

The tested compounds were constructed in a 3D model using MOE molecule builder. The partial charges of the different models were calculated using current forcefield calculations. The produced models were subjected to systematic conformational search, and then a database of different conformers for each model was saved to be used in the docking study.

The X-ray crystallographic structures of PR (PDB Id: 1SQN) was prepared for docking and the active sites were isolated using MOE site finder tool. The docking simulations were performed by MOE dock application using Triangle Matcher as placement scheme and London dG as a scoring function.

Most of molecular docking programs are treating the ligand as a flexible molecule while protein in a rigid manner. On the other hand, realistic docking experiments need to account for molecular flexibility for

Results & Discussion, Molecular modeling

both the protein and the ligand because there are many cases in which the lock-and-key model does not work well and the induced-fit model is more appropriate⁸⁴.

LigX (Ligand Explorer) tool, a new tool added in (MOE V.10.2010), was used in docking simulations in the present investigation. In LigX calculations, the receptor atoms far from the ligand are held fixed (constrained not to move) while receptor atoms near the ligand (in the active site) are allowed to move but are subject to tether restraints that discourage gross movement, **Figure 14**.

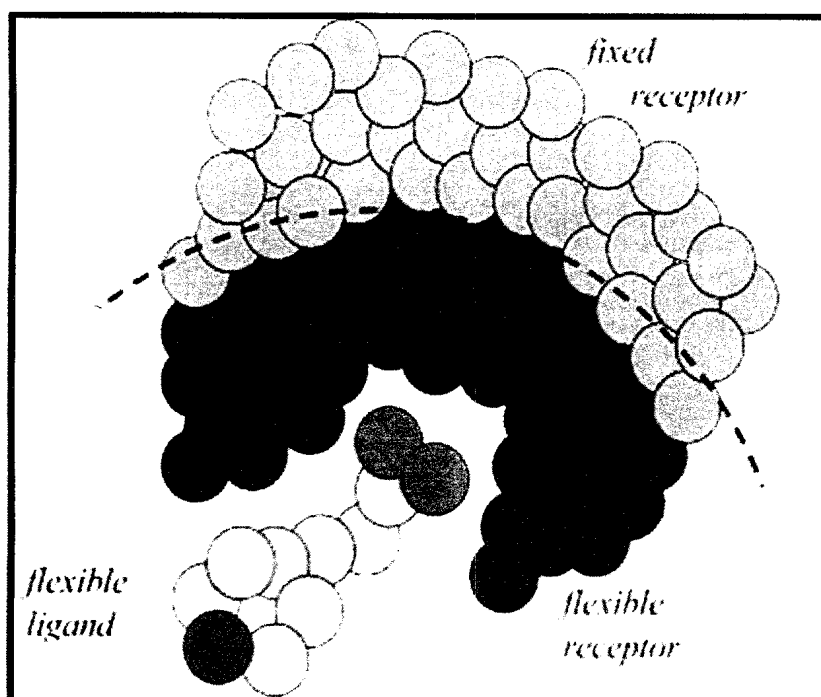


Figure (14): Flexible ligand/active site docking simulation by LigX tool.⁸⁵

Results & Discussion, Molecular modeling

From the docking studies of the target compounds **5(a-f)** and their binding energy (ΔG) **Table 6**, we can observe a rough correlation with the *in vivo* progestational activity represented in the increase in the endometrial thickness compared to that of the reference drug norethindrone acetate. The results also revealed that the change in the hydrophobic interactions due to the addition of the hydrophobic aromatic moiety to the steroid C₁₇ has no significant effect on the binding with the target in comparison to that of the hydrogen bond forming groups.

In comparison to the reference drug, norethindrone acetate **Figure 15** compounds **5a**, **5f** and **5b** showed lower binding energies (best docking scores) respectively. While compounds **5d**, **5c**, and **5e** showed higher binding energies respectively and this arrangement agree to a large extent with the arrangement of the biological activity.

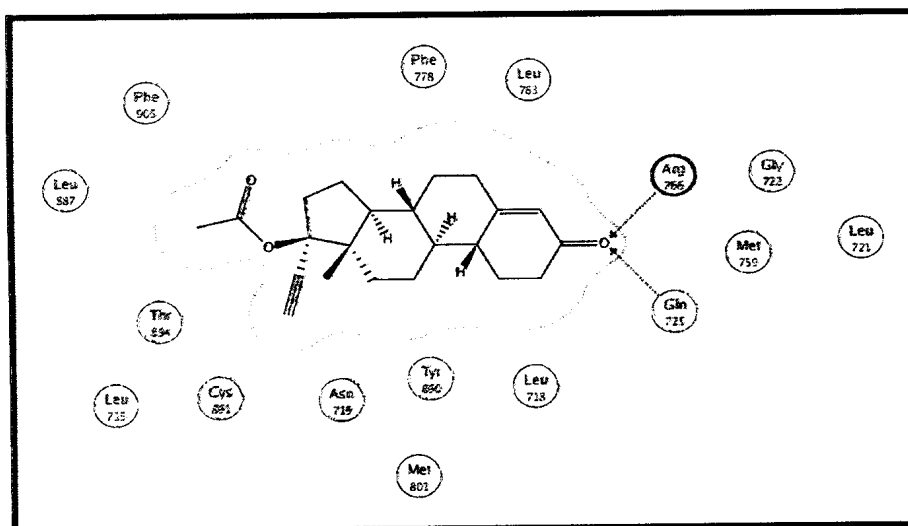


Figure (15): Two-dimensional representation of the docking pose of norethindrone acetate in the PR binding site.

Results & Discussion, Molecular modeling

Table (6): Interaction energies, ligand target interactions and *in vivo* biological activities of reference drug NETA and target compounds.

Comp. No.	ΔG (Kcal/mole)	Ligand binding groups				Endometrial Thickness (μm)
		oxygen of C3 carbonyl (\AA)	Oxygen of carboxylic carbonyl (\AA)	Oxygen of carboxylic hydroxyl (\AA)	Others	
NETA	-10.5131	Gln725(2.73) Arg766(2.67)	-	-	Hydrophobic interactions with 16 AA	302.35 \pm 2.2
5a	-12.6971	Asn719(2.82)	Arg766(2.49)	Gln725(2.77) Arg766(2.56)	Hydrophobic interactions with 19 AA	452 \pm 12.67
5b	-11.1299	Asn719(2.69)	Arg766(2.72)	Gln725(2.72) Arg766(2.41)	Hydrophobic interactions with 21 AA	375.5 \pm 13.99
5c	-8.8336	Asn719(2.65)	Arg766(2.31)	-	Hydrophobic interactions with 20AA	277.5 \pm 10.42
5d 6a	-9.7881	Gln725(2.78) Arg766(2.46)	-	-	Hydrophobic interactions with 21 AA	343.7 \pm 1.86
5e 6b	-8.0234	Asn719(2.43)	Arg766(2.31)	-	Hydrophobic interactions with 21AA	214.04 \pm 2.21
5f 6c	-11.3694	Gln725(2.52) Arg766(3.24)	Asn719(2.63)	-	Hydrophobic interactions with 19 AA	417.6 \pm 7.17

Results & Discussion, Molecular modeling

Examination of the binding modes of the target compounds; we observed that hydrogen bonding with certain amino acids and the orientation of the ligand within the active site pocket corresponding to these amino acids are the major factors affecting the ligand/target binding results.

Within compounds **5a**, **5f** and **5b** which had more favorable binding energy in comparison with the Norethindrone acetate, compound **5a** and **5b** showed four hydrogen bonds with Asn719, Arg766, Gln725 and Arg766 (as in **Table 6**) with the oxygen of C₃ carbonyl of the Steroid A-ring directed toward Asn719 while the carboxylate group project toward Gln725 and Arg766 **Figure 16, 17**.

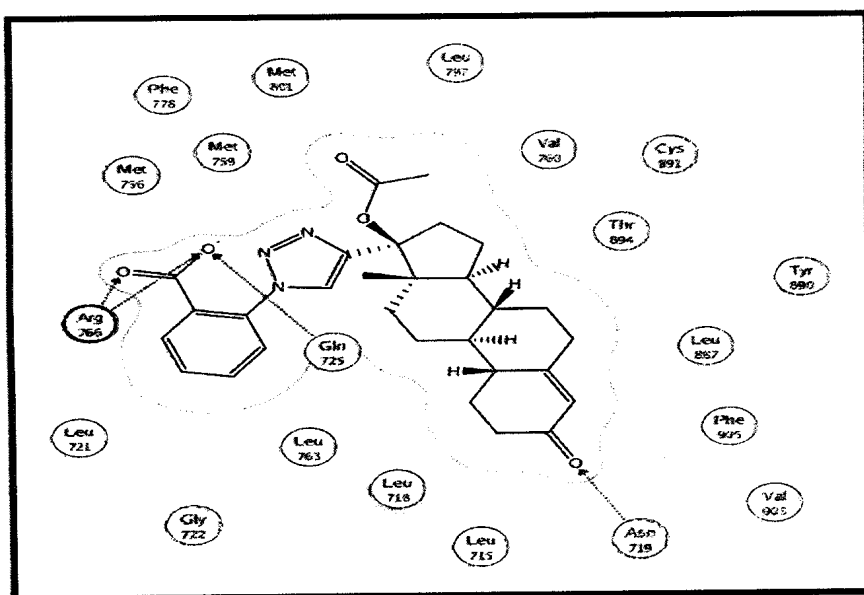


Figure (16): Two-dimensional representation of the docking pose of compound **5a** in the PR binding site.

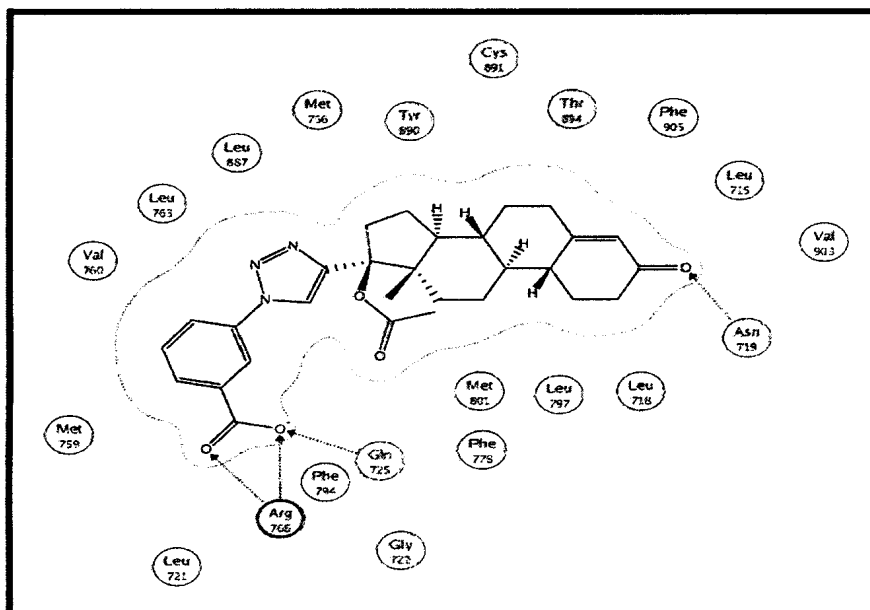


Figure (17): Two-dimensional representation of the docking pose of compound 5b in the PR binding site.

On the other hand compound **5f** exhibited reversed orientation within the receptor active site and showed three hydrogen bonds with Gln725, Arg766 and Asn719 **Figure 18**.

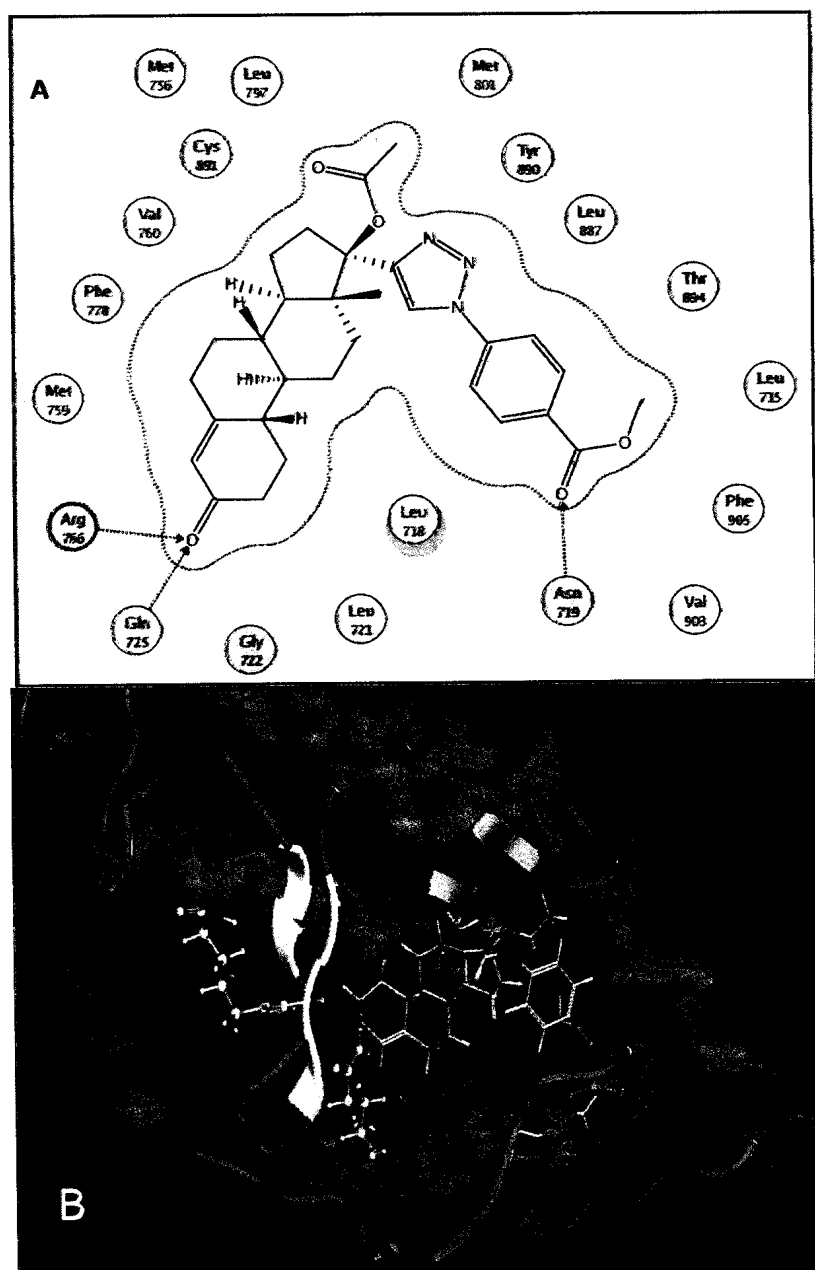


Figure (18): A) Two-dimensional representation of the docking pose of compound 5f in the PR binding site. B) 3D representation of the same pose.

Results & Discussion, Molecular modeling

Moreover, compounds **5d**, **5c** and **5e** revealed less favorable binding energy comparing with Norethindrone acetate (**table 4**). Compound **5d** (**Figure 19**) exhibited the same orientation as the reference drug and forming two hydrogen bonds between oxygen at C₃ of steroid A-ring with both Gln725 and Arg766. On the other hand, **5c** and **5e** showed an opposite orientation and forming a hydrogen bond between oxygen at C₃ of steroid A-ring and Asn719 and another between carbonyl of carboxylate moiety (acid/ester) and Arg766 **Figure 20&21**.

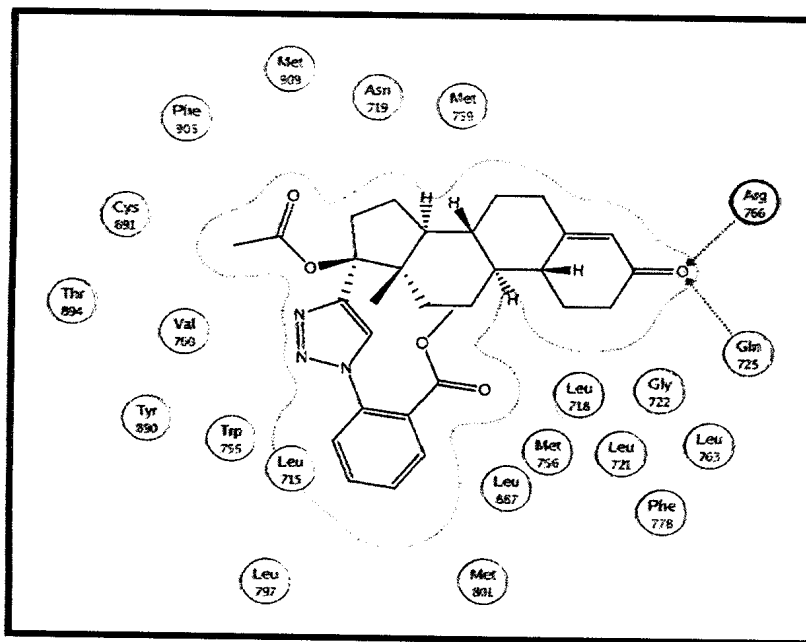


Figure (19): Two-dimensional representation of the docking pose of compound **5d** in the PR binding site.

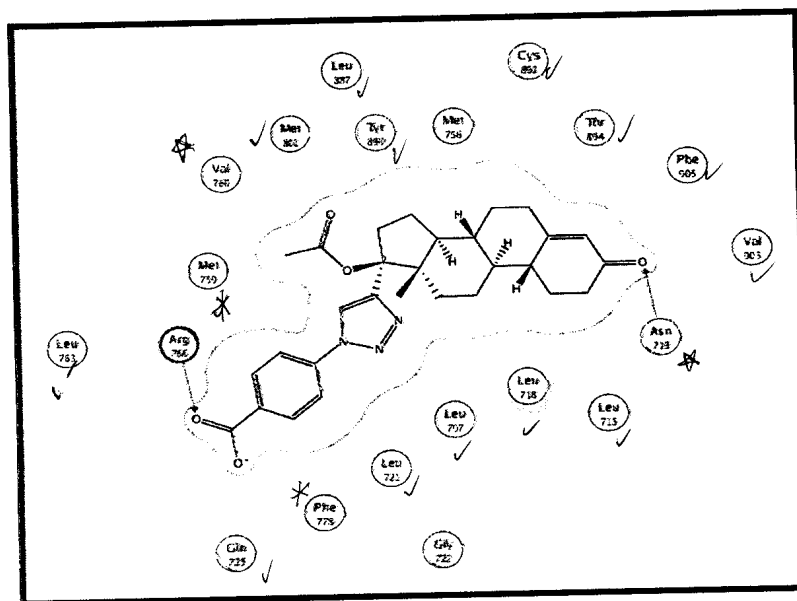


Figure (20): Two-dimensional representation of the docking pose of compound 5c in the PR binding site.

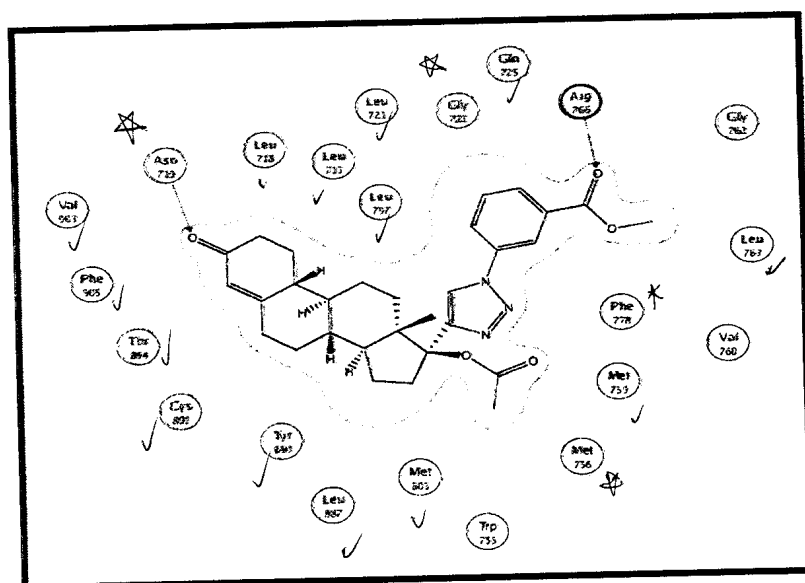


Figure (21): Two-dimensional representation of the docking pose of compound 5e in the PR binding site.

Results & Discussion, Molecular modeling

On comparison between the ester derivatives (**5d-f**) and their acid precursors (**5a-c**), it was observed that the later oriented in a manner that the carbonyl at C₃ of the steroid A-ring projected toward Asn719. On the other hand the carboxylate group of these compounds projected toward Gln725 and Arg766 forming three hydrogen bonds (**5a** and **5b**) or only one hydrogen bond (**5c**). The opposite was observed with the ester derivatives except compound **5e** which oriented in a manner similar to acid derivatives.

With regard to the position of the substitution and its effect on the binding with the receptor we observed that the *ortho* substituted derivatives showed more favorable binding energies than the corresponding *meta* isomers while the *para* substituted derivative showed the least favorable score within the acid derivatives and the best one within the ester derivatives.

From the docking simulation study, it was observed that:

- 1- Binding of the ligand with Gln725 a hydrogen bond is essential.
- 2- The newly added moieties at C17 provide important and very effective sources of additional ligand/ target binding especially hydrogen bonding.
- 3- The effect of the added moieties at C17 on the hydrophobic interactions wasn't significant.
- 4- Compound **5a**, **5b** and **5f** showed the highest scores due to their binding with the two essential amino acids Gln725 and Arg766 in addition to other hydrogen bond interaction with the active site Asn719. On the other hand compounds **5c**, **5d** and **5e** showed

Results & Discussion, Molecular modeling

lower scores than the reference drug since they bind only with two essential amino acids in the active site.

- 5- The orientation of the ligands within the active site in such a manner in which the carbonyl at C3 of the steroid A-ring bind with Gln725 isn't essential for the binding to elicit the predicted biological activity.

3.3.5) Physicochemical calculations:

The term "physicochemical properties" refers to the influence of the organic functional groups within a molecule on its acid-base properties, water solubility, partition coefficient, crystal structure, stereochemistry, and so on. All these properties influence the absorption, distribution, metabolism, excretion, and toxicity of the molecule. To design better medicinal agents, the medicinal chemist needs to understand the relative contributions that each functional group makes to the overall physicochemical properties of the molecule. Studies of this type involve modification of the molecule in a systematic fashion and determination of how these changes affect biological activity. Such studies are referred to structure-activity relationships (SAR) that is, what structural features of the molecule contributes to, or takes away from, the desired biological activity of the molecule of interest.³

In the present investigation the effect of the structural modification on the physicochemical properties of norethindrone acetate and consequently on its biological activity was attempted. These properties were calculated using Molecular Operating Environment (MOE[®]) version 10.2010⁸⁵ and the molinspiration server, **Table 7.**⁸⁶

The first properties studied were that of Lipinski rule which states that poor absorption or permeation is more likely when there are more than 5 H-bond donors, 10 H-bond acceptors, the molecular weight (Mwt) is greater than 500 and the calculated Log P (CLogP) is greater than 5.⁸⁷ The only slight violation observed was with the molecular weight which was 503.5990 for the acid derivatives (**5a-c**) and 517.6260 for the ester derivatives (**5d-f**). This violation can be neglected if we know that molecular weight increase up to 550 D is permissible.⁸⁸

Results & Discussion, Molecular modeling

Examination of the cLogP of the synthesized derivatives indicated that a slight increase in lipophilic characters by the added phenyl triazole moiety in the acid derivatives (**5a-c**) and the ester derivatives (**5d-f**) still not exceed the allowed upper limit 5.

The added acid moiety provided the newly synthesized derivatives (**5a-c**) with a hydrogen bond donor capacity which eliminated by the esterification process in (**5d-f**). The effect of the added moiety was very significant since the hydrogen bond acceptor property was increased from three in norethindrone acetate to eight due to the triazole three nitrogens and the carboxyl/methyl carboxylate two oxygens.

Table (7): Calculated properties of the synthesized compounds (**5a-f**) in addition to Norethindrone acetate.

Compound	M.wt.	cLog P(O/W)	Lip-don	Lip-acc	Volume	TPSA	LogS
NETA	340.4630	3.7070	0	3	333.749	43.376	-5.4856
5a	503.5990	3.7990	1	8	458.363	111.393	-6.1313
5b	503.5990	3.8380	1	8	458.363	111.393	-6.1313
5c	503.5990	3.8010	1	8	458.363	111.393	-6.1313
5d	517.6260	4.0630	0	8	475.891	100.399	-6.5436
5e	517.6260	4.1020	0	8	475.891	100.399	-6.5436
5f	517.6260	4.0650	0	8	475.891	100.399	-6.5436

Results & Discussion, Molecular modeling

Because the solubility (logS) of organic molecules in water should be considered in the design of drugs, due to its significant impact on many ADME-concerned properties of drugs, such as uptake, distribution, transport, and eventually bioavailability⁸⁹, the effect of the structural modification on the calculated log solubility in water LogS (calculated from an atom contribution linear atom type model)⁸⁹ was also studied. The results revealed that the added moiety diminished the value of water solubility LogS from -5.4856 to -6.1313 in the acid derivatives (**5a-c**) and to -6.5436 in the ester derivatives(**5d-f**) and these results was in agree with the increase of the log P values in the synthesized derivatives.

Another very helpful parameter for the prediction of absorption in drug design is the topological polar surface area (TPSA) defined as the sum of surfaces of polar atoms in a molecule. This parameter is easy to understand and, most importantly, provides good correlation with experimental transport data. It has been successfully applied for the prediction of intestinal absorption, Caco-2 monolayers penetration, and blood-brain barrier crossing.⁹⁰ It was reported that orally active drugs that are transported passively by the transcellular route should not exceed a polar surface area of about 120 Å² and for brain penetration they can be tailored by decreasing the polar surface to <60-70 Å².⁹¹ Calculations revealed that the structural modification of norethindrone acetate raised the polar surface area significantly in both acid and ester derivatives from 43.376 Å² to 111.393 Å² and 100.399 Å² respectively. This was predicted due to the polarity of triazole nitrogens in addition to the carboxyl/methyl carboxylate oxygens.

Finally because the volume is a fundamental physical property of molecules that is important in understanding their structure, function, and interactions⁹², the effect of the structural modification of norethindrone

Results & Discussion, Molecular modeling

acetate on the molecular volume was studied. As predicted the volume of both acid (**5a-c**) and ester (**5d-f**) derivatives was increased to 458.363 Å³ and 475.891 Å³ respectively in comparison to 333.749 Å³ for norethindrone acetate.

From these calculations we can conclude that:

- 1- The planned structural modification of norethindrone acetate had slightly increased the Lipinski parameters to the extent not affect the drugability of these targets.
- 2- The modification provided the target compounds with additional hydrogen bond donors and acceptors within Lipinski's limitations which had a significant effect on progesterone receptor binding as docking studies revealed.
- 3- The modification slightly diminished the predicted water solubility of the target compounds but our design for introduction of the carboxyl group provides a wide capability of salt formation with several bases that can enhance water solubility.
- 4- The increase of polar surface area of the target compounds due to the modification was within the reported limit for orally active drugs that are transported passively by the transcellular route.
- 5- The increase in the molecular volume of the target compounds wasn't a problem due to the known flexibility of the progesterone receptor active site that accommodate the ligands bulkiness and this was confirmed by the docking and *in vivo* progestational screening studies.

4. EXPERIMENTAL

4.1. CHEMISTRY

4. EXPERIMENTAL

4.1 CHEMISTRY

Materials and Apparatus:

- Melting points were determined using electrothermal apparatus (Stuart Scientific, England), and were uncorrected.
- Elemental analyses were performed on AnalysenSysteme GmbH-D-63452-Hanau apparatus Germany, Microanalytical Center, Faculty of Science, Assiut University, Assiut, Egypt, and Perkin Elmer 2400 CHN elemental analyzer, Microanalytical Center, Faculty of Science, Cairo University, Cairo, Egypt as well as the Regional Center for Mycology and Biotechnology, Al-Azhar University, Cairo, Egypt.
- Thin layer chromatography (TLC) was used for monitoring chemical reactions and was carried out using silica gel 60 F₂₅₄ precoated sheets 20 X 20 cm, layer thickness 0.2 mm (E. Merck, Germany), and spots were visualized using UV-lamp at λ_{\max} 254 nm, Column chromatography was carried out on Fluka silica gel 60 (particle size 0.063 – 0.02 mm.)
- IR-spectra were recorded as KBr disk using Shimadzu IR 400-91527 Spectrophotometer (Shimadzu Corp., Kyoto, Japan) at the Central Laboratory, Faculty of Pharmacy, Assiut University Assiut, Egypt.
- ¹H-NMR spectra were performed on Varian EM-360L NMR Spectrophotometer (60 MHz) (USA), Faculty of Pharmacy, and JEOL-JNM-LA400 FT-NMR Spectrometer (400 MHz) (Japan), Faculty of Science, Assiut University. Chemical shifts are expressed in δ values (ppm) relative to tetramethyl silane (TMS) as an internal standard, and coupling constants *J* were expressed in (Hz). CDCl₃ (7.29ppm) and

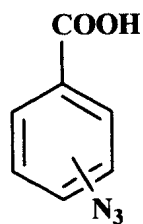
Experimental, Chemistry

DMSO-d₆ (2.5 ppm.) were used as solvents. Deuterium oxide was used for the detection of exchangeable protons.

¹³C-NMR spectra were performed on JEOL-JNM-LA400 FT-NMR Spectrometer (400 MHz) (Japan), Faculty of Science, Assiut University, CDCl₃ (77ppm) was used as solvent.

- All the chemicals used for the synthesis of the target compounds were of commercially available reagent grade and used without further purification except the solvents, which were purified before use.

4.1.1) General method for synthesis of azido benzoic acids (2a-c)⁹³



(2 a-c)

In a 150 mL round-bottomed flask , a solution of sodium nitrite (1.06 g , 15.4 mmol) in cold water (5°C) (3 mL) was added portion wise to a stirred cold mixture of the respective amino benzoic acid (1a-c) (2.0g, 14.5 mmol) , water (10 mL) and concentrated sulphuric acid (3 mL) . To the resultant clear mixture, a solution of sodium azide (1.20 g, 18.45 mol) in water (3 mL) was then added with vigorous stirring. A white product was precipitated, the stirring was continued for further 10 min. The precipitate was washed thoroughly with water, filtered under suction, crystallized from the proper solvents to afford the pure products (2a-c) . Physical data are shown in **Table (8)**.

Table (8): Physical data of *o*-, *m*- and *p*-azidobenzoic acid (2a-c).

No.	M.p. (°C)		Yield (%)	(Cryst. Solv.)
	Found	Reported ^{68, 94}		
2a	141-143 °C	142-143 °C	83%	Hexane
2b	162-165 °C	163-165 °C	89%	Hexane
2c	188-190 °C	188-191 °C	95%	H ₂ O / Ethanol

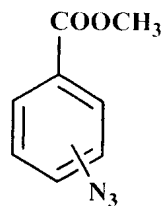
Spectral data of *o*-, *m*- and *p*-Azidobenzoic acid (2a-c).

***o*-Azidobenzoic acid (2a)** IR (KBr, cm⁻¹): 3670-3060 (OH), 2100 (N₃), 1684 (C=O). ¹H-NMR (60 MHz, CDCl₃, δ ppm, J Hz): 7.09-7.42 (m, 2H, H3,5); 7.42-7.81 (m, 1H, H4); 8.03-8.29 (d, 1H, J = 9, H6); 11.21 (br.s, exchangeable, 1H, COOH).

***m*-Azidobenzoic acid (2b)** IR (KBr, cm⁻¹): 3625-3380 (OH), 2345 (N₃), 1647 (C=O). ¹H-NMR (60 MHz, CDCl₃, δ ppm): 7.13-8.09 (m, 4H, H2,4-6); 9.16 (s, exchangeable, 1H, COOH).

***p*-Azidobenzoic acid (2c)** IR (KBr, cm⁻¹): 3755-3090 (OH), 2095 (N₃), 1668 (C=O). ¹H-NMR (60 MHz, CDCl₃, δ ppm, J Hz): 7.03-7.33 (d, 2H, J = 8, H3,5); 7.93- 8.29 (d, 2H, J = 8, H2,6); 8.63 (s, exchangeable, 1H, COOH).

4.1.2) General method for synthesis of methyl azidobenzoates (3a-c)⁹⁵



(3a-c)

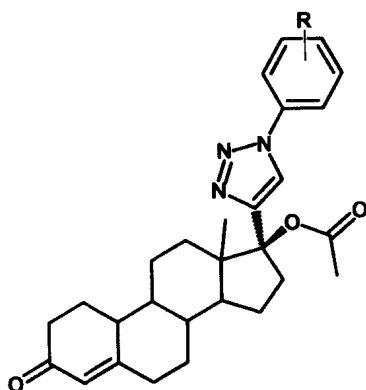
A mixture of the respective Azidobenzoic acid (**2a-c**) (2g, 0.0122 mol), absolute methanol (5mL, 0.125mol) and concentrated sulphuric acid (0.36 g 0.2 mL) was refluxed for 4 hours. The solvent was evaporated under reduced pressure and allowed to cool. The product was extracted with chloroform (2×50 mL) and the organic layer washed with sodium bicarbonate solution (20%) until effervescence ceases, then with water, and dried over anhydrous magnesium sulphate. The chloroform was evaporated under vacuum and the product was collected. Compounds 3a and 3b are dark red oils, while compound 3c is reddish white powder with m.p. 38°C as reported.⁶⁹ Yields were 63%, 75%, 80% respectively. Spectral data for compounds (**3a-c**) are shown below. The products were used without further purification in the next reactions.

Methyl o-azidobenzoate (3a) IR (KBr, cm⁻¹): 2955 (-C-H), 2095 (N₃), 1713 (C=O). ¹H-NMR (60 MHz, CDCl₃, δ ppm): 3.89 (s, 3H, CH₃); 6.93-8.00 (m, 4H, H3-6).

Methyl m-azidobenzoate (3b) IR (KBr, cm⁻¹): 2985 (-C-H), 2090 (N₃), 1715 (C=O). ¹H-NMR (60 MHz, CDCl₃, δ ppm): 3.86 (s, 3H, CH₃); 6.83-7.73 (m, 4H, H2,4-6).

Methyl p-azidobenzoate (3c) IR (KBr, cm⁻¹): 2100 (N₃), 1710 (C=O). ¹H-NMR (60 MHz, DMSO-d₆, δ ppm, J Hz): 3.86 (s, 3H, CH₃); 7.00-7.33 (d, 2H, J = 8.5, H3,5); 7.76-8.06 (d, 2H, J = 8.5, H2,6).

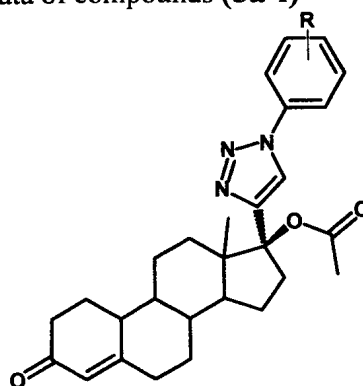
4.1.3) General method for synthesis of 17- α (1-substituted-1,2,3-triazol-4-yl)-19-nortestosterone acetate (5a-f)



5(a-f)

Norethindrone acetate (4) (250 mg, 0.73 mmol) and the respective azide (2 a-c, 3 a-c) (2.92 mmol) were suspended in a mixture of water and tert-butyl alcohol 1:1 (12 mL). An aqueous solution of sodium ascorbate (14.5 mg, 0.073 mmol, water 300 μ L) was added, followed by copper (II) sulphate pentahydrate solution (1.8 mg, 0.0073 mmol, in water 100 μ L). The heterogeneous mixture was stirred vigorously under nitrogen overnight, at which point it cleared and TLC monitoring (hexane/ethylacetate) indicated complete consumption of the steroid. The reaction mixture was diluted with water (50 mL), extracted with ethyl acetate (3 \times 20mL), dried via filtering over anhydrous magnesium sulphate. The organic layer was evaporated under vacuum, and the residues were purified by column chromatography using gradient elution of (hexane/ethyl acetate) to afford the target products. Physical data are shown in **Table 9**.

Table (9): Physical data of compounds (5a-f)



No.	R	m.p. (°C)	Yield (%)	Mol. Formula	Elemental Analyses		
					Calc. /Found	C%	H%
5a	<i>o</i> -COOH	145-148	45%	C ₂₉ H ₃₃ N ₃ O ₅ (Mol. Wt. 503.589)	69.17	6.60	8.34
					69.21	6.58	8.49
5b	<i>m</i> -COOH	151-153	70%	C ₂₉ H ₃₃ N ₃ O ₅ (Mol. Wt. 503.589)	69.17	6.60	8.34
					69.28	6.69	8.57
5c	<i>p</i> -COOH	184-186	55%	C ₂₉ H ₃₃ N ₃ O ₅ (Mol. Wt. 503.589)	69.17	6.60	8.34
					69.24	6.71	8.62
5d	<i>o</i> -COOCH ₃	93-96	50%	C ₃₀ H ₃₅ N ₃ O ₅ (Mol. Wt. 517.616)	69.61	6.82	8.12
					69.68	6.85	8.27
5e	<i>m</i> -COOCH ₃	97-99	75%	C ₃₀ H ₃₅ N ₃ O ₅ (Mol. Wt. 517.616)	69.61	6.82	8.12
					69.70	6.88	8.32
5f	<i>p</i> -COOCH ₃	119-122	60%	C ₃₀ H ₃₅ N ₃ O ₅ (Mol. Wt. 517.616)	69.61	6.82	8.12
					69.57	6.95	8.33

Spectral data of 17- α (1-substituted 1, 2, 3-triazol-4-yl) - 19-nortestosterone acetate (5a-f):

Compound (5a) IR (KBr, cm^{-1}): 2590-3695 (OH), 1718 (C=O acetyl), 1651 broad (C=O ketonic overlapped with COOH carbonyl). $^1\text{H-NMR}$ (400 MHz, CDCl_3 , δ ppm, J Hz): 8.03-8.01(d, 1H, Ar H6); 7.68-7.64 (m, 1H, Ar H4); 7.58-7.52 (m, 3H, Ar H3,5, triazole H5); 5.81 (s, 1H, steroidal C4-H). 3.05-0.64 (unresolved multiplets of cycloaliphatic protons of the steroidal nucleus in addition to acetyl and C18 methyl protons).

Compound (5b) IR (KBr, cm^{-1}): 2530-3435(OH), 1718 (C=O acetyl), 1651 broad (C=O ketonic and COOH carbonyl). $^1\text{H-NMR}$ (400 MHz, CDCl_3 , δ ppm, J Hz) : 8.34 (s, 1H, Ar H2); 8.14-8.12 (m, 2H, Ar H4,6) ; 7.84 (s, 1H, triazole H5); 7.64-7.60(t, 1H, J=8, Ar H5); 5.82 (s, 1H, steroidal C4-H) ; 3.13-0.66 (unresolved multiplets of cycloaliphatic protons of the steroidal nucleus in addition to acetyl and C18 methyl protons).

$^{13}\text{C-NMR}$ (400 MHz, CDCl_3) : δ 14.82(C18), 21.73(O=C- CH_3), 24.07(C11), 25.91(C15), 26.37(C7), 30.70(C6), 32.90(C16), 35.47(C2), 36.33(C1,C12), 40.72(C8), 42.41(C10), 46.36(C14), 47.61(C13), 48.65(C9), 88.11(C17), 119.39(ArC2), 121.15(ArC4), 124.50(ArC5), 125.33(C4), 130.02(triazole C5), 130.11(ArC6), 131.15(triazole C4), 137.12(ArC1), 150.58(ArC3), 166.86(C5), 170.51(O C O C H $_3$, C O O H), 200.37(C3).

Compound (5c) IR (KBr, cm^{-1}): 2565-3455 (OH), 1714 (C=O acetyl), 1645 (C=O ketonic) , 1615 (C=O carboxyl), $^1\text{H-NMR}$ (400 MHz, CDCl_3 , δ ppm, J Hz) : 8.23-8.21 (d, 2H, J = 8.8, Ar H2,6) ; 7.89-7.86 (d, 2H, J = 8.8, Ar H3,5) ; 7.82 (s, 1H, triazole H5) ; 5.81 (s, 1H, steroidal C4-H); 3.75-0.65 (unresolved multiplets of cycloaliphatic protons of the steroidal nucleus in addition to acetyl and C18 methyl protons).

Experimental, Chemistry

Compound (5d) IR (KBr, cm^{-1}): 1722 strong (acetyl and ester carbonyl group), 1656 (C=O ketonic). $^1\text{H-NMR}$ (400 MHz, CDCl_3 , δ ppm, J Hz) : 7.98-7.94(m, 1H, Ar H6); 7.64-7.49 (m, 4H, Ar H3,4,5+ triazole H5) ; 5.77 (s, 1H, steroidal C4-H); 3.67-3.60 (s, 1H, COOCH_3); 3.01-0.68 (unresolved multiplets of cycloaliphatic protons of the steroidal nucleus in addition to acetyl and C18 methyl protons). $^{13}\text{C-NMR}$ (400 MHz, CDCl_3) : δ 14.52(C18), 21.55(OCOCH_3), 24.07(C11), 26.02(C15), 26.57(C7), 29.45(C6), 30.83(C16), 32.77(C2), 35.47(C12), 36.44(C1), 40.75(C8), 42.45(C10), 46.13(C14), 48.91(C9, C13), 52.53(COOCH_3), 88.07(C17), 118.32(ArC3), 123.47(ArC1), 124.57(C4), 126.92(ArC6), 129.83(ArC5, triazole C5), 131.27(triazole C4), 132.63(ArC4), 150.95(ArC2), 166.46(COOCH_3), 195.03 (OCOCH_3), 218.26(C3).

Compound (5e) IR (KBr, cm^{-1}): 1719 strong (acetyl and ester carbonyl group), 1657 (C=O ketonic) . $^1\text{H-NMR}$ (400 MHz, DMSO-d_6 , δ ppm, J Hz) : 8.84 (s, 1H, Ar H2); 8.44 (m, 1H, triazole H5) ; 8.24-8.22 (m, 1H, Ar H6) ; 8.03-8.02 (d, $J = 7.6$, 1H, Ar H4) ; 7.76-7.71 (m, 1H, Ar H5); 5.67(s, 1H, steroidal C4-H); 3.90 (s, 1H, COOCH_3); 3.40-0.54(unresolved multiplets of cycloaliphatic protons of the steroidal nucleus in addition to acetyl and C18 methyl protons).

Compound (5f) IR (KBr, cm^{-1}): 1715 strong (acetyl and ester C=O group), 1655 (C=O ketonic). $^1\text{H-NMR}$ (400 MHz, DMSO-d_6 , δ ppm, J Hz) : 8.11-8.09 (d, 2H, $J = 8.8$, Ar H2,6); 8.08-8.05 (d, 2H, $J = 8.8$, Ar H3,5); 8.78(s, 1H, triazole H5); 5.63(s, 1H, steroidal C4-H); 3.83 (s, 1H, COOCH_3) ; 3.33-1.03(unresolved multiplets of cycloaliphatic protons of the steroidal nucleus in addition to acetyl and C18 methyl protons).

4.2. BIOLOGY

4.2) BIOLOGY

4.2.1) Progestational Screening:

General notes:

Animals: Adult female Wistar rats (weighing 200 -215g) were housed into 8 groups 6 per cage at 20-22°C under controlled conditions of light, with free access to rat chow and tap water. Rats showing regular estrous cycle length (4–5 days). The phases of estrous cycle were determined by observing the vaginal smear in the morning according to Cooper, *et al.*⁹⁶ Only those rats showing at least two consecutive 4-days estrous cycles were used. For all experiments the treatment was started when the animals were in estrus phase.⁹⁷

Reference standard: Norethindrone acetate was obtained as a gift from Hi pharm pharmaceutical company, El Obour City, Egypt.

Morphometric measurements: were calculated using Lieca Qwin 500 Image Analyzer in Pathology Department, National Research Centre, Cairo, Egypt.

All the *in vivo* investigational studies were carried out in Pharmacology and Pathology Departments, National Research Centre, Cairo, Egypt.

4.2.1.1) Methodology

Initial body weight before treatment and final body weight at the time of sacrifice were recorded. Then solution of the tested compounds **5(a-f)** or reference standard (Norethindrone acetate) in DMSO (0.018 mg/mL) was injected subcutaneously daily for 8 days to rat groups, while the control group received an equivalent amount of the vehicle. Twenty-four hours after the final dose, rats were killed, and their uteri were carefully excised, trimmed of extraneous tissue, blotted filter paper to remove excess fluid, weighed to calculate the uterus weight as the following:⁹⁸

Relative organ weight (kg) = [organ weight (g)/body weight (g)] ×
1000

The uteri were fixed and stained, paraffin sections were evaluated for histological changes. The thickness endometrium, myometrium and the uterine epithelial cell heights were measured using an objective lens of magnification 10, and eye lens 10, the total magnification was 100 times. Ten fields were chosen in each specimen and the mean values were taken.

4.2.1.2) Statistical analysis:

The data were expressed as mean ± SEM and analyzed using SPSS statistical software. One way analysis of variance (ANOVA) was used to assess the variation of the means among the treatments. If the variation was greater than expected by chance alone, Tukey multiple comparison tests were performed to compare each treatment group with the control and standard groups. Significance was established when the p value was less than 0.05. *In vivo* progestational screening results of the tested compounds 5(a-f) and reference drug in comparison to the control were given in **Table (4)**.

4.2.2) Anticancer Screening:

All the *in vitro* investigational studies were carried out in National Cancer Institute (NCI), Bethesda, Maryland, USA under the Development Therapeutic Program (DTP) of NCI according to reported procedure.⁹⁹

4.2.2.1) *In vitro* anticancer screening

The human tumor cell lines of the cancer screening panel are grown in RPMI 1640 medium containing 5% fetal bovine serum and 2 mM L-glutamine. For a typical screening experiment, cells are inoculated into 96 well microtiter plates in 100 μ L at plating densities ranging from 5,000 to 40,000 cells/well depending on the doubling time of individual cell lines. After cell inoculation, the microtiter plates are incubated at 37° C, 5 % CO₂, 95 % air and 100 % relative humidity for 24 h prior to addition of experimental drugs.

After 24 h, two plates of each cell line are fixed *in situ* with TCA, to represent a measurement of the cell population for each cell line at the time of compound addition (Tz). The 60 human cancer cell lines used in the screen are Leukemia (L) lines CCRF-CEM, HL-60(TB), K-562, MOLT-4, RPMI-8226, SR; Non small cell lung cancer (NSCLC) lines A549/ATCC, HOP-62, NCI-H226, NCI-H23, NCI-H322M, NCI-H460, NCI-H522; Colon cancer (CL) lines COLO 205, HCC-2998, HCT-116, HCT-15, HT29, SW-620; Central nervous system cancer (CNSC) lines SF-268, SF-295, SF-539, SNB-19, SNB-75, U251; Melanoma (M) lines LOX IMVI, MALME-3M, M14, SK-MEL-2, SK-MEL-28, SK-MEL-5, UACC-257, UACC-62; Ovarian cancer (OC) lines IGR-OV1, OVCAR-3, OVCAR-4, OVCAR-5, OVCAR-8, NCI/ADR-RES, SK-OV-3; Renal cancer (RC) lines 786-0, A498, ACHN, CAKI-1, RXF 393, SN12C, TK-10, UO-31; Prostate cancer (PC) line PC-3, DU-145 and Breast cancer

(BC) lines MCF7, NCI/ADR-RES, MDA-MB-231/ATCC, HS 578T, MDA-MB-468, BT-549, T-47D .

4.2.2.2) Addition of experimental agents:

Experimental compounds (**5a-f**) are solubilized in dimethylsulfoxide at 400-fold the desired final maximum test concentration and stored frozen prior to use. At the time of compound addition, an aliquot of frozen concentrate is thawed and diluted to twice the desired final maximum test concentration with complete medium containing 50 µg/ml gentamicin. Additional four, 10-fold or ½ log serial dilutions are made to provide a total of five compound concentrations plus control. Aliquots of 100 µl of these different compound dilutions are added to the appropriate microtiter wells already containing 100 µl of medium, resulting in the required final concentrations.

4.2.2.3) Endpoint measurement:

Following compound addition, the plates are incubated for an additional 48 h at 37°C, 5 % CO₂, 95 % air, and 100 % relative humidity. For adherent cells, the assay is terminated by the addition of cold TCA. Cells are fixed *in situ* by the gentle addition of 50 µl of cold 50 % (w/v) TCA (final concentration, 10 % TCA) and incubated for 60 minutes at 4°C. The supernatant is discarded, and the plates are washed five times with tap water and air dried. Sulforhodamine B (SRB) solution (100 µl) at 0.4 % (w/v) in 1 % acetic acid is added to each well, and plates are incubated for 10 minutes at room temperature. After staining, unbound dye is removed by washing five times with 1 % acetic acid and the plates are air dried. Bound stain is subsequently solubilized with 10 mM trizma base, and the absorbance is read on an automated plate reader at a wavelength of 515 nm. For suspension cells, the methodology is the same except that the assay is terminated by fixing settled cells at the bottom of

the wells by gently adding 50 µl of 80 % TCA (final concentration, 16 % TCA).

4.2.2.4) Calculation of Percentage Growth (PG) inhibition

Using the seven absorbance measurements [time zero (Tz), control growth, (C), and test growth in the presence of tested compound at the five concentration levels (Ti)], the percentage growth is calculated at each of the compound concentrations levels. Compounds which exhibit significant growth inhibition are evaluated against the 60 cell panel at five concentration levels.

Percentage growth inhibition is calculated as:

$$[(Ti-Tz)/(C-Tz)] \times 100 \text{ for concentrations for which } Ti \geq Tz$$

$$[(Ti-Tz)/Tz] \times 100 \text{ for concentrations for which } Ti < Tz.$$

4.2.2.5) Calculation of special concentration parameters:

Three dose response parameters are calculated for each experimental agent. Growth inhibition of 50 % (GI50) is calculated from $[(Ti-Tz)/(C-Tz)] \times 100 = 50$, which is the compound concentration resulting in a 50% reduction in the net protein increase (as measured by SRB staining) in control cells during the drug incubation. The compound concentration resulting in total growth inhibition (TGI) is calculated from $Ti = Tz$. The LC50 (concentration of compound resulting in a 50% reduction in the measured protein at the end of the compound treatment as compared to that at the beginning) indicating a net loss of cells following treatment is calculated from $[(Ti-Tz)/Tz] \times 100 = -50$. Values are calculated for each of these three parameters if the level of activity is reached; however, if the effect is not reached or is exceeded, the value for that parameter is expressed as greater or less than the maximum or minimum concentration tested.

4.3 MOLECULAR MODELING

4.3) MOLECULAR MODELING

Molecular modeling and docking simulation studies were carried out at the Department of Medicinal Chemistry, Faculty of Pharmacy, Assiut University, Assiut, Egypt.

Software and hardware:

All the molecular modeling calculations and docking simulation studies were performed using Molecular Operating Environment (MOE[®]) version 10.2010, Chemical Computing Group (CCG) Inc., Montreal, Canada.⁸⁵ The computational software operated under “Windows XP” installed on an Intel Pentium IV PC with a 1.6 GHz processor and 512 MB memory. All the interaction energies and different calculations were automatically calculated.

General methodology:

4.3.1) Target compounds optimization

The target compounds were constructed into a 3D model using the builder interface of the MOE program. After checking their structures and the formal charges on atoms by 2D depiction, the following steps were carried out:

- The target compounds were subjected to a conformational search.
- All conformers were subjected to energy minimization, all the minimizations were performed with MOE until a RMSD gradient of 0.01 Kcal/mole and RMS distance of 0.1 Å with MMFF94X force-field and the partial charges were automatically calculated.
- The obtained data base was then saved as MDB file to be used in the docking calculations.

4.3.2) Optimization of the enzymes active site

The X-ray crystallographic structures of progesterone receptor complexed with norethindrone (PDB Id: 1SQN) was obtained from the Protein Data Bank through the internet.^{100,56} The enzymes were prepared for docking studies by:

- The ligand molecules, norethindrone, was removed from progesterone receptor active sites.
- Hydrogen atoms were added to the system with their standard geometry.
- The atoms connection and type were checked for any errors with automatic correction.
- Selection of the receptor and its atoms potential were fixed.
- MOE Alpha Site Finder was used for the active site search in the enzyme structure using all default items. Dummy atoms were created from the obtained alpha Spheres.

4.3.3) Docking of the target molecules to the progesterone receptor active sites

Docking of the conformation database of the target compounds was done using MOE-Dock software. The following methodology was generally applied:

- The enzyme active site file was loaded and the Dock tool was initiated. The program specifications were adjusted to:
 - Dummy atoms as the docking site.
 - Triangle matcher as the placement methodology to be used.

- London dG as Scoring methodology to be used and was adjusted to its default values.
- The MDB file of the ligand to be docked was loaded and Dock calculations were run automatically.
- The obtained poses were studied and the poses showed best ligand-enzyme interactions were selected and stored for energy calculations.

4.3.4) Exploring the binding mode and energy calculations of the target molecules

The best pose for each ligand was explored using LigX tool. In LigX calculations, the following steps were applied:

- The ligand is verified in the active site.
- Protonate 3D application was used to optimally place hydrogens and partial charges on the receptor-ligand complex atoms.
- Applying tether and minimize tool to constrain the receptor atoms far from the ligand (held fixed), while receptor atoms near the ligand (in the active site) are allowed to move with restraints.
- Using properties and minimize tools, the properties of the ligand and the energy calculations were calculated and displayed.

The 2D ligand interactions were obtained for each compound and different stereo views of the ligands inside the active site were saved as both MOE and photo files.

5. REFERENCES

REFERENCES

1. B. S. Apgar, G. Greenberg, Using progestins in clinical practice, *Am. Fam. Physician*, **2000**, 62, 1839-1846.
2. J. A. Maybin, H. O. D. Critchley, Steroid regulation of menstrual bleeding and endometrial repair, *Rev. Endocr. Metab. Disord.*, **2012**, 13, 253-263.
3. T. L. Lemke, D. A. Williams, "Foye's Principles of Medicinal Chemistry", 6th edition, Lippincott Williams & Wilkins, Philadelphia, **2008**, pp 1311-1317.
4. F. Z. Stanczyk, All progestins are not created equal, *Steroids*, **2003**, 68, 879-890.
5. R. Bursi, M. B. Groen, Application of (quantitative) structure-activity relationships to progestagens: from serendipity to structure-based design, *Eur. J. Med. Chem.*, **2000**, 35, 787-796.
6. T. Levy, S. Gurevitch, I. Bar-Hava, J. Ashkenazi, A. Magazanik, R. Homburg, R. Orvieto, Z. Ben-Rafael, Pharmacokinetics of natural progesterone administered in the form of a vaginal tablet, *Hum. Reprod.*, **1999**, 14, 606-610.
7. F. Z. Stanczyk, M. R. Henzl, Use of the name "Progestin", *Contraception* **2001**, 64, 1-2.
8. A. E. Schindler, C. Campagnoli, R. Druckmann, J. Huber, J. R. Pasqualini, K. W. Schweppe, J. H. H. Thijssen, Classification and pharmacology of progestins, *Maturitas*, **2003**, 46S1,S7-S16.
9. F. Z. Stanczyk, Pharmacokinetics and potency of progestins used for hormone replacement therapy and contraception, *Rev. Endocr. Metab. Disord*, **2002**, 3, 211-224.

References

10. R. A. Lobo, "Treatment of the Postmenopausal Woman: Basic And Clinical Aspects", 3rd edition, Academic Press/Elsevier, 2007, pp 779-796.
11. A. E. Schindler, Progestational effects of dydrogesterone *in vitro*, *in vivo* and on the human endometrium, *Maturitas*, 2009, 65, Supplement 1, S3-S11.
12. X. Ruan, H. Seeger, A. O. Mueck, The pharmacology of nomegestrol acetate, *Maturitas*, 2012, 71, 345–353.
13. N. Kumar, S. S. Koide, Y. Y. Tsong, K. Sundaram, Nestorone®: a progestin with a unique pharmacological profile, *Steroids*, 2000, 65, 629 – 636.
14. Z. Tuba, C. W. Bardin, A. Dancsi, E. Francsics-Czinege, C. Molnár, J. Csörgei, G. Falkay, S. S. Koide, N. Kumar, K. Sundaram, V. Dukát–Abrók, G. Balogh, Synthesis and biological activity of a new progestogen, 16-methylene-17 α -hydroxy-18-methyl-19-norpregn-4-ene-3,20-dione acetate, *Steroids*, 2000, 65, 266 –274.
15. F. Stanczyk, S. Roy, Metabolism of levonorgestrel, norethindrone, and structurally related contraceptive steroids, *Contraception*, 1990, 42, 67-96.
16. J. Yasuda, H. Honjo, H. Okada, Metabolism of lynestrenol: Characterization of 3-hydroxylation using rabbit liver microsomes *in vitro*, *J. Steroid Biochem.*, 1984, 21, 777-780.
17. N. Goldstuck, Progestin potency-Assessment and relevance to choice of oral contraceptives, *Middle East Fertil. Soc. J.*, 2011, 16, 248-253.

References

18. P. G. Crosignani, C. Nappi, S. Ronsini, V. Bruni, S. Marelli, D. Sonnino, Satisfaction and compliance in hormonal contraception: the result of a multicentre clinical study on women's experience with the ethinylestradiol/norelgestromin contraceptive patch in Italy, *BMC Womens Health*, **2009**, *9*,1-11.
19. M. Oettel, A. Kurischko, STS 557, A new orally active progestin with antiprogestational and contragestational properties in rabbits, *Contraception*, **1980**, *21*, 61-75.
20. R. Druckmann, Profile of the progesterone derivative chlormadinone acetate-pharmacodynamic properties and therapeutic applications, *Contraception*, **2009**, *79*, 272-281.
21. D. C. Collins, Sex hormone receptor binding, progestin selectivity, and the new oral contraceptives, *Am. J. Obstet. Gynecol.*, **1994**, *170*, 1508-1513.
22. L. Liang, D. Astruc, The copper(I)-catalyzed alkyne-azide cycloaddition (CuAAC) "click" reaction and its applications. An overview, *Coord. Chem. Rev.*, **2011**, 2933-2945.
23. V. V. Rostovtsev, L. G. Green, V. V. Fokin, K. B. Sharpless, A stepwise Huisgen cycloaddition process: copper(I)-catalyzed regioselective ligation of azides and terminal alkynes, *Angew. Chem. Int. Ed.*, **2002**, *41*, 2596-2599.
24. S. G. Agalave, S. R. Maujan, V. S. Pore, Click chemistry: 1,2,3-triazoles as pharmacophores, *Chem. Asian J.*, **2011**, *6*, 2696 – 2718.
25. J. Kalia, R. T. Raines, Advances in bioconjugation, *Curr. Org. Chem.*, **2010**, *14*, 138–147.

References

26. K. Nwe, M. W. Brechbiel, Growing applications of “Click Chemistry” for bioconjugation in contemporary biomedical research *Cancer Biother. Radiopharm.*, **2009**, 24, 289-302.
27. B. Peschke, M. Zundel, S. Bak, T. R. Clausen, N. Blume, A. Pedersen, F. Zaragoza, K. Madsen, C-Terminally PEGylated hGH-derivatives, *Bioorg. Med. Chem.*, **2007**, 15, 4382-4395.
28. A. Salic, T. J. Mitchison, A chemical method for fast and sensitive detection of DNA synthesis *in vivo*, *Proc. Natl. Acad. Sci.*, **2008**, 105, 2415-2420.
29. X.-L. Sun, C. L. Stabler, C. S. Cazalis, E. L. Chaikof, Carbohydrate and protein immobilization onto solid surfaces by sequential Diels-Alder and azide-alkyne cycloadditions, *Bioconjugate Chem.*, **2006**, 17, 52-57.
30. E. Lallana, F. Fernandez-Trillo, A. Sousa-Herves, R. Riguera, E. Fernandez-Megia, Click chemistry with polymers, dendrimers, and hydrogels for drug delivery, *Pharm. Res.*, **2012**, 29, 902-921.
31. N. G. Angelo, P. S. Arora, Nonpeptidic foldamers from amino acids: Synthesis and characterization of 1,3-substituted triazole oligomers, *J. Am. Chem. Soc.*, **2005**, 127, 17134-17135.
32. S. Srinivasachari, T. M. Reineke, Versatile supramolecular pDNA vehicles via “click polymerization” of β -cyclodextrin with oligoethyleneamines, *Biomaterials*, **2009**, 30, 928-938.
33. P. Antoni, Y. Hed, A. Nordberg, D. Nyström, H. V. Holst, A. Hult, M. Malkoch, Bifunctional dendrimers: From robust synthesis and accelerated one-pot postfunctionalization strategy to potential applications, *Angew. Chem., Int. Ed.*, **2009**, 48, 2126-2130.

References

34. D. A. Ossipov, J. Hilborn, Poly(vinyl alcohol)-based hydrogels formed by "Click Chemistry", *Macromolecules*, **2006**, *39*, 1709-1718.
35. F. Pagliai, T. Pirali, E. D. Grosso, R. D. Brisco, G. C. Tron, G. Sorba, A. A. Genazzani, Rapid synthesis of triazole-modified resveratrol analogues via click chemistry, *J. Med. Chem.*, **2006**, *49*, 467-470.
36. L. B. Peterson, B. S. J. Blagg, Click chemistry to probe Hsp90: Synthesis and evaluation of a series of triazole-containing novobiocin analogues, *Bioorg. Med. Chem. Lett.*, **2010**, *20*, 3957-3960.
37. D. Kumar, V. B. Reddy, A. Kumar, D. Mandal, R. Tiwari, K. Parang, Click chemistry inspired one-pot synthesis of 1,4-disubstituted 1,2,3-triazoles and their Src kinase inhibitory activity, *Bioorg. Med. Chem. Lett.*, **2011**, *21*, 449-452.
38. A. H. Banday, S. A. Shameem, B. D. Gupta, H. M. S. Kumar, D-ring substituted 1,2,3-triazolyl 20-keto pregnenanes as potential anticancer agents: Synthesis and biological evaluation, *Steroids*, **2010**, *75*, 801-804.
39. M. Whiting, J. C. Tripp, Y. Lin, W. Lindstrom, A. J. Olson, J. H. Elder, K. B. Sharpless, V. V. Fokin, Rapid discovery and structure-activity profiling of novel inhibitors of human immunodeficiency virus type 1 protease enabled by the copper(I)-catalyzed synthesis of 1,2,3-triazoles and their further functionalization, *J. Med. Chem.*, **2006**, *49*, 7697-7710.
40. R. V. Somu, H. Boshoff, C. Qiao, E. M. Bennett, C. E. Barry, C. C. Aldrich, Rationally designed nucleoside antibiotics that inhibit siderophore biosynthesis of *Mycobacterium tuberculosis*, *J. Med. Chem.*, **2006**, *49*, 31-34.

References

41. C. Gill, G. Jadhav, M. Shaikh, R. Kale, A. Ghawalkar, D. Nagargoje, M. Shiradkar, Clubbed [1,2,3] triazoles by fluorine benzimidazole: A novel approach to H37Rv inhibitors as a potential treatment for tuberculosis, *Bioorg. Med. Chem. Lett.*, **2008**, 18, 6244-6247.
42. V. S. Pore, N. G. Aher, M. Kumar, P. K. Shukla, Design and synthesis of fluconazole/bile acid conjugate using click reaction, *Tetrahedron*, **2006**, 62, 11178-11186.
43. N. G. Aher, V. S. Pore, N. N. Mishra, A. Kumar, P. K. Shukla, A. Sharma, M. K. Bhat, Synthesis and antifungal activity of 1,2,3-triazole containing fluconazole analogues, *Bioorg. Med. Chem. Lett.*, **2009**, 19, 759-763.
44. P. M. Chaudhary, S. R. Chavan, F. Shirazi, M. Razdan, P. Nimkar, S. P. Maybhate, A. P. Likhite, R. Gonnade, B. G. Hazara, M. V. Deshpande, S. R. Deshpande, Exploration of click reaction for the synthesis of modified nucleosides as chitin synthase inhibitors, *Bioorg. Med. Chem.*, **2009**, 17, 2433-2440.
45. V. Sumangala, B. Poojary, N. Chidananda, J. Fernandes, N. S. Kumari, Synthesis and antimicrobial activity of 1,2,3-triazoles containing quinoline moiety, *Arch. Pharm. Res.*, **2010**, 33, 1911-1918.
46. O. A. Phillips, E. E. Udo, M. E. Abdel-Hamid, R. Varghese, Synthesis and antibacterial activity of novel 5-(4-methyl-1H-1,2,3-triazole) methyl oxazolidinones, *Eur. J. Med. Chem.*, **2009**, 44, 3217-3227.
47. O. A. Phillips, E. E. Udo, M. E. Abdel-Hamid, R. Varghese, Synthesis and antibacterial activities of N-substituted-glycinyll 1H-1,2,3-triazolyl oxazolidinones, *Eur. J. Med. Chem.*, **2013**, 66, 246-257.

References

48. B. Zhang, E. Zhang, L. Pang, L. Song, Y. Li, B. Yu, H. Liu, Design and synthesis of novel D-ring fused steroidal heterocycles, *Steroids*, **2013**, 78, 1200-1208.
49. N. Fan, J. Tang, H. Li, X. Li, B. Luo, J. Gao, Synthesis and cytotoxic activity of some novel steroidal C-17 pyrazolanyl derivatives, *Eur. J. Med. Chem.*, **2013**, 69, 182-190.
50. A. H. Banday, B. P. Mir, I. H. Lone, K. A. Suri, H. M. S. Kumar, Studies on novel D-ring substituted steroidal pyrazolines as potential anticancer agents, *Steroids*, **2010**, 75, 805-809.
51. A. H. Banday, S. Singh, M. S. Alam, D. M. Reddy, B. D. Gupta, H. M. S. Kumar, Synthesis of novel steroidal D-ring substituted isoxazoline derivatives of 17-oxoandrostanes, *Steroids*, **2008**, 73, 370-374.
52. Z. Szarka, R. Skoda-Földes, J. Horváth, Z. Tuba, L. Kollár, Synthesis of steroidal diacyl hydrazines and their 1,3,4-oxadiazole derivatives, *Steroids*, **2002**, 67, 581-586.
53. R. M. Mohareb, N. N. E. El-Sayed, M. A. Abdelaziz, The Knoevenagel reactions of pregnenolone with cyanomethylene reagents: Synthesis of thiophene, thieno[2,3-b]pyridine, thieno[3,2-d]isoxazole derivatives of pregnenolone and their in vitro cytotoxicity towards tumor and normal cell lines, *Steroids*, **2013**, 78, 1209-1219.
54. J. A. R. Salvador, R. M. A. Pinto, S. M. Silvestre, Steroidal 5 α -reductase and 17 α -hydroxylase/17,20-lyase (CYP17) inhibitors useful in the treatment of prostatic diseases, *J. Steroid Biochem. Mol. Biol.*, **2013**, 137, 199-222.

References

55. M. Togashi, S. Borngraeber, B. Sandler, R. J. Fletterick, P. Webb, J. D. Baxter, Conformational adaptation of nuclear receptor ligand binding domains to agonists: Potential for novel approaches to ligand design, *J. Steroid Biochem. Mol. Biol.*, **2005**, 93, 127-137.
56. K. P. Madauss, S. Deng, R. J. H. Austin, M. H. Lambert, I. McLay, J. Pritchard, S. A. Short, E. L. Stewart, I. J. Uings, S. P. Williams, Progesterone receptor ligand binding pocket flexibility: crystal structures of the norethindrone and mometasone furoate complexes, *J. Med. Chem.*, **2004**, 47, 3381-3387.
57. J. Hou, X. Liu, J. Shen, G. Zhao, P. G. Wang, The impact of click chemistry in medicinal chemistry, *Expert Opin. Drug Discov.*, **2012**, 7, 489-501.
58. S. Bräse, C. Gil, K. Knepper, V. Zimmermann, Organic azides: An exploding diversity of a unique class of compounds, *Angew. Chem. Int. Ed.*, **2005**, 5188-5240.
59. R. N. Butler, A. Fox, S. Collier, L. A. Burke, Pentazole chemistry: The mechanism of the reaction of aryl diazonium chlorides with azide ion at -80°C: Concerted *versus* stepwise formation of arylpentazoles, detection of a pentazene intermediate, a combined ¹H and ¹⁵N NMR experimental and *ab initio* theoretical study, *J. Chem. Soc., Perkin Trans. 2*, **1998**, 2243-2247.
60. S. M. Capitosti, T. P. Hansen, M. L. Brown, Facile Synthesis of an azido-labeled thalidomide analogue, *Org. Lett.*, **2003**, 5, 2865 - 2867.
61. K. A. H. Chehade, H. P. Spielmann, Facile and efficient synthesis of 4-azidotetrafluoroaniline: A new photoaffinity reagent, *J. Org. Chem.*, **2000**, 65, 4949-4953.

References

62. D. R. Miller, D. C. Swenson, E. G. Gillan, Synthesis and structure of 2,5,8-triazido-s-heptazine: An energetic and luminescent precursor to nitrogen-rich carbon nitrides, *J. Am. Chem. Soc.*, **2004**, 126, 5372-5373.
63. W. Stadlbauer, W. Fiala, M. Fischer, G. Hojas, Thermal cyclization of 4-azido-3-nitropyridines to furoxanes [1], *J. Heterocycl. Chem.*, **2000**, 37, 1253 – 1256.
64. J. Gavenonis, T. D. Tilley, Tantalum alkyl and silyl complexes of the bulky(terphenyl) imido ligand $[2,6-(2,4,6\text{-Me}_3\text{C}_6\text{H}_2)_2\text{C}_6\text{H}_3\text{N=}]^2-$ ($[\text{Ar}^*\text{N=}]^2-$). Generation and reactivity of $[(\text{Ar}^*\text{N=})(\text{Ar}^*\text{NH})\text{Ta}(\text{H})(\text{OSO}_2\text{CF}_3)]$, Which reversibly transfers hydride to an aromatic ring of the arylamide ligand, *Organometallics*, **2002**, 21, 5549 –5563.
65. Q. Liu, Y. Tor, Simple conversion of aromatic amines into azides, *Org. Lett.*, **2003**, 5, 2571–2572.
66. Y. H. Kim, K. Kim, S. B. Shim, Facile synthesis of azides: Conversion of hydrazines using dinitrogen tetroxide, *Tetrahedron Lett.*, **1986**, 27, 4749-4752.
67. V. T. Bhat, N. R. James, A. Jayakrishnan, A photochemical method for immobilization of azidated dextran onto aminated poly(ethylene terephthalate) surfaces, *Polym. Int.*, **2008**, 57, 124–132.
68. Y. Xiong, D. Bernardi, S. Bratton, M. D. Ward, E. Battaglia, M. Finel, R. R. Drake, A. Radomska-Pandya, Phenylalanine 90 and 93 are localized within the phenol binding Site of Human UDP-glucuronosyl transferase 1A10 as determined by photoaffinity labeling , mass spectrometry, and site-directed mutagenesis, *Biochemistry*, **2006**, 45, 2322-2332.

References

69. K. Lamara, R. K. Smalley, 3_H -azepines and related systems. Part 4. Preparation of 3_H -azepin-2-ones and 6_H -azepino[2,1-b]quinazolin-12-ones by photo-induced ring expansions of aryl azides, *Tetrahedron*, **1991**, 47, 2277-2290.
70. H. A. Hassan, Synthesis and characterization of some new 1,2,3-triazole, Pyrazolin-5-one and thiazolidinone derivatives, *Journal of Al-Nahrain University*, **2013**, 16, 53-59.
71. F. Santoyo-González, F. Hernández-Mateo, Azide-alkyne 1,3-dipolar cycloadditions: a valuable tool in carbohydrate chemistry, *Top. Heterocycl. Chem.*, **2007**, 7, 133-177.
72. J. E. Hein, V. V. Fokin, Copper-catalyzed azide-alkyne cycloaddition (CuAAC) and beyond: new reactivity of copper (I) acetylides, *Chem. Soc. Rev.*, **2010**, 39, 1302-1315.
73. P. L. Golas, K. Matyjaszewski, Marrying click chemistry with polymerization: expanding the scope of polymeric materials, *Chem. Soc. Rev.*, **2010**, 39, 1338-1354.
74. I. Coblenz Society, Inc., "Evaluated infrared reference spectra" in NIST chemistry webBook, NIST standard reference database number 69, Eds. P.J. Linstrom and W.G. Mallard, National institute of standards and technology, Gaithersburg MD, 20899, <http://webbook.nist.gov/cgi/cbook.cgi?ID=C68224&Mask=80#Top>.
75. Coblenz Society, Inc., "Evaluated infrared reference spectra" in NIST chemistry webBook, NIST standard reference database number 69, Eds. P.J. Linstrom and W.G. Mallard, National institute of standards and technology, Gaithersburg MD, 20899, <http://webbook.nist.gov/cgi/cbook.cgi?ID=C51989&Mask=80>.

References

76. B-Y. Lu, Z-M. Li, Y-Y. Zhu, X. Zhao, Z-T. Li, Assessment of the intramolecular C-H...X (X=F, Cl, Br) hydrogen bonding of 1,4-diphenyl-1,2,3-triazoles, *Tetrahedron*, **2012**, 68, 8857 - 8862.
77. E. Pretsch, T. Clerc, J. Seibl, W. Simon, in "*Tabellen zur Strukturaufklärung organischer Verbindungen mit spektroskopischen Methoden*", Springer Berlin Heidelberg, **1981**, vol. 15, pp. 55-107.
78. R. M. Silverstein, F. X. Webster, "*Specrometric identification of organic compounds*", 6th edition, John Wiley & sons Inc., New York, **1998**, pp. 236-249.
79. N. Ai, M. D. Krasowski, W. J. Welsh, S. Ekins, Understanding nuclear receptors using computational methods, *Drug Discov. Today*, **2009**, 14, 486-494.
80. X. Gao, Z. Nawaz, Progesterone receptors-animal models and cell signaling in breast cancer: Role of steroid receptor coactivators and corepressors of progesterone receptors in breast cancer, *Breast Cancer Res.*, **2002**, 4, 182-186.
81. S. P. Williams, P. B. Sigler, Atomic structure of progesterone complexed with its receptor, *Nature*, **1998**, 393, 392-396.
82. Z. Zhang, A. M. Olland, Y. Zhu, J. Cohen, T. Berrodin, S. Chippari, C. Appavu, S. Li, J. Wilhem, R. Chopra, A. Fensome, P. Zhang, J. Wrobel, R. J. Unwalla, C. R. Lyttle, R. C. Winneker, Molecular and pharmacological properties of a potent and selective novel nonsteroidal progesterone receptor agonist tanaproget, *J. Biol. Chem.*, **2005**, 280, 28468-28475.
83. R. C. Winneker, A. Fensome, P. Zhang, M. R. Yudt, C. C. McComas, R. J. Unwalla, A new generation of progesterone receptor modulators, *Steroids*, **2008**, 73, 689-701.

References

84. C. F. Wong, Flexible ligand-flexible protein docking in protein kinase systems, *Biochim. Biophys. Acta*, **2008**, 1784, 244-251.
85. Molecular operating Environment (MOE), Chemical Computing group Inc., Montreal, Quebec, Canada, <http://www.chemcomp.com>.
86. S. G. Molinspiration Cheminformatics, Slovak Republic, <http://www.molinspiration.com>.
87. C. A. Lipinski, F. Lombardo, B. W. Dominy, P. J. Feeney, Experimental and computational approaches to estimate solubility and permeability in drug discovery and development settings., *Adv. Drug Delivery Rev.*, **2012**, 64, 4-17.
88. Y. Qiu, Y. Chen, G. G. Z. Zhang, L. Liu, W. Porter, "Developing Solid Oral Dosage Forms: Pharmaceutical Theory and Practice", 1st edition, Academic Press, New York, **2008**, pp 282.
89. T. J. Hou, K. Xia, W. Zhang, X. J. Xu, ADME evaluation in drug discovery. 4. Prediction of aqueous solubility based on atom contribution approach, *J. Chem. Inf. Comput. Sci.*, **2004**, 44, 266-275.
90. P. Ertl, B. Rohde, P. Selzer, Fast calculation of molecular polar surface area as a sum of fragment-based contributions and its application to the prediction of drug transport properties, *J. Med. Chem.*, **2000**, 43, 3714-3717.
91. J. Kelder, P. D. J. Grootenhuis, D. M. Bayada, L. P. C. Delbressine, J.-P. Ploemen, Polar molecular surface as a dominating determinant for oral absorption and brain penetration of drugs, *Pharm. Res.*, **1999**, 16, 1514-1519.
92. M. L. Connolly, Computation of molecular volume, *J. Am. Chem. Soc.*, **1985**, 107, 1118-1124

References

93. V. T. Bhat, N. R. James, A. Jayakrishnan, A photochemical method for immobilization of azidated dextran onto aminated poly (ethylene terephthalate) surfaces, *Polym. Int.*, **2008**, 57, 124–132.
94. D. Harrison, A. C. B. Smith, The synthesis of some cyclic hydroxamic acids from o- aminocarboxylic acids, *J. Chem. Soc.*, **1960**, 2157-2160.
95. A. I. Vogel, A. R. Tatchell, B. S. Furnis, A. J. Hannaford, P. W. G. Smith, "*Vogel's Textbook of Practical Organic Chemistry*", 5th Edition, Longman, United Kingdom, **1989**, pp 1077.
96. R. L. Cooper, J. M. Goldman, J. G. Vandenberg, "*Monitoring of the estrous cycle in the laboratory rodent by vaginal lavage*. In: Heindel JJ, Chapin RE, eds. *Methods in Reproductive Toxicology: Female Reproductive Toxicology*", Academic Press, San Diego, **1993**, pp 45-56.
97. D. R. Murthy, C. M. K. Reddy, S. B. Patil, Effect of benzene extract of *Hibiscus rosa sinesis* on the estrous cycle and ovarian activity in albino mice, *Biol. Pharm. Bull.*, **1997**, 20, 756-758.
98. T. S. El-Alfy, M. H. Hetta, N. Z. Yassin, R. F. Abdel-Rahman, E. M. Kadry, Estrogenic activity of *Citrus medica* L. leaves growing in Egypt, *J. App. Pharm. Sci.*, **2012**, 02, 180-185.
99. <http://dtp.nci.nih.gov/branches/btb/ivclsp.html>.
100. <http://www.rcsb.org/pdb/explore.do?structureId=1SQN>.

ARABIC SUMMARY

الملخص العربي

المخلص العربي

تصميم وتشبيد مشتقات 17 ألفا-(1- مستبدل-3،2،1- تريازول-4-ويل)- خلاص 19-

نورستستيرون باستخدام "كيمياء كليك" ذات فاعلية بروجستيرون وكمضادات للسرطان

البروجيستيينات هي مركبات مشيدة تضاهي في تأثيرها بعض (أو كل) تأثيرات البروجيستيرون. ويعتبر الهدف الرئيسي من البحث المتعلق بهذه المركبات هو تصميم مشتقات فعالة عن طريق الفم استنادا الي معرفة المسارات الأيضية للبروجيستيرون. ولقد طورت هذه البروجيستيينات من أجل استخدامها في تنظيم دورة الطمث ومنع تضخم بطانة الرحم وعلاج النزيف الرحمي الغير طبيعي إضافة الي استخدامها في العلاج الهرموني التعويضي وتنظيم الحمل.

الجدير بالذكر أن وجود ذرات غير متجانسة (نيروجين أو أوكسجين أو كبريت) في الحلقة A والحلقة D من الإستيرويدات تحدث امتدادا في الفاعلية البيولوجية لهذه المركبات لتصبح ذات تأثيرات أخرى مثل التأثير المضاد للميكروبات والالتهاب والسرطان إضافة الي التأثير الخافض للكوليستيرول في الدم والتأثير المدر للبول. وفي محاولة الاستفاده من هذا التأثير فقد تم ادخال العديد من الحلقات التي تحوي ذرات غير متجانسة علي المركبات الستيرويدية.

بناءا علي الملاحظات السابقة تم تحضير مجموعة من المركبات عبارة عن مشتقات لعقار خلاص النورايتندرون حاملا مستبدلات 3،2،1- تريازول في الحلقة D باستخدام تفاعل "كليك" وذلك من خلال التفاعل بين مجموعة الايثينيل الطرفية لخلاص النورايتندرون (4) ومجموعة من المستبدل فينيل أزيد (2a-c) و (3a-c) الذين تم اختيارهم بناءا علي دراسة النمجة الجزيئية المبدئية التي تمت علي مستقبل هرمون البروجيستيرون .

تمت موانمة ظروف تفاعل "كليك" من حيث درجة الحرارة المناسبة والوقت المناسب للتفاعل والمذيب المناسب وكذلك النحاس الأحادي المستخدم كعامل حفاز من أجل الحصول علي ناتج جيد من المركبات المستهدف تحضيرها (5a-f).

تم تحضير ستة مركبات وسيطة وهي :

- ٢- أزيدو- حمض البنزويك (2a).
- ٣- أزيدو- حمض البنزويك (2b).
- ٤- أزيدو- حمض البنزويك (2c).
- ميثيل ٢- أزيدو- بنزوات (3a).
- ميثيل ٣- أزيدو- بنزوات (3b).
- ميثيل ٤- أزيدو- بنزوات (3c).

وتم التأكد من التركيب البنائي لهذه المركبات باستخدام قياسات الأشعة دون الحمراء والرنين النووي المغناطيسي المشع للبروتون إضافة الي مقارنة درجة الإنصهار الخاصة بالمركبات بتلك المنشورة مسبقاً.

تم استخدام هذه المركبات في تفاعل "كليك" مع مركب خلاص النور ايتندرون (4) لتحضير المركبات المستهدفة وهي :

- ٢- (٤)-(١٧)-أسيتوكسي-١٣-ميثيل-٣-أوكسو-٢،٣،٤،٦،٧،٨،٩،١٠،١١،١٢،١٣،١٤،١٥-سيكلوبنتا [أ] فينانثرين-١٧-ايد-١،٢،٣-تريازول-١-اويل) حمض البنزويك (5a).
- ٣- (٤)-(١٧)-أسيتوكسي-١٣-ميثيل-٣-أوكسو-٢،٣،٤،٦،٧،٨،٩،١٠،١١،١٢،١٣،١٤،١٥-سيكلوبنتا [أ] فينانثرين-١٧-اويل) حمض البنزويك (5b).
- ٤- (٤)-(١٧)-أسيتوكسي-١٣-ميثيل-٣-أوكسو-٢،٣،٤،٦،٧،٨،٩،١٠،١١،١٢،١٣،١٤،١٥-سيكلوبنتا [أ] فينانثرين-١٧-اويل) حمض البنزويك (5c).

- ميثيل ٢-(٤)-(١٧)-أسيتوكسي-١٣-ميثيل-٣-أوكسو-،٦٤٣،٨٠٧،٩٠٩،١٠١١،١٢،١٣،١٤،١٥،١٦،١٧- أربعة عشر هيدرو-١-يد- سيكلوبنتا [أ] فينانثرين-١٧-ويل)-١-يد-٣،٢،١- تريازول-١-ويل) بنزوات (5d).
- ميثيل ٣-(٤)-(١٧)-أسيتوكسي-١٣-ميثيل-٣-أوكسو-،٦٤٣،٨٠٧،٩٠٩،١٠١١،١٢،١٣،١٤،١٥،١٦،١٧- أربعة عشر هيدرو-١-يد- سيكلوبنتا [أ] فينانثرين-١٧-ويل)-١-يد-٣،٢،١- تريازول-١-ويل) بنزوات (5e).
- ميثيل ٤-(٤)-(١٧)-أسيتوكسي-١٣-ميثيل-٣-أوكسو-،٦٤٣،٨٠٧،٩٠٩،١٠١١،١٢،١٣،١٤،١٥،١٦،١٧- أربعة عشر هيدرو-١-يد- سيكلوبنتا [أ] فينانثرين-١٧-ويل)-١-يد-٣،٢،١- تريازول-١-ويل) بنزوات (5f).

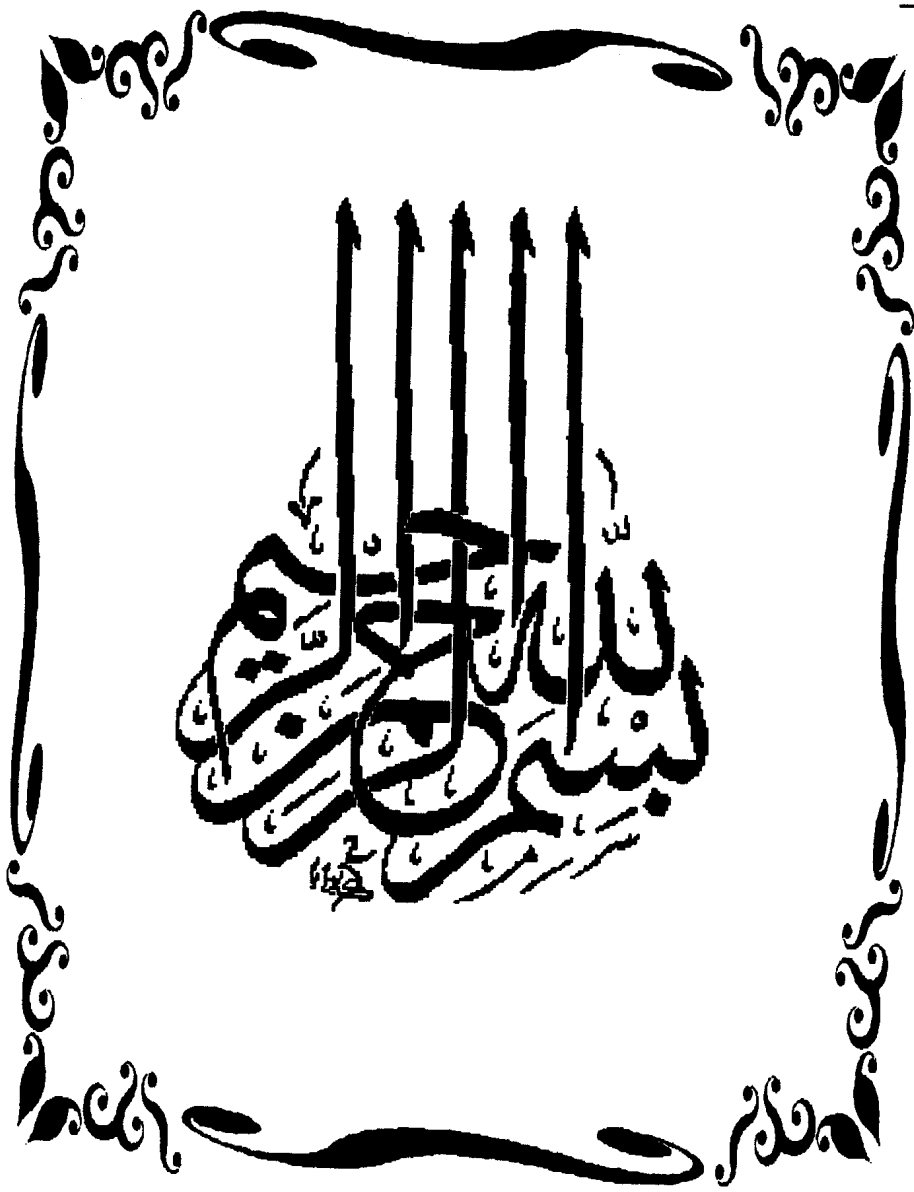
تم تنقية المركبات التي تم تحضيرها باستخدام كروماتوجرافيا السوائل وتم التأكد من التركيب البنائي لهذه المركبات باستخدام التحليل الكمي لعناصر الكربون والنيتروجين والهيدروجين بالإضافة الي قياسات الأشعة دون الحمراء والرنين النووي المغناطيسي للبروتون والكربون المشع.

تمت دراسة الفاعلية البيولوجية للمركبات المشيدة (5a-f) لتقييم نشاطها البروجيستيروني علي رحم الفئران الحية مصحوبا باستخدام مركب خلات النوراينثندرون كعقار مرجعي . أظهر التشريح المجهرى للرحم أن كل المركبات التي تم دراستها أبدت نشاطا بروجيستيرونيا بفاعلية عالية تم استنتاجه من خلال التأثير الملاحظ لهذه المركبات علي طبقة الاندوميتريم والذي أدى إلي زيادة سمكها مع انتشار الغدد الإفرازية مقارنة بالحيوانات التي أستخدمت كمرجع تم حقنه بالمذيب فقط . تبين من خلال هذه الدراسة أن المركبات 5a و 5b و 5d و 5f أبدت نشاطا بروجيستيرونيا أكثر من العقار المرجعي في حين أبدت المركبات 5c و 5e نشاطا بروجيستيرونيا أقل منه.

تمت أيضا دراسة التأثير المضاد للسرطان للمركبات المشيدة (5a-f) وفقا لبروتوكول المعهد الدولي للسرطان NCI بالولايات المتحدة الأمريكية حيث تمت الدراسة علي ٦٠ خط للخلايا السرطانية البشرية والمشتقة من تسعة أنواع للسرطان (سرطان الدم- سرطان الرئة- سرطان القولون- سرطان الجهاز العصبي المركزي- سرطان الجلد- سرطان المبيض- سرطان الكلية- سرطان البروستاتا سرطان الثدي).

وقد أبدت المركبات المختبرة فاعليات مختلفة تجاه الخلايا السرطانية المستخدمة في الدراسة وأبدت المركبات ذات الفاعلية نشاطا غير انتقائي واسع الطيف. ولوحظ من خلال هذه الدراسة أن مشتقات الإستر (5d-f) أبدت فاعلية أكثر من نظيراتها من المشتقات الحامضية (5a-c) وأبدى المركب 5e من بين مشتقات الإستر أعلى فاعلية حيث استطاع تثبيط حوالي ٥٠% من نمو الخلايا السرطانية SNB-75 لسرطان الجهاز العصبي المركزي كما استطاع تثبيط حوالي ٥٦% من نمو الخلايا السرطانية A498 لسرطان الكلية إضافة لتثبيطه لحوالي ٥٦.٧% من نمو الخلايا السرطانية PC-3 لسرطان البروستاتا.

تم عمل دراسة للإرساء الجزيئي للمركبات التي تم تحضيرها باستخدام برنامج MOE (إصدار ٢٠١٠.١٠) لتقييم ارتباط هذه المركبات بمستقبل البروجيسترون مقارنة بعقار النورايثندرون أسيتات. وقد أبدت الدراسة تأثيرا واضحا لإضافة المجموعات الكيميائية الجديدة علي الإرتباط مع الموقع النشط لمستقبل البروجيسترون. أعطت المركبات 5f, 5b, 5a أفضل النتائج لارتباطهم مع الحمضين الأمينيين الأساسيين في الموقع النشط للمستقبل Gln725 و Arg766 إضافة الي روابط هيدروجينية أخرى مع الحمض الأميني Asn719. علي الجانب الاخر أبدت المركبات 5c, 5d, 5e نتائج أقل من العقار المرجعي لارتباطها مع حمضين أميينيين فقط في الموقع النشط للمستقبل. تم أيضا دراسة تأثير التعديل الكيميائي الذي تم علي الخصائص الفيزيوكيميائية للمركبات المحضرة مقارنة بالمركب الأولي خلات النورايثندرون وأبدت هذه النتائج قصورا محدودا متوقعا في القابلية للذوبان في الماء للمركبات المخلقة ولكن التصميم المعتمد مسبقا لهذه المركبات يسمح بإمكانية تحضير أملاح مختلفة مع مجموعة الكربوكسيل في المشتقات الحامضية يمكن من خلالها زيادة القابلية للذوبان في الماء.





تصميم وتشبيد مشتقات ١٧ ألفا- (١- مستبدل- ١, ٢, ٣-
تريازول-٤-ويل)- خلايا ١٩- نور تستستيرون باستخدام "كيمياء
كليك" ذات فاعلية بروجستيرون وكمضادات للسرطان

رسالة مقدمة من

الصيدلي / زين العابدين حسيب محمد أحمد

بكالوريوس العلوم الصيدلانية - كلية الصيدلة - جامعة أسيوط
(٢٠٠٧)

للاستيفاء الجزئي للحصول على درجة الماجستير في العلوم الصيدلانية
(كيمياء صيدلانية طبية)

تحت إشراف

الأستاذ الدكتور

عادل فوزي يوسف

أستاذ الكيمياء الصيدلانية الطبية المتفرغ
كلية الصيدلة - جامعة أسيوط

الأستاذ الدكتور

نوال أبوبكر القوصي

أستاذ الكيمياء الصيدلانية الطبية

كلية الصيدلة - جامعة أسيوط

الأستاذ الدكتور

نادية محمد أحمد محفوظ

أستاذ الكيمياء الصيدلانية الطبية

كلية الصيدلة - جامعة أسيوط

كلية الصيدلة - جامعة أسيوط

١٤٣٥ هـ - ٢٠١٤ م